AD NUMBER
ADB000295
LIMITATION CHANGES
TO: **Approved for public release; distribution is unlimited.**
FROM: **Distribution authorized to U.S. Gov't. agencies only; Test and Evaluation; SEP 1974. Other requests shall be referred to US Army Air Mobility Research and Development Lab., Fort Eustis, VA 23604.**
AUTHORITY
USAASC ltr, 22 Oct 1990

USAAMRDL-TR- 74-50

AD B000295

A METHOD FOR PREDICTING THE AERODYNAMIC PERFORMANCE OF CENTERBODY-PLUG IR SUPPRESSORS

United Aircraft Research Laboratories
United Aircraft Corporation
East Hartford, Conn. 06108

September 1974

Final Report for Period March 1973 - June 1974

Distribution limited to U. S. Government agencies only; test and evaluation; September 1974. Other requests for this document must be referred to the Eustis Directorate, U.S. Army Air Mobility Research and Development Laboratory, Fort Eustis, Virginia 23604.

Prepared for

EUSTIS DIRECTORATE
U. S. ARMY AIR MOBILITY RESEARCH AND DEVELOPMENT LABORATORY
Fort Eustis, Va. 23604

EUSTIS DIRECTORATE POSITION STATEMENT

The object of this contractual effort was to develop a computerized, calculational procedure for predicting the aerodynamic static pressure distributions, local pressure recovery coefficients, and separation region locations inside center-plug infrared suppressors. The analysis is applicable to incompressible, subsonic, turbulent flow, with provisions made for both film-convection cooling and optional plume dilution. Comparisons of program predicted values and measured results reveal that additional modifications and refinements are necessary to improve prediction accuracy. Since significant differences have been found between measured and predicted results, it is recommended that computer program use be limited to cases in which extrapolations may be made from known results.

The conclusions contained in this report are concurred in by this Directorate.

The technical monitor for this contract was C. C. Gentry, Military Operations Technology Division.

Unclassified

SECURITY CLASSIFICATION OF THIS PAGE (When Data Entered)

REPORT DOCUMENTATION PAGE		READ INSTRUCTIONS BEFORE COMPLETING FORM
1. REPORT NUMBER USAAMRDL-TR-74-50	2. GOVT ACCESSION NO.	3. RECIPIENT'S CATALOG NUMBER
4. TITLE (and Subtitle) A METHOD FOR PREDICTING THE AERODYNAMIC PERFORMANCE OF CENTERBODY-PLUG IR SUPPRESSORS		5. TYPE OF REPORT & PERIOD COVERED Final March 1973 - June 1974
		6. PERFORMING ORG. REPORT NUMBER
7. AUTHOR(s) Olof L. Anderson		8. CONTRACT OR GRANT NUMBER(s) DAAJ02-73-C-0037
9. PERFORMING ORGANIZATION NAME AND ADDRESS United Aircraft Research Laboratories United Aircraft Corporation East Hartford, Conn. 06108		10. PROGRAM ELEMENT, PROJECT, TASK AREA & WORK UNIT NUMBERS
11. CONTROLLING OFFICE NAME AND ADDRESS Eustis Directorate, U.S. Army Air Mobility Research and Development Laboratory Fort Eustis, Va. 23604		12. REPORT DATE September 1974
		13. NUMBER OF PAGES 159
14. MONITORING AGENCY NAME & ADDRESS(if different from Controlling Office)		15. SECURITY CLASS. (of this report) Unclassified
		15a. DECLASSIFICATION/DOWNGRADING SCHEDULE

16. DISTRIBUTION STATEMENT (of this Report)

Distribution limited to U. S. Government agencies only; test and evaluation; September 1974. Other requests for this document must be referred to the Eustis Directorate, U. S. Army Air Mobility Research and Development Laboratory, Fort Eustis, Virginia 23604.

17. DISTRIBUTION STATEMENT (of the abstract entered in Block 20, if different from Report)

18. SUPPLEMENTARY NOTES

19. KEY WORDS (Continue on reverse side if necessary and identify by block number)

Diffusers, Internal Flow, Numerical Analysis, Aerodynamic Performance, IR Suppressors

20. ABSTRACT (Continue on reverse side if necessary and identify by block number)

An important consideration in the design of military aircraft engine exhaust diffusers is the need to reduce infrared radiation emanating from the engine, coupled with the need to maximize shaft horsepower. To aid the engineer in the solution of this problem, advanced mathematical techniques developed in this report have been applied to the solution of turbulent compressible swirling flow through curved-wall annular diffusers. This analysis has

DD FORM 1 JAN 73 1473 EDITION OF 1 NOV 65 IS OBSOLETE

Unclassified

SECURITY CLASSIFICATION OF THIS PAGE (When Data Entered)

20. developed a generalized method for calculating an orthogonal coordinate system for arbitrary curved-wall annular ducts with cooling slots which is based on the Schwartz-Christoffel transformation. In addition, this analysis has developed a stable implicit numerical integration scheme for solving a nonlinear parabolic partial differential equation which does not require an iterative procedure to maintain second-order accuracy. Finally, it is noted that the procedure does not require an iterative procedure coupling the inviscid and viscous portion of the flow field but treats the entire flow field as a whole.

A computer program has been developed using this analysis and applied to sample cases to demonstrate the capability of the analysis. Cases with and without slot-cooled walls have been calculated and compared with experimental data taken from the ST9 demonstrator IR suppression diffuser operating at different slot cooling flow rates for one engine operating condition. The results are in fair agreement with the experimental data, but additional work is required in order to obtain better theoretical predictions.

TABLE OF CONTENTS

Page

LIST OF ILLUSTRATIONS

LIST OF TABLES

INTRODUCTION

An important consideration in the design of military aircraft is the minimization of the infrared radiation emanating from the aircraft engine. The infrared signature of the engine can be controlled through proper design of an engine diffuser; however, great care must be taken to assure that the proposed diffuser does not adversely affect engine performance. Therefore, the design engineer is faced with the complex problem of designing an engine which provides minimum turbine back pressure with an efficient exhaust diffuser in order to maximize shaft horsepower and at the same time minimize radiation through the use of curved wall diffusers and cooled walls.

The satisfaction of these sometimes conflicting requirements has proven to be extremely difficult in the past, and engineers often have been forced to rely on empirical design methods based on correlations of limited experimental data. For example, diffuser performance maps based on empirical correlations have been published by Reneau (Ref. 1) for incompressible two-dimensional flow and by Sovran (Ref. 2) for incompressible annular flow in straight-wall diffusers. Regions of stall on these performance maps have been defined by Fox (Ref. 3) for two-dimensional diffusers and by Howard (Ref. 4) for straight-wall annular diffusers. In addition, Sovran (Ref. 2) has developed empirical correlations for the effect of inlet blockage on performance, and Runstadler (Ref. 5) has developed correlations for the effect of inlet Mach number. Although these empirical design criteria provide some insight into the effect of variables such as area ratio, length, inlet blockage and Mach number on performance, these criteria are not adequate for

---

(1) Reneau, L. R., J. P. Johnson, and S. J. Kline: Performance and Design of Straight, Two-Dimensional Diffusers. Transactions of ASME, Journal of Fluid Mechanics, Vol. 89, March 1969, pp. 141-160.

(2) Sovran, G., and E. D. Klomp: Optimum Geometries for Rectilinear Diffusers. Fluid Mechanics of Internal Flow, Elsevier Publishing Co., 1967.

(3) Fox, R. W., and S. J. Kline: Flow Regime Data and Design Methods for Curved Subsonic Diffusers. Journal of Basic Engineering, Transactions of the ASME, Series D, Vol. 84, No. 3, September 1962, pp. 303-312.

(4) Howard, J., H. Henseler, and A. Thornton-Trump: Performance and Flow Regimes for Annular Diffusers. ASME Paper 67, WA/FE-21, 1967.

(5) Runstadler, P. W., and R. C. Dean: Straight Channel Diffuser Performance at High Inlet Mach Numbers. Transactions of ASME, Journal of Basic Engineering, Vol. 91, September 1969, pp. 397-422.

designing curved-wall IR suppressing diffusers. For curved-wall annular diffusers, only a few studies such as those by Dietz and Thompson (Ref. 6) and Thayer (Ref. 7) are available to provide design information. In particular, Thayer has developed some general design requirements for diffusers of this type through his investigation of the effects of swirl and Mach number on diffuser performance.

The development of analytical design methods has generally lagged behind empirical design methods. Conventional solutions, such as those used by Sovran (Ref. 2), divide the flow field into an irrotational free-stream flow and a boundary layer flow. These methods which divide the flow field into viscous and inviscid portions require an iteration between the potential flow pressure field and the boundary layer displacement thickness. This iteration frequently fails to converge when the boundary layers comprise a significant portion of the total flow field. In addition, these iterative methods cannot account conveniently for phenomena such as inlet swirl and inlet flow distortion. Recently Anderson (Refs. 8 and 9) introduced a new method for solving the swirling diffuser flow problem which solves a single set of equations of motion for the entire flow field in the diffuser, thereby enabling compatibility between the inviscid flow and boundary layer to be achieved without the need for matching a boundary layer solution to an inviscid flow solution through an iterative procedure. The method has shown good agreement between theory and experiment for incompressible flow (Ref. 9) and has been extended more recently by Anderson (Ref. 10) to the prediction of compressible flow. Theoretical predictions again have been in good agreement with experimental data.

---

(6) Dietz, A. E., and J. F. Thompson: Advanced Experimental Infrared Energy Suppression System for the T-53-L-11 or T-53-L-13 Turbine Engine. Hayes Internal Report No. 1172, 1968.

(7) Thayer, E. B.: Evaluation of Curved-Wall Annular Diffusers. ASME Paper 71-WA/FE-35, September 1972.

(8) Anderson, O. L.: A Comparison of Theory and Experiment for Incompressible, Turbulent, Swirling Flows in Axisymmetric Ducts. AIAA Paper No. 72-42, 10th Aerospace Sciences Meeting, January 1972.

(9) Anderson, O. L.: Numerical Solutions of Incompressible Turbulent Swirling Flows Through Axisymmetric Annular Ducts. United Aircraft Research Laboratories Report No. H213577-1, March 1968.

(10) Anderson, O. L.: User's Manual for a Finite-Difference Calculation of Turbulent Swirling Compressible Flow in Axisymmetric Ducts With Struts. United Aircraft Research Laboratories Report L911211-1, Contract No. NAS3-15402, 1972.

The method derived in Ref. 10 requires construction of a gereralized orthogonal coordinate system from a solution of the plane potential flow through the duct in question. This potential flow solution serves as an approximate streamline coordinate system upon which the viscous solution of the equations of motion is based. The equations of motion are written in the approximate streamline coordinate system, and boundary layer approximations may be made in this new system since the potential flow streamlines approximate the real streamlines. With the boundary layer approximations, the equations of motion reduce to a set of parabolic partial differential equations which apply to the flow field under investigation. In Ref. 10, the solution to the potential flow problem was obtained through an approximate geometric construction which yielded good results when the curvature on both walls was small and nearly the same. This geometric solution sometimes failed when the curvature varied significantly from wall to wall. Even when the solution did not fail, significant errors could arise due to the small curvature approximation inherent in the method. Thus the procedure of Ref. 10 is limited in the types of geometries to which it can apply. With this limitation in mind, a new solution procedure not limited to the small curvature approximations was developed. This new method obtains the solution to the plain potential flow problem using an exact numerical solution based on the Schwartz-Christoffel transformation (Refs. 11 and 12).

It is possible to solve the governing equations by an explicit or an implicit numerical integration. In an explicit method for solving the equations of motion, the allowable streamwise step size is related to the transverse step size through numerical stability conditions. If the solution is to be numerically stable, a finer transverse grid requires a smaller streamwise step size. This restriction is particularly troublesome in the case of slot cooled walls, where a very fine transverse grid is desired to define the coolant film accurately. Therefore, under the present effort, the explicit numerical integration technique of Ref. 10 was replaced by an implicit technique based on the method of Keller (Ref. 13). In this new method, the

---

(11) Kober, H.: Dictionary of Conformal Representations. Dover Publications, Inc., 1957.

(12) Gaier, Dieter: Konstruktive Methoden der Konformen Abbildung, Springer Tracts in Natwal Philosophy, Vol. 8, 1963.

(13) Keller, H. B., and T. Cebeci: Accurate Numerical Methods for Boundary Layer Flows-II Two-Dimensional Turbulent Flows. AIAA 9th Aerospace Sciences Meeting, New York, January 25-27, 1971, AIAA Paper No. 71-164.

equations of motion are linearized in such a way that an iteration is not required to obtain a solution. The method, however, retains important features such as second-order accuracy and from the point of view of linear stability analysis has no restrictions on step size in either the streamwise or the transverse directions (Ref. 14). However, in practice the step size is restricted by the need to minimize truncation errors arising from the finite-difference scheme. Truncation errors will cause loss of accuracy and may lead to numerical instabilities through nonlinear effects. In addition, powerful matrix inversion methods are available in the numerical solution (Refs. 15 and 16).

Under the present effort, advanced mathematical techniques have been applied to the solution of turbulent compressible swirling flow through curved-wall annular diffusers with slot-cooled walls. From this analysis, a computer program has been developed and sample cases calculated and compared with experimental test results obtained from an IR suppressing diffuser with slot-cooled walls at different simulated engine operating conditions.

---

(14) Keller, H. B.: A New Difference Scheme for Parabolic Problems. Numerical Solution of Partial-Differential Equation-II SYNSPADE 1970 Ed. by Hubbard, B. Academic Press, New York.

(15) Keller, H. B.: Accurate Difference Methods for Linear Ordinary Differential Systems Subject to Linear Constraints. SIAM J. Namer, Anal. Vol. 6, No. 1, March 1969.

(16) Briley, W. R., and H. McDonald: An Implicit Numerical Method for the Multidimensional Compressible Navier-Stokes Equations. United Aircraft Research Laboratories Report M911363-6, November 1973.

ANALYSIS

The present analysis solves the problem of axisymmetric swirling flow through typical IR suppressing diffuser geometries in a two-step procedure. In the first step, a proper coordinate system is constructed; in the second step, a set of boundary layer type parabolic partial differential equations is solved using a forward marching implicit numerical integration procedure. For flow over a flat plate, the proper coordinate system consists of lines parallel to the plate (termed the streamwise coordinate) and a second set of lines perpendicular to the plate (termed the transverse or normal coordinate). If the equations of motion are written in this Cartesian coordinate system and the boundary layer approximations are made, a set of parabolic partial differential equations is obtained. For this simple problem, it is obvious that the boundary layer approximations (namely, that the transverse velocity is small compared to the streamwise velocity and that the streamwise derivatives are small compared to the transverse derivatives) are valid. In the case of more complicated geometries such as curved-wall diffusers, the coordinate system in which the boundary layer approximations can be made is not as simple as in the Cartesian coordinates described above. Rather, it is a coordinate system in which one coordinate approximates the streamlines and the other is normal to the streamlines. Such suitable coordinates can be obtained from the plain potential flow solution for the duct under investigation since it is apparent that in view of the constraining effect of the walls, the potential flow streamlines approximate the real streamlines provided large regions of flow separation do not occur.

This problem has been discussed in more detail by Anderson (Ref. 10), where it was shown that the solution to the plane potential flow problem through a given duct can be used to construct an orthogonal coordinate system uniquely suited to solve for the turbulent flow through the duct. Although the direct problem of determining the velocity potential s and stream function n in terms of the cartesian coordinates R and Z may be solved easily, the equations of motion for the turbulent flow require that n and s be explicitly the independent variables so that the coordinate functions R(n,s) and Z(n,s) can be obtained (Ref. 10). Although an approximate solution to this problem was presented in Ref. 10, the solution is inaccurate for ducts having large curvature. In order to alleviate this curvature limitation, an exact numerical solution has been obtained to the inverse problem using the Schwartz-Christoffel transformation (Ref. 11). In addition, the Schwartz-Christoffel transformation provides a method for obtaining an orthogonal coordinate system for a duct with slots. The method for solving for the generalized orthogonal coordinate system is derived in the next section.

The boundary layer approximations to the equations of motion for turbulent swirling flow with normal pressure gradients are derived in Ref. 10 where these equations were solved using an explicit numerical integration method. For slot-cooling problems, however, this explicit method is unsuitable because the inner layer of the turbulent boundary layers cannot be described accurately if a reasonable streamwise step is to be taken. Therefore, under the present effort, an implicit method of numerically integrating the equations of motion was developed. This method is derived in the following section entitled, "Conformal Mapping Solution". The implicit method is unconditionally stable, and the linearization technique used permits integration of the equations of motion without any iteration such as that used by Keller (Ref. 13).

Conformal Mapping Solution

Schwartz-Christoffel Transformation

If a curved-wall duct is represented by straight line segments in the w complex plane to form a many sided polygon, the Schwartz-Christoffel transformation (Ref. 11) may be used to transform this polygon in the w plane into the upper half of the z plane, as shown in Fig. 1. Under this transformation, the source flow at the duct inlet in the physical plane becomes a point source at the origin of the z plane. Source flows resulting from inlet cooling slots become point sources on the real axis of the z plane. The potential flow solution as a result of this source distribution in the z plane can be found easily by superposition of elementary source solutions leading to a definition of the streamlines n and potential lines s in the z plane. Then given n and s in the z plane, R(n,s) and Z(n,s) can be obtained by going back to the w plane and rotating and scaling as shown in Fig. 2. This procedure is explained in more detail in the following paragraphs.

The conformal mapping method has several important advantages over other methods of determining R and Z as a function of s and n. First, the inverse problem can be solved exactly in a straightforward manner as opposed to most other procedures, which lead to approximate solutions. Second, real ducts do have discontinuities along the wall boundaries for which the Schwartz-Christoffel transformation is ideally suited. Third, the technique developed in this report determines the wall slope and integrates the slope to obtain the wall contour. Thus the first derivatives and metric scale coefficients required for integration of the viscous flow equations are obtained directly rather than by numerical differentiation, leading to a more accurate solution.

Solution in z Plane

The complex potential for a source located at the origin of the z plane, which represents inflow at the duct entrance plane, is given by

$$F = \ln z = s + in \tag{1}$$

The complex potential can be solved explicitly. Thus, as shown in Fig. 1,

$$s = \ln r = \frac{1}{2} \ln \left(x^2 + y^2\right) \tag{2}$$

$$n = \phi = \tan^{-1}\left(y/x\right) \tag{3}$$

Equations (2) and (3) describe the potential flow in the z plane in the absence of any slot cooling. Since the walls contain poles representing corners of the duct in the physical plane, a finite upper half plane bounded by

$$\xi \leq \phi \leq \pi - \xi \tag{4}$$

$$r_0 \leq r \leq r_L \tag{5}$$

is defined. Thus n and s are bounded by

$$\xi \leq n \leq \pi - \xi \tag{6}$$

$$\ln r_o \leq s \leq \ln r_L \tag{7}$$

and the solution lies completely within a bounded domain free of singularities.

Solution in w Plane

The Schwartz-Christoffel transformation is given by

$$\frac{dw}{dz} = \frac{1}{z} \prod_{I=2}^{Nr+1} \left(z - b_I\right)^{-\alpha_I/\pi} \tag{8}$$

where b_I is the location of the poles on the x axis of the z plane, representing corners in the physical plane, and α_I is the corresponding corner angle (defined in Fig. 1) in the w plane. The b_I's and α_I's are, therefore, real constants. When the values of b_I are known, any point (n,s) in the z plane corresponds uniquely with a point in the w plane. The central problem is to find the values for the b_I's which are unique for the duct under consideration. Let

$$w = \xi + i z \tag{9}$$

$$z = x + iy \tag{10}$$

Then, because of orthogonality,

$$\frac{dw}{dz} = \frac{\partial \xi}{\partial x} - i\frac{\partial \xi}{\partial y} = \frac{\partial \eta}{\partial y} + i\frac{\partial \eta}{\partial x} \tag{11}$$

The real and imaginary parts of Eq. (8) are evaluated as follows:

$$r_J = \left[\left(x - b_J \right)^2 + y^2 \right]^{1/2} \tag{12}$$

$$\phi_J = \tan^{-1} \left[y / \left(x - b_I \right) \right] \tag{13}$$

$$\bar{r}_J = r_J^{-\alpha_J/\pi} \tag{14}$$

$$\bar{\phi}_J = -\alpha_J \phi_J / \pi \tag{15}$$

$$\bar{x}_J = \bar{r}_J \cos \bar{\phi}_J \tag{16}$$

$$\bar{y}_J = \bar{r}_J \sin \bar{\phi}_J \tag{17}$$

Then Eq. (8) reduces to

$$\frac{dw}{dz} = \prod_{J=1}^{Np+1} (\bar{x}_J + i y_J) = \tilde{x} + i\tilde{y} \tag{18}$$

which can be evaluated by repeated application of the product rule for complex numbers,

$$\tilde{x}_{J+1} = \tilde{x}_J \cdot \bar{x}_{J+1} - \tilde{y}_J \cdot \bar{y}_{J+1} \tag{19}$$

$$\tilde{y}_{J+1} = \tilde{x}_J \cdot \bar{y}_{J+1} + \tilde{y}_J \cdot \bar{x}_{J+1} \tag{20}$$

Finally, comparing Eq. (18) with Eq. (11) results in

$$\tilde{x} = \frac{\partial \xi}{\partial x} = \frac{\partial \eta}{\partial y} \tag{21}$$

$$\tilde{y} = -\frac{\partial \xi}{\partial y} = \frac{\partial \eta}{\partial x} \tag{22}$$

which lead to differential equations relating ξ, η, and x,y. As shown subsequently, these relations allow the construction of the required potential solution in the physical, w plane.

Differential Equations

The next step in the solution requires the derivation of the differential equations valid along an n or s coordinate. From Eqs. (2) and (3),

$$\frac{\partial s}{\partial x} = \frac{\partial n}{\partial y} = \frac{x}{x^2 + y^2} \tag{23}$$

$$\frac{\partial s}{\partial y} = -\frac{\partial n}{\partial y} = \frac{y}{x^2 + y^2} \tag{24}$$

A determinant, D, is defined by

$$D = - \left[\left(\frac{\partial s}{\partial x} \right)^2 + \left(\frac{\partial s}{\partial y} \right)^2 \right] \tag{25}$$

Then

$$dx = \frac{1}{D} \left[\frac{\partial s}{\partial y} dn - \frac{\partial s}{\partial x} ds \right] = \frac{1}{D} \left[- \frac{\partial n}{\partial x} dn - \frac{\partial n}{\partial y} ds \right] \tag{26}$$

$$dy = \frac{1}{D} \left[- \frac{\partial s}{\partial x} dn - \frac{\partial s}{\partial x} ds \right] = \frac{1}{D} \left[- \frac{\partial n}{\partial y} dn + \frac{\partial n}{\partial x} ds \right] \tag{27}$$

Hence along a streamline dn = 0 and

$$\frac{\partial x}{\partial s} = - \frac{1}{D} \frac{\partial s}{\partial x} \tag{28}$$

$$\frac{\partial y}{\partial s} = - \frac{1}{D} \frac{\partial s}{\partial y} \tag{29}$$

Along a potential line ds = 0 and

$$\frac{\partial x}{\partial n} = - \frac{1}{D} \frac{\partial n}{\partial x} \tag{30}$$

$$\frac{\partial y}{\partial n} = - \frac{1}{D} \frac{\partial n}{\partial y} \tag{31}$$

Equations (29) through (31) allow construction of the solution in the z plane. Finally, using Eqs. (11), (21), and (22), an integration may be carried out along streamlines or potential lines to construct the solution in the w plane.

$$\frac{\partial \xi}{\partial s} = \frac{\partial \xi}{\partial x}\frac{\partial x}{\partial s} + \frac{\partial \xi}{\partial y}\frac{\partial y}{\partial s} = \frac{\partial \eta}{\partial n} \tag{32}$$

$$\frac{\partial \eta}{\partial s} = \frac{\partial \eta}{\partial x}\frac{\partial x}{\partial s} + \frac{\partial \eta}{\partial y}\frac{\partial y}{\partial s} = -\frac{\partial \xi}{\partial n} \tag{33}$$

Hence, integration along streamlines in the w plane is obtained through Eqs. (32) and (33) together with Eqs. (27) and (29), and integration along potential lines in the w plane through Eqs. (32) and (33) together with Eqs. (30) and (31). The metric scale coefficients are the same in both directions and are given by

$$v = \left[\left(\frac{\partial \xi}{\partial s}\right)^2 + \left(\frac{\partial \xi}{\partial n}\right)^2\right]^{1/2} = \frac{dF}{dz}\Big/\frac{dw}{dz} \tag{34}$$

which is the same as the magnitude of the potential flow velocity obtained from the complex conjugate. It should be noted that the solution is equivalent to a solution for the wall slopes, Eqs. (32) and (33), or the metric scale coefficient. Hence the wall slopes and metric scale coefficients are solved for directly and the wall contour is obtained by integration. The determination of the b_I's which define the duct is discussed subsequently.

Solution Near a Source

Consider the solution in the neighborhood of the inlet source as $z \Rightarrow 0$. From Eq. (8),

$$\frac{dw}{dz} = \frac{C_1}{z} \tag{35}$$

where C_1 is a complex constant given by

$$C_1 = \prod_{I=2}^{NP+1} (b_I)^{-d_I/n} \tag{36}$$

Integration of Eq. (35) leads to the equation

$$W = C_1 \ln z + C_2 = C_1 (s + in) + C_2 \tag{37}$$

Thus the solution in the neighborhood of the inlet is

$$\xi - \xi_0 = C_{1R} (s - s_0) - C_{1R} (n - n_0) \tag{38}$$

$$\eta - \eta_0 = C_{1I} (s - s_0) + C_{1R} (n - n_0) \tag{39}$$

where C_{1R} and C_{1I} are the real and imaginary parts of C_1. Therefore, the inlet is a straight duct with an angle $(\alpha)_0$ to the axis of symmetry (see Fig. 1)

$$\alpha_0 = \tan^{-1} (C_{1R}/C_{1R}) \tag{40}$$

From Eq. (34), the metric scale coefficient is given by

$$V_0 = \left| C_{1I}^{\,2} + C_{1R}^{\,2} \right|^{1/2} \tag{41}$$

However, at the inlet, From Eq. (2) and Eq. (3)

$$S - S_0 = \ln\left(r/r_0\right) \tag{42}$$

$$n - n_0 = \phi \tag{43}$$

and from Eq. (4),

$$\Delta n = n - 2\xi \tag{44}$$

Therefore, inlet height is given by

$$h_0 = \frac{\Delta n}{v_0} \tag{45}$$

Transformation to R,Z Plane

Since the inlet of the duct starts out with an angle α_0, as shown in Fig. 1, the transform to the (r,z) plane shown in Fig. 2 is obtained through a rotation of an angle α_0 and is given by

$$r - r_0 = \cos\alpha_0\left(\eta - \eta_0\right) - \sin\alpha_0\left(\xi - \xi_0\right) \tag{46}$$

$$z - z_0 = \cos\alpha_0\left(\xi - \xi_0\right) + \sin\alpha_0\left(\eta - \eta_0\right) \tag{47}$$

Finally, the transformation to the (R,Z) plane is obtained through a translation and scaling using the inlet height h_o:

$$R = R_{HO} + \frac{R_{TO} - R_{HO}}{h_o}\left(r - r_o\right) \tag{48}$$

$$Z = \frac{\left(R_{TO} - R_{HO}\right)}{h_o}\left(z - z_o\right) \tag{49}$$

The streamline coordinates are scaled, noting that

$$\xi \leq n \leq n - \xi \tag{50}$$

$$0 \leq n \leq 1 \tag{51}$$

$$0 \leq S \leq S_L \tag{52}$$

Thus

$$n = \frac{n - \xi}{n - 2\xi} = \frac{n - \xi}{\Delta n} \tag{53}$$

$$S = \frac{s - s_o}{n - 2\xi} = \frac{s - s_o}{\Delta n} \tag{54}$$

$$V = \frac{1}{R_{TO} - R_{HO}} \quad \frac{V}{V_0} \tag{55}$$

For numerical convenience

$$S_0 = -\left(\pi - 2\xi\right) \; S_L/2 \tag{56}$$

Then from Eq. (42)

$$r_0 = \exp S_0 \tag{57}$$

and the solution in the z plane is located.

Locating Poles

The location of the poles b_I in the z plane must be obtained by an iterative method. It is noted that the location of the corners and the corresponding angle change of the polygon representing the physical duct in the (R,Z) plane is known. Specifically, the location of these corners can be expressed in terms of the distance X(J) along the wall from the inlet to the J^{th} corner. Each corner represents a pole in the z plane. If a guess is made for the b_I's, then Eqs. (32) and (33) may be integrated along the wall streamlines. Since the location of each pole is known in the (R,Z) plane, the distance $\check{X}(J)$ to the J^{th} pole is computed and compared to the known X(J). An iteration procedure based on Newton's method is used to obtain a new guess for the b_I's. In the iterative procedure the duct contour is defined by specifying the wall radius at JL equally spaced mesh points. Define

$$\Delta Z = Z_L / (JL - 1) \tag{58}$$

$$Z_J = \Delta Z\ (J-1) \tag{59}$$

Then the hub and tip contours (outer wall and inner wall) in the physical plane are known at each of the J points.

$$R_H(J) = R_H\left(Z_J\right) \tag{60}$$

$$R_T(J) = R_T\left(Z_J\right) \tag{61}$$

$$\theta_H(J) = \tan^{-1}\left(\frac{dR_H}{dZ}\right)_J \tag{62}$$

$$\theta_T(J) = \tan^{-1}\left(\frac{dR_T}{dZ}\right)_J \tag{63}$$

The α_J's for the Schwartz-Christoffel transformation are then given by

$$\alpha_H(J) = \theta_H(J) - \theta_H(J-1) \tag{64}$$

$$\alpha_T(J) = \theta_T(J+1) - \theta_T(J) \tag{65}$$

where they have been defined as the change in wall angle moving around the duct contour (polygon) in a counterclockwise direction. Since the polygon is composed of straight line segments, the distance along the wall from the inlet to the J^{th} point is given by

$$X_H(J) = \sum_{I=2}^{J} \left\{ \left[R_H(I) - R_H(I-1)\right]^2 + \Delta Z^2 \right\}^{1/2} \tag{66}$$

$$X_T(J) = \sum_{I=2}^{J} \left\{ \left[R_T(I) - R_T(I-1)\right]^2 + \Delta Z^2 \right\}^{1/2} \tag{67}$$

If an initial guess is used for the solution using the approximate solution described in Ref. 10, then the poles may be located using Eq. (42); Eq. (32) and Eq. (33) may be integrated along the walls (streamlines) and the distance along the wall to each corner determined from

$$X_H^{\nu}(J) = \int_0^{S_J} \frac{ds}{V_H} \tag{68}$$

$$X_T^{\nu}(J) = \int_0^{S_J} \frac{ds}{V_T} \tag{69}$$

These $X_H^{\nu}(J)$ and $X_T^{\nu}(J)$ in general will not agree with that calculated using Eqs. (66) and (67). However, at each pole in the (R,Z) plane we may obtain a new guess for b_I using Newton's method

$$S_H^{\nu+1}(J) = S_H^{\nu}(J) + V_H^{\nu}(J)\left[X_H^{\nu}(J) - X_H(J)\right] \tag{70}$$

$$\overset{\nu+1}{S}_T(J) = \overset{\nu}{S}_T(J) + \overset{\nu}{V}_T(J) \left[\overset{\nu}{X}_T(J) - X_T(J) \right] \tag{71}$$

Convergence occurs when

$$\xi_J = \left| X^{\nu}(J) - X(J) \right| \le \xi_M \tag{72}$$

for all J. Once the $\overset{\nu+1}{S}(J)$ are known, the new location of the poles may be obtained using Eqs. (42) and (54).

Duct With Slots

Inlet slots in a duct must satisfy the Kutta condition that the streamline leaves tangent to the slot lip. Thus the Kutta condition is equivalent to stating that the static pressure on each side of the slot lip is the same. Because of the Kutta condition, the coordinates for ducts with slots may be calculated by overlaying solutions of successively larger ducts without slots. This procedure is shown schematically in Fig. 3. The coordinates are calculated for duct 1 from station (1) to station (2). Then the cordinates are calculated for duct 2 from station (2) to station (3). Thus the Kutta condition is satisfied at the slot lip by construction of the streamline (wall) for duct 1 tangent to the slot inlet. This process may be repeated for any number of slots.

Implicit Method of Solution

Mach Number Transformation

At low Mach numbers, the extremely small variation of the pressure and temperature within the diffuser leads to large numerical errors in the solution of the equations if the actual pressure and temperature are treated as dependent variables. Therefore, a Mach number transformation was devised in which the dependent variables are the difference of the local pressure and temperature from the mean inlet flow conditions. For the purpose of the transformation, $\bar{\Pi}$, $\bar{\theta}$, $\bar{I}$ are defined as the mean inlet pressure, temperature, and entropy, respectively, and $\tilde{\Pi}$, $\tilde{\theta}$, $\tilde{I}$, $\tilde{Q}$ are defined by the relations

$$\Pi = \bar{\Pi}_1 + \gamma M_r^2 \tilde{\Pi} \tag{73}$$

$$\Theta = \bar{\Theta}_1 + (\gamma - 1) M_r^2 \tilde{\Theta} \tag{74}$$

$$I = \bar{I}_1 + (\gamma - 1) M_r^2 \tilde{I} \tag{75}$$

$$Q = (\gamma - 1) M_r^2 \tilde{Q} \tag{76}$$

where

$$\bar{I}_1 = \frac{\gamma}{\gamma - 1} \ln \bar{\Theta}_1 - \ln \bar{\Pi}_1 \tag{77}$$

The variables $\tilde{\Pi}$, $\tilde{\theta}$, $\tilde{I}$, $\tilde{Q}$ are the new dependent variables. It should be noted that for very small Mach numbers, Eq. (73) becomes

$$\tilde{\Pi} = \frac{\Pi - \bar{\Pi}_1}{\gamma M_r^2} = O(1) \tag{78}$$

When this transformation is applied to the equations of motion as given in Ref. 10, all the terms in the equations become the same order, allowing an accurate numerical solution to be obtained. In the previous formulation, some terms in the governing equations were considerably larger than others, leading to numerical errors.

Basic Equations of Motion

Under the present effort the Mach number transformation, Eqs. (73) through (77), is applied to the equations of motion derived by Anderson (Ref. 10). In addition, the equations are arranged as first-order equations to facilitate the application of an implicit numerical integration method. The governing equations are:

Continuity Equations

$$\frac{\partial \Psi}{\partial \eta} - \left[\frac{G}{XV}\right] P U_s = 0 \tag{79}$$

Streamwise Stress Component

$$\left(\frac{\mu_T}{\mu_r}\right)\left\{\frac{\partial U_s}{\partial \eta} + \left[\frac{1}{XV}\frac{\partial V}{\partial n}\right] U_s\right\} - \left[\frac{N_R}{XV}\right]\Sigma_{ns} = 0 \tag{80}$$

Tangential Stress Component

$$\left(\frac{\mu_T}{\mu_r}\right)\left\{\frac{\partial U_\phi}{\partial \eta} - \left[\frac{1}{XR}\frac{\partial R}{\partial n}\right] U_\phi\right\} - \left[\frac{N_R}{XV}\right]\Sigma_{n\phi} = 0 \tag{81}$$

Normal Momentum Equations

$$\frac{\partial \tilde{\Pi}}{\partial \eta} + \left[\frac{1}{XV}\frac{\partial V}{\partial n}\right] P U_s^2 - \left[\frac{1}{XR}\frac{\partial R}{\partial n}\right] P U_\phi^2 = 0 \tag{82}$$

Entropy Equation

$$(\gamma-1) M_r^2 \Upsilon = \frac{\gamma}{\gamma-1} \ln\left[(\gamma-1) M_r^2 \tilde{\Theta}\right] - \ln\left[\gamma M_r^2 \tilde{\Pi}\right] \tag{83}$$

Heat Flux Equation

$$\left(\frac{1}{PRE}\ \frac{\mu^E}{\mu^r}\right)\ \frac{\partial\tilde{\Theta}}{\partial\eta} + \left[\frac{N_R}{XV}\right]\tilde{Q} \tag{84}$$

Equation of State

$$\overline{\Pi}_1 + \gamma M_r^2\ \tilde{\Pi} = P\left[\overline{\Theta}_1 + (\gamma-1)M_r^2\ \tilde{\Theta}\right] \tag{85}$$

Streamwise Momentum Equation

$$\begin{aligned} &\frac{\partial\Sigma_{ns}}{\partial\eta} + \left[\frac{V}{XG}\ \frac{\partial}{\partial n}\left(\frac{G}{V}\right) - \frac{1}{XV}\ \frac{\partial V}{\partial n}\right]\Sigma_{ns} \\ &- \left[\frac{V}{G}\right]\frac{\partial\Psi}{\partial\eta}\ \frac{\partial U_s}{\partial S} + \left[\frac{V}{G}\right]\frac{\partial\Psi}{\partial S}\ \frac{\partial U_s}{\partial\eta} + \left[\frac{1}{XR}\ \frac{\partial R}{\partial S}\right]PU_\phi^2 \\ &- \frac{1}{X}\ \frac{\partial\tilde{\Pi}}{\partial S} = -\left[\frac{Hs}{XV}\right] \end{aligned} \tag{86}$$

Tangential Momentum Equation

$$\begin{aligned} &\frac{\partial\Sigma_{n\phi}}{\partial\eta} + \left[\frac{V}{XG}\ \frac{\partial}{\partial n}\left(\frac{G}{V}\right) + \frac{1}{XR}\ \frac{\partial R}{\partial n}\right]\Sigma_{n\phi} \\ &- \left[\frac{V}{G}\right]\frac{\partial\Psi}{\partial\eta}\ \frac{\partial U\phi}{\partial S} + \left[\frac{V}{G}\right]\frac{\partial\Psi}{\partial S}\ \frac{\partial U\phi}{\partial\eta} \\ &- \left[\frac{1}{XR}\ \frac{\partial R}{\partial S}\right]PU_\phi U_s = -\left[\frac{H\phi}{XV}\right] \end{aligned} \tag{87}$$

Energy Equation

$$\frac{\partial \tilde{Q}}{\partial \eta} + \left[\frac{V}{XG}\frac{\partial}{\partial n}\left(\frac{G}{V}\right)\right]\tilde{Q}$$

$$+ \frac{\gamma-1}{\gamma}\left[\frac{V}{G}\right]\Theta\left\{\frac{\partial \Psi}{\partial \eta}\frac{\partial \tilde{I}}{\partial S} - \frac{\partial \Psi}{\partial S}\frac{\partial \tilde{I}}{\partial \eta}\right. \tag{88}$$

$$\left. - \frac{N_R}{XV}\left(\frac{\mu r}{\mu r}\right)\left\{\Sigma_{ns}^{\;2} + \Sigma_{n\phi}^{\;2}\right\}\right\} = \left[\frac{\Phi B}{XV}\right]$$

It is noted upon examination of Eqs. (79) through (88) that no derivatives of density appear explicitly; therefore, a Mach number transformation was not applied to the density.

Boundary Conditions

For annular flow fields within ducts having both an inner and an outer wall, the proper set of boundary conditions is (see Ref. 10):

$$\left.\begin{aligned} &\Psi(S,0) = \Psi_H(S) \\ &Us(S,0) = 0. \\ &U_\phi(S,0) = 0. \\ &\tilde{Q}\,(S,0) = 0. \text{ adiabatic wall} \\ \text{or}\quad &\Theta\,(S,0) = \Theta_H \end{aligned}\right\} \tag{89}$$

$$\left.\begin{aligned} &\Psi(S,1) = \Psi_T(S) \\ &U_s(S,1) = 0. \\ &U_\phi(S,1) = 0. \\ &\tilde{Q}\,(S,1) = 0. \text{ adiabatic wall} \\ \text{or}\quad &\Theta\,(S,1) = \Theta_T(S) \end{aligned}\right\} \tag{90}$$

where S is the streamwise coordinate and n is the transverse coordinate. The transverse grid is normalized so that the walls occur at $n = 0$ and $n = 1$.

For axisymmetric flow, in which no inner wall is present, the equations of motion contain a removable singularity at the origin or axis of symmetry. The boundary conditions (Eq. (89)) must be replaced by boundary conditions based on a Taylor series expansion of the flow variables about the centerline. From Eq. (86) at a small distance h from the centerline, the expansion for Σ_{ns} is given by

$$\Sigma_{ns} = \frac{1}{2}\left[(VPU_s)\frac{\partial U_s}{\partial S} + V\frac{\partial \Pi}{\partial S}\right]_0 h + o(h^3) \tag{91}$$

The remainder is neglected because it is of higher order than the order of the difference approximation. Then Eq. (80) and Eq. (91) yield

$$U_s = U_{so} + \frac{1}{4}\frac{N_R}{(\mu_T \mu_r)_0}\left[VPU_s \frac{\partial V_s}{\partial S} + V\frac{\partial \Pi}{\partial S}\right]_0 h^2 + o(h^5) \tag{92}$$

which serves as a boundary condition for U_s.

The expansion of $\Sigma_{n\phi}$ about the centerline is obtained from Eq. (87):

$$\Sigma_{n\phi} = o(h^5) \tag{93}$$

Hence, from Eq. (81),

$$U_{\phi 1} = o(h^6) = 0 \tag{94}$$

since it is of higher order than the difference approximation. The heat flux equation (Eq. (84)) and the energy equation (Eq. (88)) are used to find a boundary condition for Q:

$$Q = -\frac{1}{2}\,\frac{\gamma-1}{\gamma}\left[vPU_s\Theta\,\frac{\partial I}{\partial S}\right]_0 h + o\left(h^3\right) \tag{95}$$

$$\Theta = \Theta_0 + \frac{1}{4}\,\frac{\gamma-1}{\gamma}\,\frac{N_R}{XV}\left[vPU_s\Theta\,\frac{\partial I}{\partial S}\right]_0 h^2 + o\left(h^4\right) \tag{96}$$

And, finally, a boundary condition for ψ is obtained from Eq. (79)

$$\Psi = 2\Pi\left(PU_s\right)_0 h^2 \tag{97}$$

The boundary conditions may then be applied at a distance h from the center-line. However, a great simplification may be obtained if h is chosen such that

$$h/(v\Delta\eta) \ll 1 \tag{98}$$

which implies that the first point is very near the centerline. Then we have the axisymmetric boundary conditions

$$\left.\begin{aligned} \Psi\,(S,0) &= 0. \\ \Sigma_{ns}(S,0) &= 0. \\ U_\phi\,(S,0) &= 0. \\ \tilde{Q}\,(S,0) &= 0. \end{aligned}\right\} \tag{99}$$

Finite Difference Approximation

These equations are reduced to finite difference equations using the second-order finite difference scheme of Keller (Refs. 14 and 15). The following notation for S and η is introduced:

$$\left.\begin{aligned} \Delta S^J &= S^J - S^{J-1} \\ \Delta\eta_K &= \eta_K - \eta_{K-1} \\ S^{J-1/2} &= \frac{1}{2}\left(S^J + S^{J-1}\right) \\ \eta_{K-1/2} &= \frac{1}{2}\left(\eta_K + \eta_{K-1}\right) \end{aligned}\right\} \qquad (100)$$

and for any dependent variable g (z,s) $g^{J-\frac{1}{2}}$ and $g_{K-\frac{1}{2}}$ are defined by

$$\left.\begin{aligned} g^{J-1/2} &= \frac{1}{2}\left(g^J + g^{J-1}\right) \\ g_{K-1/2} &= \frac{1}{2}\left(g_K + g_{K-1}\right) \end{aligned}\right\} \qquad (101)$$

The equations of motion, Eqs. (79) through (88), are linearized by performing a Taylor series expansion in the S coordinate, as suggested by Briley and McDonald (Ref. 16). Let any dependent variable g be given by

$$g^J = g^{J-1} + \Delta g \qquad (102)$$

where

$$\frac{\Delta g}{|g^J|} << 1 \qquad (103)$$

Then we have the following product rules (Ref. 16):

$$
\left.
\begin{aligned}
(fg)^J &= f^J g^{J-1} + f^{J-1} g^J - (fg)^{J-1} \\
(fg)^{J-1/2} &= \frac{1}{2}\left(f^J g^{J-1} + f^{J-1} g^J\right) \\
(fgh)^J &= (fg)^{J-1} h^J + (gh)^{J-1} f^J + (fh)^{J-1} g^J - 2\,(fgh)^{I-1} \\
\left(\frac{\partial g}{\partial S}\right)_K^{J-1/2} &= \frac{g_K^J - g_K^{J-1}}{\Delta S} \\
\left(\frac{\partial g}{\partial S} f\right)_K^{J-1/2} &= \frac{g^J - g^{J-1}}{\Delta S}\, f_K^{J-1}
\end{aligned}
\right\} \qquad (104)
$$

Substitution of Eq. (104) into the equations of motion, Eqs. (79) through (88), yields the following results.

Continuity Equation

$$
\Psi_K^J - \Psi_{K-1}^J - \frac{\Delta 2}{2}\left[\frac{G}{XV}\right]_{K-1/2}^J \left\{ \left(P_K^J + P_{K-1}^J\right) U_{SK-1/2}^{J-1} + P_{K-1/2}^{J-1}\left(U_{SK}^J + U_{SK-1}^J\right) \right\} \qquad (105)
$$

$$
= -\,\Delta\eta \left[\frac{G}{XV}\right]_{K-1/2}^J \left(P U_s\right)_{K-1/2}^{J-1}
$$

Streamwise Stress Component

$$
\left(\frac{\mu_T}{\mu_r}\right)_{K-1/2}^{J-1} \left\{ \left(U_{SK}^J - U_{SK-1}^J\right) + \frac{\Delta\eta}{2}\left[\frac{1}{XV}\,\frac{\partial V}{\partial \eta}\right]_{K-1/2}^J \left(U_{SK}^J + U_{SK-1}^J\right) \right\} \qquad (106)
$$

$$
- \frac{\Delta\eta}{2}\left[\frac{N_R}{XV}\right]_{K-1/2}^J \left(\Sigma_{nSK}^J + \Sigma_{nSK-1}^J\right) = 0
$$

Tangential Stress

$$
\left(\frac{\mu_T}{\mu_r}\right)_{K-1/2}^{J-1} \left\{ \left(U_{\phi K}^J - U_{\phi K-1}^J\right) - \frac{\Delta\eta}{2}\left[\frac{1}{XR}\,\frac{\partial R}{\partial \eta}\right]_{K-1/2}^J \left(U_{\phi K}^J + U_{\phi K-1}^J\right) \right\} \qquad (107)
$$

$$
- \frac{\Delta\eta}{2}\left[\frac{N_R}{XV}\right]_{K-1/2}^J \left(\Sigma_{n\phi K}^J + \Sigma_{n\phi K-1}^J\right) = 0
$$

Normal Momentum Equation

$$\tilde{\Pi}_K^J - \tilde{\Pi}_K^{J-1} + \frac{\Delta\eta}{2}\left[\frac{1}{XV}\frac{\partial V}{\partial \eta}\right]_{K-1/2}^{J}\left\{2\left(PU_s\right)_{K-1/2}^{J-1}\left(U_{SK}^J + U_{SK-1}^J\right) + \left(U_S^2\right)_{K-1/2}\left(P_K^J + P_{K-1}^J\right)\right\}$$

$$- \frac{\Delta\eta}{2}\left[\frac{1}{XR}\frac{\partial R}{\partial \eta}\right]_{K-1/2}^{J}\left\{2\left(PU_\phi\right)_{K-1/2}^{J-1}\left(U_{\phi K}^J + U_{\phi K-1}^J\right) + \left(U_\phi^2\right)_{K-1/2}^{J-1}\left(P_K^J + P_{K-1}^J\right)\right\} \quad (108)$$

$$= 2\Delta\eta\left\{\left[\frac{1}{XV}\frac{\partial V}{\partial \eta}\right]_{K-1/2}^{J}\left(PU_s^2\right)_{K-1/2}^{J-1} - \left[\frac{1}{X^R}\frac{\partial R}{\partial \eta}\right]_{K-1/2}^{J-1}\left(PU_\phi^2\right)_{K-1/2}^{J-1}\right\}$$

Entropy Equation

$$\tilde{I}_K^J - \tilde{I}_K^{J-1} = \frac{\gamma}{\gamma - 1}\left\{\frac{\tilde{\Theta}^J - \tilde{\Theta}^{J-1}}{\Theta^{J-1}} - \frac{\tilde{\Pi}^J - \tilde{\Pi}^{J-1}}{\Pi^{J-1}}\right\} \quad (109)$$

Heat Flux Equation

$$\left(\frac{1}{P_{er}}\frac{\mu_\xi}{\mu_r}\right)_{K-1/2}^{J-1}\left(\tilde{\Theta}_K^J - \tilde{\Theta}_{K-1}^J\right) + \frac{\Delta\eta}{2}\left[\frac{N_R}{XV}\right]_{K-1/2}^{J}\left(\tilde{Q}_K^J + \tilde{Q}_{K-1}^J\right) = 0 \quad (110)$$

Equation of State

$$\gamma M_r^2\ \tilde{\Pi}_K^J - P_K^J\ \overline{\Theta}_1 - (\gamma - 1) M_r^2\left[P_K^J\tilde{\Theta}_K^{J-1} + P_K^{J-1}\tilde{\Theta}_K^J\right]$$

$$= -\overline{\Pi} - (\gamma - 1) M_r^2\left(P\tilde{\Theta}\right)^{J-1} \quad (111)$$

Streamwise Momentum Equation

$$\left(\Sigma^{J}_{nSK} - \Sigma^{J}_{nSK-1}\right) + \frac{\Delta\eta}{2}\left[\frac{V}{XG}\frac{\partial}{\partial\eta}\left(\frac{G}{V}\right) - \frac{1}{XV}\frac{\partial V}{\partial\eta}\right]^{J-1/2}_{K-1/2}\left(\Sigma^{J}_{nSK} + \Sigma^{J}_{nSK-1}\right)$$

$$- \frac{1}{\Delta S}\left[\frac{V}{G}\right]^{J-1/2}_{K-1/2}\left(\Psi^{J-1}_{K} - \Psi^{J-1}_{K-1}\right)\left(U^{J}_{SK} + U^{J}_{SK-1}\right)$$

$$+ \frac{1}{\Delta S}\left[\frac{V}{G}\right]^{J-1/2}_{K-1/2}\left(U^{J-1}_{SK} - U^{J-1}_{SK-1}\right)\left(\Psi^{J}_{K} + \Psi^{J}_{K-1}\right)$$

$$+ \Delta\eta\left[\frac{1}{XR}\frac{\partial R}{\partial S}\right]^{J-1/2}_{K-1/2}\left\{2\left(PU_{\phi}\right)^{J-1}_{K-1/2}\left(U^{J}_{\phi K} + U^{J}_{\phi K-1}\right) + \left(U^{2}_{\phi}\right)^{J-1}_{K-1/2}\left(P^{J}_{K} + P^{J}_{K-1}\right)\right\}$$

$$- \frac{\Delta\eta}{\Delta S}\left[\frac{1}{X}\right]^{J-1/2}_{K-1/2}\left(\tilde{\Pi}^{J}_{K} + \tilde{\Pi}^{J}_{K-1}\right) \tag{112}$$

$$= -\left(\Sigma^{J-1}_{nSK} - \Sigma^{J-1}_{nSK-1}\right) - \frac{\Delta\eta}{2}\left[\frac{V}{XG}\frac{\partial}{\partial\eta}\left(\frac{G}{V}\right) - \frac{1}{XV}\frac{\partial V}{\partial\eta}\right]^{J-1/2}_{K-1/2}\left(\Sigma^{J-1}_{nSK} + \Sigma^{J-1}_{nSK-1}\right)$$

$$- \frac{1}{\Delta S}\left[\frac{V}{G}\right]^{J-1/2}_{K-1/2}\left(\Psi^{J-1}_{K} - \Psi^{J-1}_{K-1}\right)\left(U^{J-1}_{SK} + U^{J-1}_{SK-1}\right)$$

$$+ \frac{1}{\Delta S}\left[\frac{V}{G}\right]^{J-1/2}_{K-1/2}\left(U^{J-1}_{SK} - U^{J-1}_{SK-1}\right)\left(\Psi^{J-1}_{K} + \Psi^{J-1}_{K-1}\right)$$

$$+ \Delta\eta\left[\frac{1}{XR}\frac{\partial R}{\partial S}\right]^{J-1/2}_{K-1/2}\left(PU_{\phi}^{2}\right)^{J-1}_{K-1/2}$$

$$- \frac{\Delta\eta}{\Delta S}\left[\frac{1}{X}\right]^{J-1/2}_{K-1/2}\left(\tilde{\Pi}^{J-1}_{K} + \tilde{\Pi}^{J-1}_{K-1}\right) - 2\Delta\eta\left[\frac{H_s}{XV}\right]^{J-1/2}_{K-1/2}$$

Tangential Momentum Equation

$$\left(\Sigma^{J}_{n\phi K} - \Sigma^{J}_{n\phi K-1}\right) + \frac{\Delta\eta}{2}\left[\frac{V}{XG}\frac{\partial}{\partial n}\left(\frac{G}{V}\right) - \frac{1}{XR}\frac{\partial R}{\partial n}\right]^{J-1/2}_{K-1/2}\left(\Sigma^{J}_{n\phi K} + \Sigma^{J}_{n\phi K-1}\right)$$

$$-\frac{1}{\Delta S}\left[\frac{V}{G}\right]^{J-1/2}_{K-1/2}\left(\Psi^{J-1}_{K} - \Psi^{J-1}_{K-1}\right)\left(U^{J}_{\phi K} + U^{J}_{\phi K-1}\right) + \frac{1}{\Delta S}\left[\frac{V}{G}\right]^{J-1/2}_{K-1/2}\left(U^{J-1}_{\phi K} - U^{J-1}_{\phi K-1}\right)\left(\Psi^{J}_{K} + \Psi^{J}_{K-1}\right)$$

$$-\Delta\eta\left[\frac{1}{XR}\frac{\partial R}{\partial S}\right]^{J-1/2}_{K-1/2}\left\{\left(PU_{\phi}\right)^{J-1}_{K-1/2}\left(U^{J}_{SK} + U^{J}_{SK-1}\right)\right.$$

$$\left. + \left(PU_{S}\right)^{J-1}_{K-1/2}\left(U^{J}_{\phi K} + U^{J}_{\phi K-1}\right) + \left(U_{S}U_{\phi}\right)^{J-1}_{K-1/2}\left(P^{J}_{K} + P^{J}_{K-1}\right)\right\} \qquad (113)$$

$$= -\left(\Sigma^{J-1}_{n\phi K} - \Sigma^{J-1}_{n\phi K-1}\right) - \frac{\Delta\eta}{2}\left[\frac{V}{XG}\frac{\partial}{\partial n}\left(\frac{G}{V}\right) - \frac{1}{XR}\frac{\partial R}{\partial n}\right]^{J-1/2}_{K-1/2}\left(\Sigma^{J-1}_{n\phi K} + \Sigma^{J-1}_{n\phi K-1}\right)$$

$$-\frac{1}{\Delta S}\left[\frac{V}{G}\right]^{J-1/2}_{K-1/2}\left(\Psi^{J-1}_{K} - \Psi^{J-1}_{K-1}\right)\left(U^{J-1}_{\phi K} \quad U^{J-1}_{\phi K-1}\right) + \frac{1}{\Delta S}\left[\frac{V}{S}\right]^{J-1/2}_{K-1/2}\left(U^{J-1}_{\phi K} + U^{J-1}_{\phi K-1}\right)\left(\Psi^{J-1}_{K} + \Psi^{J-1}_{K-1}\right)$$

$$-\Delta\eta\left[\frac{1}{XR}\frac{\partial R}{\partial S}\right]^{J-1/2}_{K-1/2}\left(PU_{S}U_{\phi}\right)^{J-1}_{K-1/2} - 2\Delta\eta\left[\frac{H_{\phi}}{XV}\right]^{J-1/2}_{K-1/2}$$

Energy Equation

$$\left(\tilde{Q}^{J}_{K} - \tilde{Q}^{J}_{K-1}\right) + \frac{\Delta\eta}{2}\left[\frac{V}{XG}\frac{\partial}{\partial n}\left(\frac{G}{V}\right)\right]^{J-1/2}_{K-1/2}\left(Q^{J}_{K} + Q^{J}_{K-1}\right)$$

$$+\frac{\gamma-1}{\gamma}\frac{1}{\Delta S}\left[\frac{V}{G}\right]^{J-1/2}_{K-1/2}\Theta^{J-1}_{K-1/2}\left(\Psi^{J-1}_{K} - \Psi^{J-1}_{K-1}\right)\left(\tilde{I}^{J}_{K} + \tilde{I}^{J}_{K-1}\right)$$

$$-\frac{\gamma-1}{\gamma}\frac{1}{\Delta S}\left[\frac{V}{G}\right]^{J-1/2}_{K-1/2}\Theta^{J-1}_{K-1/2}\left(\tilde{I}^{J-1}_{K} - \tilde{I}^{J-1}_{K-1}\right)\left(\Psi^{J}_{K} + \Psi^{J}_{K-1}\right) \qquad (114)$$

$$-\Delta\eta\left[\frac{N_R}{XV}\right]^{J-1/2}_{K-1/2}\left(\frac{\mu_r}{\mu_T}\right)_{K-1/2}\left\{\Sigma^{J-1}_{nSK-1/2}\left(\Sigma^{J}_{nSK} + \Sigma^{J}_{nSK-1}\right) + \Sigma^{J-1}_{n\phi K-1/2}\left(\Sigma^{J}_{n\phi K} + \Sigma^{J}_{n\phi K-1}\right)\right\}$$

$$= -\left(\tilde{Q}_{K} - \tilde{Q}_{K-1}\right) - \frac{\Delta\eta}{2}\left[\frac{V}{XG}\frac{\partial}{\partial n}\left(\frac{G}{V}\right)\right]^{J-1/2}_{K-1/2}\left(Q^{J-1}_{K} + Q^{J-1}_{K-1}\right)$$

$$+\frac{\gamma-1}{\gamma}\frac{1}{\Delta S}\left[\frac{V}{G}\right]^{J-1/2}_{K-1/2}\Theta^{J-1}_{K-1/2}\left(\Psi^{J-1}_{K} - \Psi^{J-1}_{K-1}\right)\left(\tilde{I}^{J-1}_{K} + \tilde{I}^{J-1}_{K-1}\right)$$

$$-\frac{\gamma-1}{\gamma}\frac{1}{\Delta S}\left[\frac{V}{G}\right]^{J-1/2}_{K-1/2}\Theta^{J-1}_{K-1/2}\left(\tilde{I}^{J-1}_{K} - \tilde{I}^{J-1}_{K-1}\right)\left(\Psi^{J-1}_{K} - \Psi^{J-1}_{K-1}\right) + 2\Delta\eta\left[\frac{\Phi_B}{XV}\right]^{J-1}_{K-1/2}$$

With mass flow bleed at the wall, $\psi_H(s)$ and $\psi_T(s)$ are given by

$$\Psi_H^J = \Psi_H^{J-1} - \Delta S_J \left(\frac{G\overset{o}{M}}{V}\right)_H^{J-1/2} \tag{115}$$

$$\Psi_T^J = \Psi_J^{J-1} + \Delta S_J \left(\frac{G\overset{o}{M}}{V}\right)_T^{J-1/2} \tag{116}$$

Solution of Matrix Equation

The solution of these equations is obtained using the method of block-tridiagonal factorization (Refs. 15 and 17). If the column matrix $\bar{\bar{f}}^K$ is defined by

$$\bar{\bar{f}}^K = \left(\Psi_K^J, U_{SK}^J, U_{\phi K}^T, \tilde{\Pi}_K^J, \tilde{I}_K^J, \tilde{\Theta}_K^J, P_K^J, \Sigma_{nSK}^J, \Sigma_{n\phi K}^J, \tilde{Q}_K^J\right)^T \tag{117}$$

then the difference equations, Eqs. (105) through (114), may be written as a matrix equation

$$\bar{\bar{R}}^K \bar{\bar{f}}^K - \bar{\bar{L}}^K \bar{\bar{f}}^{K-1} = \bar{\bar{T}}^K \tag{118}$$

where $\bar{\bar{R}}^K$ and $\bar{\bar{L}}^K$ are the coefficients of the dependent variables and $\bar{\bar{T}}^K$ is the right-hand side of these equations. If $\eta_1 = 0$ is at the first mesh point and $\eta_{KL} = 1$ is at the last mesh point, equations are written at each of the η_K transverse locations where $2 \le K \le KL$ and ten boundary conditions are required. Note that Eqs. (109) and (111) involve only the K^{th} mesh point. Then we may use these two equations as boundary conditions plus the eight conditions given by Eqs. (89) and (90) or Eqs. (89) and (99).

---

(17) Varah, J. M.: On the Solution of Block-Tridiagonal Systems Arising from Certain Finite-Difference Equations. Mathematics of Computation, Vol. 26, No. 1, March 1969.

A 5X10 $\bar{\bar{M}}$ matrix for the boundary conditions may then be written for each end point such that the matrix equations become

$$\left.\begin{aligned} \bar{\bar{M}}^{1}\,\bar{\bar{f}}^{1} &= \bar{\bar{\tau}}^{1} \\ \bar{\bar{M}}^{KL}\,\bar{\bar{f}}^{KL} &= \bar{\bar{\tau}}^{KL} \end{aligned}\right\} \tag{119}$$

The complete set of matrix equations is written

$$\underset{\sim}{\bar{\bar{A}}}\;\bar{\bar{f}} = \bar{\bar{Q}} \tag{120}$$

where

$$\underset{\sim}{\bar{\bar{A}}} = \begin{Bmatrix} \bar{\bar{M}}^{1} & 0 & & & & & \\ -\bar{\bar{L}}^{1} & \bar{\bar{R}}^{1} & & & & 0 & \\ & -\bar{\bar{L}}^{2} & \bar{\bar{R}}^{2} & & & & \\ & & \ddots & \ddots & & & \\ & & & -\bar{\bar{L}}^{K} & \bar{\bar{R}}^{K} & & \\ & & & & -\bar{\bar{L}}^{KL} & \bar{\bar{R}}^{KL} & \\ & 0 & & & & 0 & \bar{\bar{M}}^{KL} \end{Bmatrix} \tag{121}$$

$$\tilde{Q} = \left\{\bar{\bar{\tau}}^{1},\ \bar{\bar{\tau}}^{K},\ \bar{\bar{\tau}}^{KL}\right\}^{T} \tag{122}$$

The matrix $\bar{\bar{A}}$ is made block tridiagonal by splitting as follows:

$$\bar{\bar{A}}^1 = \left\{ \begin{array}{ll} m^1_{IJ} & I = 1,5 \\ & J = 1,10 \\ \hdashline -\ell^2_{IJ} & I = 1,5 \\ & J = 1,10 \end{array} \right\} \tag{123}$$

$$\bar{\bar{A}}^K = \left\{ \begin{array}{ll} r^K_{IJ} & I = 6,10 \\ & J = 1,10 \\ \hdashline -\ell^{K+1}_{IJ} & I = 1,5 \\ & J = 1,10 \end{array} \right\} \quad (K = 2, KL-1) \tag{124}$$

$$\bar{\bar{A}}^{KL} = \left\{ \begin{array}{ll} r^{KL}_{IJ} & I = 6,10 \\ & J = 1,10 \\ \hdashline m^{KL}_{IJ} & I = 1,5 \\ & J = 1,10 \end{array} \right\} \tag{125}$$

$$\bar{\bar{B}}^K = \left\{ \begin{array}{ll} -\ell^K_{IJ} & I = 6,10 \\ & J = 1,5 \\ \hdashline & 0 \end{array} \right\} \quad (K = 2, KL) \tag{126}$$

$$\bar{\bar{C}}^R = \left\{ \begin{array}{ll} & 0 \\ \hdashline r^{K+1}_{IJ} & I = 1,5 \\ & J = 1,10 \end{array} \right\} \quad (K = 1, KL-1) \tag{127}$$

Hence we have a block tridiagonal matrix:

$$\underset{\sim}{\bar{\bar{A}}} = \begin{Bmatrix} \bar{\bar{A}}^1 & \bar{\bar{C}}^1 & & & & \\ \bar{\bar{B}}^2 & \bar{\bar{A}}^2 & \bar{\bar{C}}^2 & & & \\ & \bar{\bar{B}}^K & \bar{\bar{A}}^K & \bar{\bar{C}}^K & & \\ & & \bar{\bar{B}}^{KL-1} & \bar{\bar{A}}^{KL-1} & \bar{\bar{C}}^{KL-1} & \\ & & & \bar{\bar{B}}^{KL} & \bar{\bar{A}}^{KL} & \end{Bmatrix} \tag{128}$$

The matrix $\bar{\bar{Q}}$ splits as follows:

$$\bar{\bar{q}}^1 = \left\{ \bar{\bar{T}}^1, \bar{\bar{T}}_I^2 (I = 1,5) \right\}^T \tag{129}$$

$$\bar{\bar{q}}^K = \left\{ \bar{\bar{T}}_I^K (I = 6,10), \bar{\bar{T}}_I^K (I = 1,5) \right\} \tag{130}$$

$$\bar{\bar{q}}^{KL} = \left\{ \bar{\bar{T}}_I^{KL} (I = 6,10), \bar{\bar{T}}^{KL} \right\} \tag{131}$$

The matrix equations (Eq. (120)) are solved using the method of block tri-diagonal factorization (Ref. 17) with the recursion formulas given by

$$\bar{\bar{D}}^1 = \bar{\bar{A}}^1 \tag{132}$$

$$\bar{\bar{E}}^K = (\bar{\bar{D}}^K)^{-1} \bar{\bar{C}}^K \qquad 1 \leq K \leq KL - 1 \tag{133}$$

$$\bar{\bar{D}}^K = \bar{\bar{A}}^K - \bar{\bar{B}}^K \bar{\bar{E}}^{K-1} \qquad 2 \le K \le KL \tag{134}$$

$$\bar{\bar{Z}}^1 = (\bar{\bar{D}}^1)^{-1} \bar{\bar{Q}}^1 \tag{135}$$

$$\bar{\bar{Z}}^K = (\bar{\bar{D}}^K)^{-1} \left[\bar{\bar{Q}}^K - \bar{\bar{B}}^K \bar{\bar{Z}}^{K-1} \right] \qquad 2 \ge K \le KL \tag{136}$$

and the solution is obtained by backward substitution.

$$\bar{\bar{f}}^{KL} = \bar{\bar{Z}}^{KL} \tag{137}$$

$$\bar{\bar{f}}^K = \bar{\bar{Z}}^K - \bar{\bar{E}}^K \bar{\bar{f}}^{K+1} \qquad (KL-1 > Z, \ge 1) \tag{138}$$

DESCRIPTION OF TEST PROGRAM

The ST9 demonstrator IR suppressing exhaust diffuser was tested on the Pratt & Whitney Florida Research and Development Center (FRDC) D-32 test facility to verify the accuracy of the analysis described previously in this report. The FRDC facility can provide hot gas flow at a temperature of 1200 deg F and weight flows of 8.3 lb/sec. Adjustable swirl vanes upstream of the diffuser provide swirling flow from 0 deg up to 30 deg, thus simulating typical turbine exit flows at different engine operating conditions. In addition, the facility was modified to provide coolant flow rates up to 10 percent of diffuser airflow rates and to provide slot cooling on the diffuser walls. Complete wall static pressure and temperature instrumentation was provided to measure the effect of wall cooling rates on pressure recovery and wall temperature at different simulated engine operating conditions.

Description of Test Facility

A schematic of the FRDC D-32 test facility is shown in Fig. 4. The diffuser inlet flow simulating a typical turbine exit flow is provided by compressed air from the D-Area J57 slave engine. The compressor air flows through a stand heater burner and swirl generator with adjustable vanes shown in Fig. 5. Coolant airflow is supplied to the inner and outer walls of the exhaust diffuser from the D-Area 350-psig air system. As shown in Fig. 6, the coolant to the outer wall, inner wall, and base louvers is separately regulated. A schematic of the ST9 demonstrator IR suppressing exhaust diffuser is shown in Fig. 7. The manifold providing the coolant flow separately to the inner and outer walls and base is shown as well as the location of the louvers or slots on the diffuser wall. Throughout the test program, no coolant flow was supplied to the base in order to eliminate effects of base cooling flow on inner wall static pressure. Photographs of the test facility with the diffuser in place taken after completion of testing are shown in Figs. 8 and 9. No apparent damage or deterioration to the suppressor occurred during the test program.

Description of Instrumentation

Wall pressures were measured by thirty-one static pressure taps located on the inner and outer walls of the diffuser with the data recorded manually on manometer boards. The exact axial locations of these pressure taps, denoted PW01 through PW31, are given on Table 1 and are shown schematically on Fig. 10. Plenum static pressures in the three manifolds are denoted PB01,

PB02, and PB03 for the outer wall, inner wall, and base, respectively. Wall temperatures were measured by sixteen thermocouples located on the inner and outer walls with the data recorded manually on the thermocouple readouts. The locations of these thermocouples are given in Table 1 and are shown on Fig. 11. These thermocouples are labeled TW01 through TW16. In addition, the bulk temperature of the coolant flow was measured by thermocouples labeled TB01 through TB06 as shown on Table 1 and Fig. 11.

The inlet flow distribution was measured by two total pressure rakes and two wall static pressure taps. In addition, a measurement of circumferential distortion was made through four midspan total pressure rakes located at several circumferential stations.

A midspan total temperature probe was used to measure the bulk temperature of the diffuser flow. The location of all the inlet flow instrumentation is shown on Fig. 12. Diffuser inlet and coolant flow rates were measured separately by orifices located as shown in Fig. 12.

Test Results

A summary of the results of the test program are presented in the test log, Table 2, and a complete set of test results in Table 3. Eleven tests were conducted over a period of two days at three simulated power settings and three different coolant flows per power setting. Two tests, 2.01 and 6.01, are considered to be invalid due to flow perturbations while data was being recorded. Each test was repeated to provide valid data. The main results of the test program are briefly discussed in the following paragraphs.

The effects of film cooling on pressure recovery, wall pressures, and wall temperatures were evaluated by testing coolant flows of 2.5, 5, and 10 percent of diffuser inlet flow. The largest effect of this coolant flow variation was on louver wall temperature, as shown for the outer wall in Fig. 13. Locations of the outer wall cooling louvers are shown in Fig. 7. Surface temperatures increased rapidly with reduced coolant flow and the greatest change occurred in louver 4.

The effects of coolant flow on wall pressure distributions are shown in Fig. 14 for a swirl angle of zero degrees. Changes in wall pressure with coolant flow were less significant at swirl angles of 16 and 21 deg than at zero degrees. Reducing coolant flow rate from 10 to 2.5 percent on inlet flow resulted in a general increase in wall pressures of about 0.03 psi for both inner and outer walls. Note that the increased wall pressures were not restricted to the cooled section of the suppressor but also extended upstream to the inlet static pressures. This results in a decrease in

pressure recovery (C_p) from 0.63 to 0.58 with coolant flow as shown in Fig. 15, where the pressure coefficient C_p is given by

$$C_p = \frac{P - P_1}{P_{01} - P_1} \tag{139}$$

However, the influence of coolant flow on C_p is small at zero swirl and negligible at swirl angles of 16 and 21 deg. Hence, the slight ejector-effect of the film coolant at zero swirl disappears at higher swirl angles.

COMPARISON OF EXPERIMENT AND THEORY

A set of calculations were made to demonstrate the capability of the computer program and assess the code by comparing the theoretical predictions with experimental data. These calculations include a solution obtained for turbulent flow through a 6-deg conical diffuser, termed Fraser Flow "A" (Ref. 18), a baseline calculation for the ST9 demonstrator diffuser model tests with no film cooling, and a set of three cases for the flow through the ST9 demonstrator IR suppression diffuser corresponding to tests logged in Table 2. The calculations were numerically stable; however, truncation errors associated with the linearization of the differential equations were found to be sensitive to streamwise step size. The sensitivity to step size was particularly acute for the slot cooling cases. Since the slot height was only one percent of the diffuser inlet height in these cases, the streamwise step size had to be very small (of the order of the slot height) to allow adequate definition of the resultant flow field development. Since the computing time is proportional to the number of streamwise stations in the calculation field, efforts should be made to select the optimum step size in order to minimize computing time and still keep truncation errors within reasonable bounds.

Fraser Flow "A"

The solution for the turbulent flow through a 6-deg conical diffuser was obtained with the current calculation procedure and compared to the experimental data of Fraser as presented in Ref. 18. For this calculation, one hundred thirty streamlines and fifty streamwise stations were used to construct the coordinate system from the Schwartz-Christoffel transformation as shown in Fig. 16. The mesh distortion parameter placed approximately twenty mesh points between $0 \leq Y^+ \leq 10$. The inlet flow was constructed from Coles' velocity profile (Ref. 18) with the inlet boundary layer thickness taken to be 0.0528 in. as specified by the Fraser data in Ref. 18.

---

(18) Coles, D. E., and E. A. Hirst: Proceedings Computation of Turbulent Boundary Layers - 1968 AFSOR-IFP-Stanford Conference, August 1968.

As demonstrated in Ref. 18, Coles' profile accurately represents the boundary layer mean velocity profiles over a wide range of flow conditions in terms of two parameters, a friction velocity, U^* and a wake parameter, π. Coles' profile expresses the mean velocity distribution by

$$U^+ = \frac{1}{\kappa} \ln Y^+ + 2\frac{\Pi}{\kappa} \sin^2\left(\frac{\Pi}{2}\frac{Y}{\delta}\right) + B \tag{140}$$

where U^+ and Y^+ are the velocity and transverse coordinate written in wall variables

$$U^+ = U/U^* = U/\sqrt{\tau_w/\rho_w} \tag{141}$$

$$Y^+ = YU^*/\nu = Y\sqrt{\tau_w/\rho_w}\,/\nu \tag{142}$$

π is the wake parameter, and B is a constant. In Eq. (140) the first term expresses the "law of the wall" and the second term expresses the "law of the wake". Specification of U^* and π uniquely determines the velocity profile. At the edge of the boundary layer $Y = \delta$ and Eq. (140) becomes

$$\frac{U}{U^*} = \frac{1}{\kappa} \ln\left(\frac{\delta U^*}{\nu}\right) + \frac{2\Pi}{\kappa} + B \tag{143}$$

When Eq. (140) is used to compute the boundary layer displacement thickness δ^*, the relation

$$\kappa \frac{\delta^* U_\infty}{\delta U^*} = 1 + \Pi \tag{144}$$

is obtained. Thus given δ and δ^*, the wake parameter π and friction velocity U^* can be determined from Eqs. (143) and (144) and then the velocity distribution is uniquely determined by Eq. (140).

It should be noted that Fraser Flow "A" is a particularly difficult flow to calculate with classical boundary layer theory which assumes a viscous flow development under the influence of a semi-infinite nominally inviscid outer flow field. The inability of classical boundary layer theory to predict the flow field development is shown in Ref. 18, where a variety of boundary layer theories were unable to predict this flow field accurately. This inability of standard boundary layer procedure to predict Fraser Flow "A" stems from two sources. First, the wall boundary layer reaches the diffuser centerline approximately halfway downstream from the diffuser throat, and in this region no potential core flow exits. Second, the Fraser Flow "A" diffuser is an optimum diffuser in that it is designed to keep a nearly separated boundary layer as the flow diffuses. Boundary layers which are on the verge of separation are very difficult to predict since small changes in pressure distribution can lead to large changes in boundary layer thickness. However, as discussed by Coles and Hirst (Ref. 18), the Fraser Flow "A" data are reliable and based upon careful development of a flow configuration with good axial symmetry. Thus the flow should be able to be predicted accurately by a calculation procedure which can properly account for the disappearance of the central potential core. The present analysis, which does not assume the existence of any potential core, yields predictions which are in good agreement with the data as shown in Figs. 17 and 18, where comparisons between experiment and theory for the pressure coefficient and wall friction coefficient are present.

Calculation Procedure For ST9 Demonstrator IR Suppression Diffuser Runs

The streamline coordinate system used to predict the flow in the FRDC diffuser as calculated from the Schwartz-Christoffel transformation is shown in Fig. 19. Since this diffuser configuration is complicated, it is helpful to describe it in some detail. First it is noted that a short "duct inlet section" has been added to the diffuser in order to insure that the initial inlet flow has no normal pressure gradient. The diffuser centerbody has a blunt "diffuser base" and a lip on the outerbody (OD) wall extending past the base. The exit centerbody (ID) and OD walls were, therefore, extended past the diffuser exit plane by the "extended free streamline" shown in Fig. 19. The ID and OD wall contours were specified at fifteen equally-spaced streamwise stations. The computer program then fitted smooth curves through these points and interpolated the curves to specify eighty streamwise stations. The input mesh points are indicated by a small circle and the diffuser wall by a double line. In addition, seven cooling slots are located on the wall at the stations specified. In order to clearly illustrate the location of the slots, the ID and OD walls were opened a small amount at each slot so that at the

exit plane the wall is separated from the wall streamline by a small amount. Finally, six struts are located in the duct. The plan view of one strut is indicated in Fig. 19 by the "strut centerline", "strut leading edge", and "strut trailing edge".

Eighty streamwise stations and one hundred thirty streamlines were calculated for the streamline coordinate system. The mesh distortion parameters were selected so that the first streamline from the wall was located at a distance of 0.000077 times the duct inlet height. This placed approximately five mesh points between $0 < Y^+ < 10$ at a slot exit plane and about forty mesh points within the slot height. In portions of the flow removed from the slots, approximately thirty mesh points were placed in the viscous sublayer. For all cases, the inlet flow was obtained from experimental data shown in Fig. 20. Instrumentation in the inlet plane of the diffuser was used to measure total pressure, static pressure, swirl angle, and total temperature as given in Table 3 for each test case. Twelve data points across the inlet are given. These data were then interpolated to fit the one hundred thirty mesh points used in the calculation, and the Mach number, velocity and static pressure, and temperature were then computed. This experimental data, however, is not accurate enough to construct the inlet boundary layer profiles. Therefore, these profiles were constructed from Coles' velocity profile by specifying the displacement thickness.

<u>Baseline Case - No Film Cooling - No Struts</u>

The first ST9 diffuser case calculated consists of the basic diffuser with no struts or slot cooling and is termed the baseline case; the baseline case has zero swirl. The predicted wall static pressure distribution is compared with the experimental data taken from earlier FRDC cold-flow model tests (Ref. 7) in Fig. 21. As shown in Fig. 21, the theoretical predictions of wall static pressure distribution without cooling and without struts is higher than the experimental data. This observation is consistent with the observation made in the Fraser Flow "A". In addition, it is noted that the analysis predicts the appearance of a separation bubble on the centerbody wall located approximately between $0.19 < Z/L < 0.26$; this prediction is in agreement with FRDC model test data which also shows a separation bubble at the same approximate location.

A number of observations can be made about this test case. The predictions of the analysis are in qualitative agreement with the data for pressure coefficient along the diffuser. The overall pressure rise is in fairly good agreement with the data, and both the analysis and the data show a separation bubble in approximately the same duct location. However, the detailed variations of pressure coefficient is not in good qualitative agreement with the data and in the region of the separation bubble, the

analytical predictions and the data show significant qualitative discrepancies. However, it should be noted that it is very difficult to maintain axisymmetric flow in curved-wall annular diffusers (see Ref. 2). This problem is compounded when separation occurs because separated flow is very sensitive to small pressure fluctuations. Therefore, the size and location of the separation may be affected by asymmetry effects which in turn may lead to discrepancies between prediction and data.

ST9 Demonstrator IR Suppression Diffusers - 2.5 Percent Cooling Rate

The 2.5 percent cooling case consists of the ST9D demonstrator IR suppression diffuser run with six struts and seven cooling slots and corresponds to test case 3.01 shown on Table 2. This test case represents the diffuser operating at 60 percent military rated power and film cooling flow rate of 2.5 percent of the diffuser flow rate. The coolant plenum total pressure and static temperatures are given in Table 3. Experimental data, obtained from Table 3, was used to construct the inlet flow profiles as described for the Fraser Flow "A" case.

A comparison of the predicted flow with the corresponding experimental data is shown in Fig. 22 and Fig. 23. The predicted wall static pressure distribution, shown in Fig. 22, indicates a significant drop in pressure in the region of the strut. This effect is caused by the strut blockage which accelerates the flow through the strut passage (see Ref. 7). The presence of the strut exhibits the separated region which is present in the baseline case, and separation was neither predicted by the analysis nor measured in the experimental test. The first slot is located on the tip wall just downstream of the strut trailing edge. As shown on Fig. 23, the wall temperature drops almost by 700 deg F at this slot and increases rapidly by almost 500 deg F as rapid mixing of the film cooling flow with the hot diffuser flow is promoted. Successive slots follow the same pattern. The predicted wall static temperature distribution is in good agreement with experimental data. The wall static pressure distribution is qualitatively correct for $Z/L < 0.6$, but shows significant quantitative discrepancies with the data. Downstream of the fourth slot, the wall static pressure decreases rapidly due to large total pressure losses, and this unrealistic solution is not plotted.

ST9 Demonstrator IR Suppression Diffuser With 5 Percent Cooling Rate

The 5 percent cooling rate case corresponds to test case 2.02 shown on Table 2. This case represents the diffuser operating at 60 percent military rated power with a film cooling flow rate of 5 percent of diffuser weight flow. A comparison of the predicted results with experimental data is shown on Figs. 24 and 25. The wall static pressure distribution shows very little

change compared to test case 3.01 with 2.5 percent cooling flow rate and is consistent with earlier observations of the data that the pressure distribution is not greatly affected by the coolant flow rate as shown in Fig. 14. The wall temperatures, however, show a significant reduction from a mean temperature of about 600 deg F for test case 3.01 down to a mean temperature of about 450 deg F for this test case. This predicted reduction in temperature with increasing coolant flow rate follows the trend in the experimental data shown in Fig. 13. Again, downstream of the fourth slot, the wall static pressure decreases rapidly due to large total pressure losses and the solution is not plotted.

ST9 Demonstrator IR Suppression Diffuser With 10 Percent Cooling Rate

The 10 percent cooling rate case corresponds to test case 1.01 as shown on Table 2 and represents the diffuser operating at 60 percent military rated power with a film cooling flow rate of 10 percent of diffuser weight flow. A comparison of the predicted results with experimental data is shown on Figs. 26 and 27. Again, the wall static pressure distribution shows very little change from the previous cases, indicating that the coolant flow rate does not greatly change the wall static pressure distribution. This observation was previously noted (see Fig. 14). The mean wall temperature shows a drop from the previous cases down to a mean temperature of about 300 deg F and demonstrates the expected behavior that increasing coolant flow rates reduce wall static temperatures as shown by the data in Fig. 13. It should be noted that part of this reduction in wall temperature comes from a reduced plenum total temperature as seen in the data of Table 3. Therefore, an accurate calculation of an IR diffuser performance must account for an overall heat balance as well as the local slot cooling effect.

Discussion of Numerical Calculations

Since this report presents new and very advanced techniques for calculating turbulent flow in ducts, some discussion of the numerical problems which were encountered is in order. In particular, suggestions are made on means to improve the predictions of the computer code for slot and film cooled problems. The Fraser Flow "A" test case represents a good test case for the purpose of checking the accuracy and reliability of the computer program. As evaluated by Coles and Hirst in Ref. 18, Fraser Flow "A" represents reliable measurements based on careful development of a flow configuration with good axial symmetry. Pressure distributions, wall friction coefficient distributions, displacement thickness, and momentum thickness distributions are presented. In addition, accurate measurements of the boundary layer profiles are given for eleven axial stations. Finally, the

Fraser Flow "A" is a clean flow showing only the effects of boundary layer growth in an adverse pressure gradient. Of special interest in this test case is the fact that the flow is in a nearly separated condition for a good part of the diffuser length. Complications arising from struts, slots, swirl or wall curvature are not present.

Before the predictions of the Fraser Flow "A" case were compared with the experimental data, the numerical accuracy for the computer program was checked for internal consistency by several means. The most important of these checks was a comparison of the mean flow variables obtained by averaging the solution for each dependent variable over the duct height and comparing the average values with the solution for these same variables obtained by integrating the one-dimensional mass flow weighted average equations. As an example, these equations show that in the absence of wall mass flow bleed and wall heat transfer, the diffuser weight flow and mass flow weighted average total temperature are constant. An examination of the detailed computer printout for the Fraser Flow "A" case shows that these variables are indeed constant to at least five decimal places, thus indicating that the numerical procedure satisfies the integral conservation laws. In regard to the prediction of Fraser Flow "A", the agreement between theory and experiment should be regarded as excellent for the skin friction and good for the pressure coefficient, particularly in view of the fact that the flow is continuously on the verge of separation. As shown by Stratford (Ref. 19), turbulent boundary layers near separation may take on a wide variety of profile shapes. The shape depends upon the upstream history of the flow and small changes in the upstream history can lead to large changes in boundary layer development. Thus the Fraser Flow "A" case is a difficult test of the basic analytical procedure, and based on this test, it is concluded that the analysis operates well in predicting flows in the absence of such complications as struts, swirl, and wall curvature.

Some indication of local errors can be estimated by examining the total and static pressures along the centerline of the Fraser Flow "A" case, which should be nearly constant since the viscous and heat transfer losses are negligible along the centerline. This comparison indicates local accumulated errors of the order of 0.1, which is quite good. From these results, it is concluded that the basic numerical procedure is accurate and that any improvements in the predictions for this basic case must come from a closer examination of the turbulent mixing length model.

---

(19) Stratford, B. S.: An Experimental Flow With Zero Skin Friction Throughout Its Pressure Rise. Journal of Fluid Mechanics, Vol. 5, 1972, pp. 17-35.

The turbulent mixing length model may be an important source of error, producing discrepancies between theoretical predictions and experimental data. Short of detailed turbulence measurements, the best method for assessing this effect is to compare predicted boundary layer growth with experimental data such as the Fraser Flow "A" test case. First, it should be noted that the Mach number for the Fraser Flow "A" is low, so that 0.1 percent error in static pressure represents a 6.5 percent error in static pressure coefficient (i.e., the error is magnified when results are expressed in terms of a pressure coefficient). Second, it is noted that there is a very close interaction among the following parameters: mixing length, boundary layer thickness or blockage, and static pressure gradient. Thus, increasing the boundary layer thickness decreases the static pressure because of effective blockage. Increasing the pressure gradient increases the boundary layer growth because of the additional work done on the boundary layer. Therefore, a comparison of the theoretically predicted pressure distribution with the experimental data yields an indication of the boundary layer growth and, by inference, the mixing length. Since the predicted pressure coefficient is larger than the experimental data, the predicted boundary layer thickness must be smaller than the measured boundary layer thickness. Hence, it is concluded that the mixing length is too small. It should be noted, however, that the pressure coefficient prediction is very good up to a $Z/L = 0.4$, at which point the boundary layers merge (see Fig. 17). Furthermore, downstream of this station the boundary layer is in a nearly separated condition as shown in Fig. 18. Therefore, it is concluded that modifications of the mixing length may be required for flows with merged boundary layers or nearly separated boundary layers.

The ST9 IR suppression diffuser case with no slots or struts introduces an additional problem in making an accurate flow field prediction. This diffuser, unlike the Fraser Flow "A" diffuser, has significant wall curvature which is known to effect the mixing length (Ref. 20). Thus turbulence can be expected to increase on a concave surface and decrease on a convex surface, modifying the boundary layer growth on these walls and changing the pressure distribution accordingly. Hence it is expected that introducing a better turbulence model which accounts for wall curvature, would produce better predictions for wall static pressure distribution than that shown in Fig. 21. An additional complication which arises in the baseline calculation is the appearance of a separation bubble. Since separation is a very complex

---

(20) Bradshaw, P.: Effects of Streamline Curvature on Turbulent Flow. AGARDograph No. 169, 1973.

phenomenon which is very sensitive to local conditions, predictions of separated regions in turbulent flow can be a strong function of the turbulence model. The turbulence model used in the present effort is an equilibrium model based on measurements of turbulence structure in unseparated flows and, therefore, some significant error may be introduced in applying a turbulence model based upon attached turbulent flow data to separated flow. Inaccuracies of the turbulence model in separated regimes will affect the predictions downstream of flow reattachment since total pressure losses produced by the separation bubble cannot be reversed.

For slot cooled wall cases, test case 3.01, 2.02, and 1.01, the comparisons indicate that the simple mixing length model used in this report may not be adequate. The turbulence model used only accounts for an inner layer mixing length influenced by the wall and an outer layer mixing length influenced by the free stream. The mixing layer developing between the cold slot flow and the hot diffuser flow is not being properly modeled, and this may adversely affect the theoretical predictions. If the turbulence model used is not appropriate in the immediate vicinity of the slot, then any inaccuracies would be compounded for diffusers which contain a succession of cooling slots such as the ST9 IR suppression diffuser. This inadequate modeling of the turbulence structure in the slot mixing region may explain the increased discrepancy between predicted and measured pressure distribution with each slot (see Figs. 22, 24, and 26). Thus, in summary, although the turbulence model appears accurate for flows in the absence of curvature, slot cooling and separation, it may need to be refined for these effects before accurate predictions for the general diffuser flow field can be made.

The numerical method used in this report can be subject to one final important source of error. Since the linearization of the equations of motion implies a certain degree of smoothness in the solution, any local errors introduced in the initial profile may produce significant errors downstream. Usually, as in the diffuser inlet flow, this initial error is dampened and causes little difficulty because the flow variables change slowly. At the slot interface, however, there is a large temperature discontinuity, and since the flow variables (especially temperature) change very rapidly, this initial error may not be dampened. Such an initial error would cause errors in entropy which would lead to inaccurate predictions of the pressure coefficient. Indications that this may be a factor are shown by the significantly larger errors in the mass flow and mass flow weighted average total temperature which are not as well behaved downstream of a slot as they are upstream of the first slot. It is, therefore, concluded that the model used to predict the initial flow and shear for each slot be improved so as to smooth out the discontinuity in the neighborhood of the slot exit plane.

CONCLUSIONS

Based on the experimental data presented in this report, it is concluded that the wall temperatures can be significantly reduced by increasing film coolant rate. For coolant flow rates less than or equal to 10 percent of diffuser flow rates, the film cooling has little effect on pressure distributions or pressure recovery.

An examination of the Fraser Flow "A" test case demonstrates that the basic numerical methods used in this report based on the Schwartz-Christoffel transformation to calculate an orthogonal coordinate system and an implicit linearized finite-difference scheme for solving the equations of motion for turbulent flow is an accurate and reliable method for solving internal flows in axisymmetric ducts of arbitrary wall curvature. Further refinement of the turbulence model in regions of merged boundary layers and nearly separated flow is indicated by the comparisons with data.

For slot cooled walls and highly curved walls, such as the ST9 IR suppression diffuser, further refinement of the turbulence model is also indicated. Specifically, the turbulence model should include the effects of wall curvature and the effects of a mixing layer between the hot and cold flows. Finally, the initial profiles setting up the slot cooled flow need smoothing of the temperature and density discontinuity in order to minimize nonlinear errors in the calculation. It is felt that if the indicated refinements and modifications were made, the resulting computer code would have a unique capability for predicting the development of flow fields in axisymmetric diffusers, including the effects of wall curvature, struts, swirl, and film cooling.

REFERENCES

1. Reneau, L. R., J. P. Johnson, and S. J. Kline: Performance and Design of Straight, Two-Dimensional Diffusers. Transactions of ASME, Journal of Fluid Mechanics, Vol. 89, March 1969, pp. 141-160.

2. Sovran, G., and E. D. Klomp: Optimum Geometries for Rectilinear Diffusers. Fluid Mechanics of Internal Flow. Elsevier Publishing Co., 1967.

3. Fox, R. W., and S. J. Kline: Flow Regime Data and Design Methods for Curved Subsonic Diffusers. Journal of Basic Engineering, Transactions of the ASME, Series D, Vol. 84, No. 3, September 1962, pp. 303-312.

4. Howard, J., H. Henseler, and A. Thornton-Trump: Performance and Flow Regimes for Annular Diffusers. ASME Paper 67, WA/FE-21, 1967.

5. Runstadler, P. W., and R. C. Lean: Straight Channel Diffuser Performance at High Inlet Mach Numbers. Transactions of ASME, Journal of Basic Engineering, Vol. 91, September 1969, pp. 397-422.

6. Dietz, A. E., and J. F. Thompson: Advanced Experimental Infrared Energy Suppression System for the T-53-L-11 or T-53-L-13 Turbine Engine. Hayes International Report No. 1172, 1968.

7. Thayer, E. B.: Evaluation of Curved-Wall Annular Diffusers. ASME Paper 71-WA/FE-35, September 1972.

8. Anderson, O. L.: A Comparison of Theory and Experiment for Incompressible, Turbulent, Swirling Flows in Axisymmetric Ducts. AIAA Paper No. 72-42, 10th Aerospace Sciences Meeting, January 1972.

9. Anderson, O. L.: Numerical Solutions of Incompressible Turbulent Swirling Flows Through Axisymmetric Annular Ducts. United Aircraft Research Laboratories Report No. H213577-1, March 1968.

10. Anderson, O. L.: User's Manual for a Finite-Difference Calculation of Turbulent Swirling Compressible Flow in Axisymmetric Ducts with Struts. United Aircraft Research Laboratories Report L911211-1, Contract No. NAS3-15402, 1972.

11. Kober, H.: Dictionary of Conformal Representations. Dover Publications, Inc., 1957.

12. Gaier, Dieter: Konstruktive Methoden der Konformen Abbildung, Springer Tracts in Natwal Philosophy, Vol. 8, 1963.

13. Keller, H. B., and T. Cebeci: Accurate Numerical Methods for Boundary Layer Flows-II Two-Dimensional Turbulent Flows. AIAA 9th Aerospace Sciences Meeting, New York, January 25-27, 1971, AIAA Paper No. 71-164.

14. Keller, H. B.: A New Difference Scheme for Parabolic Problems. Numerical Solution of Partial Differential Equation-II SYNSPADE 1970 Ed. by Hubbard, B. Academic Pressure, New York.

15. Keller, H. B.: Accurate Difference Methods for Linear Ordinary Differential Systems Subject to Linear Constraints, SIAM J. Namar, Anal. Vol. 6, No. 1, March 1969.

16. Briley, W. R., and H. McDonald: An Implicit Numerical Method for the Multidimensional Compressible Navier-Stokes Equations. United Aircraft Research Laboratories Report M911363-3, November 1973.

17. Varah, J. M.: On the Solution of Block-Tridiagonal Systems Arising from Certain Finite-Difference Equations. Mathematics of Computation, Vol. 26, No. 120, October 1972.

18. Coles, D. E., and E. A. Hirst: Proceedings Computation of Turbulent Boundary Layers - 1968 AFSOR-IFP-Stanford Conference, August 1968.

19. Stratford, B. S.: An Experimental Flow With Zero Skin Friction Throughout Its Pressure Rise. Journal of Fluid Mechanics, Vol. 5, 1972, pp. 17-35.

20. Bradshaw, P.: Effects of Streamline Curvature on Turbulent Flow. AGARDograph No. 169, 1973.

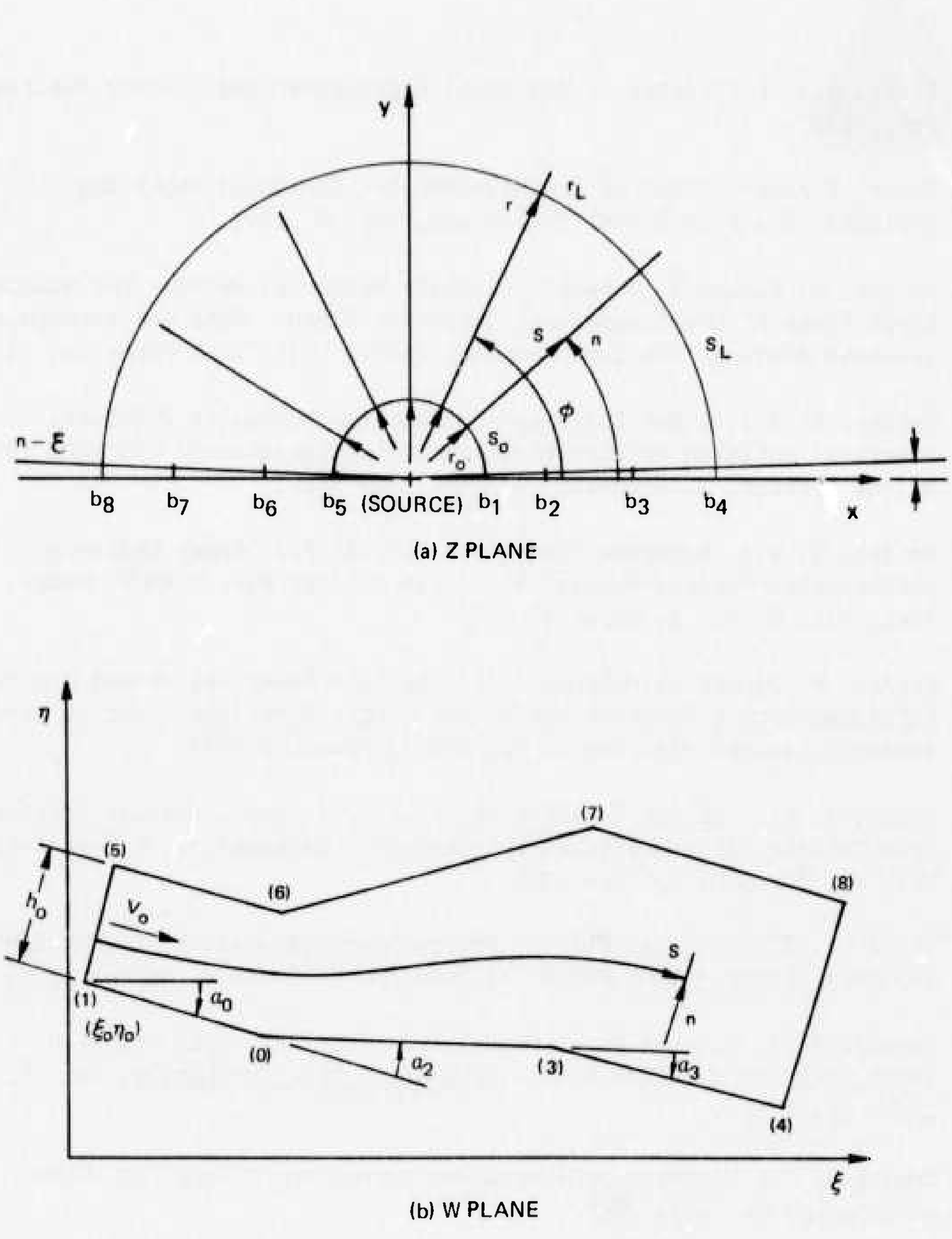

FIG. 1 CONFORMAL MAPPING OF DUCT.

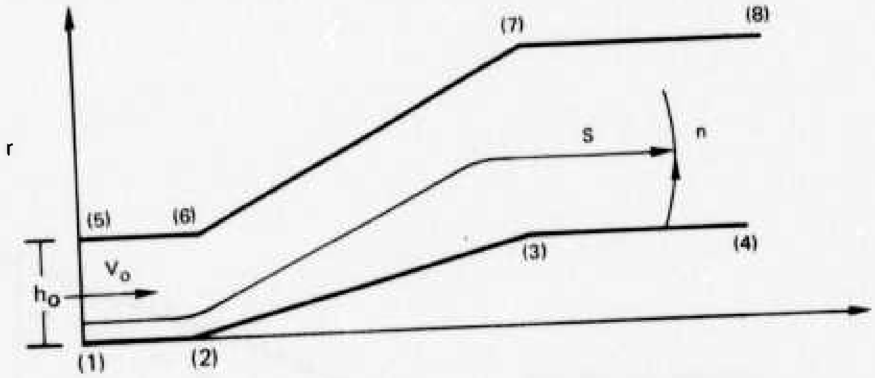

(a) r (n,S) , z (n,s) PLANE

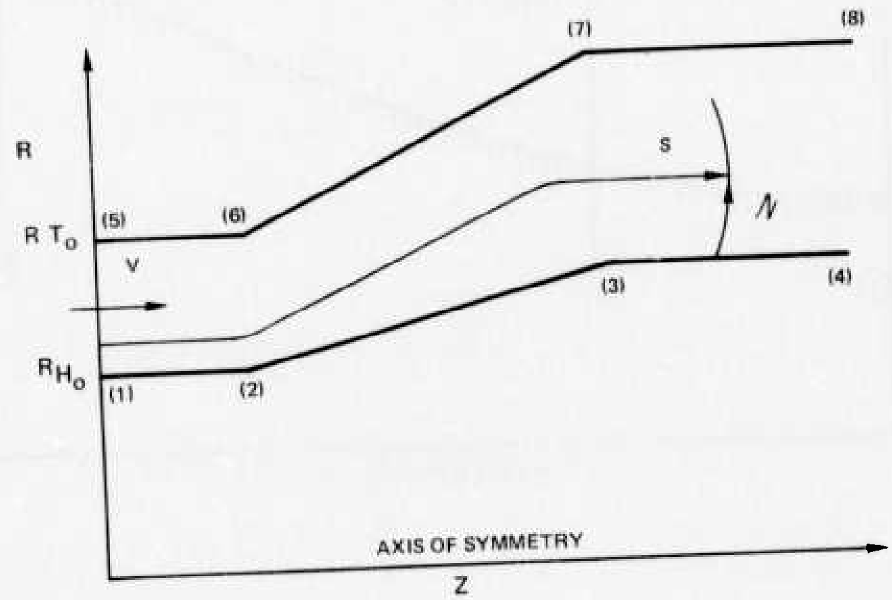

(b) R ($\mathcal{N}$,S) , Z ($\mathcal{N}$,S) PLANE

FIG. 2. ROTATING AND SCALING DUCT.

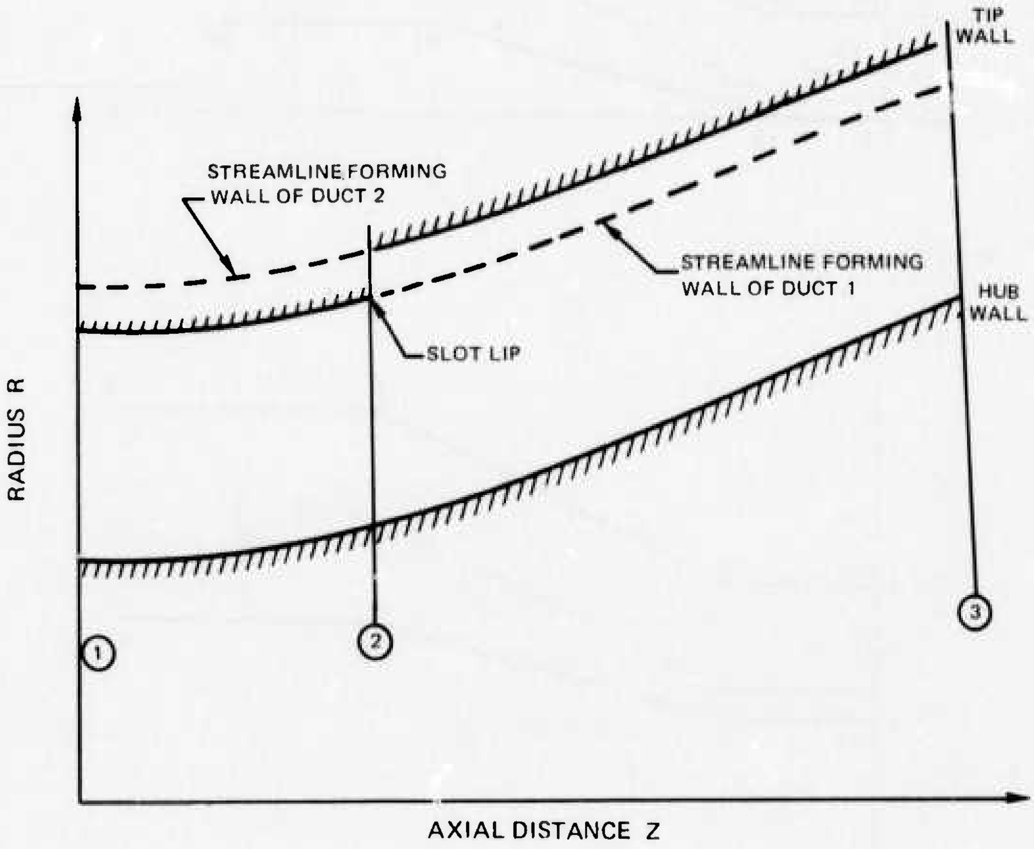

FIG. 3. CONSTRUCTION OF SLOT IN DUCT.

b

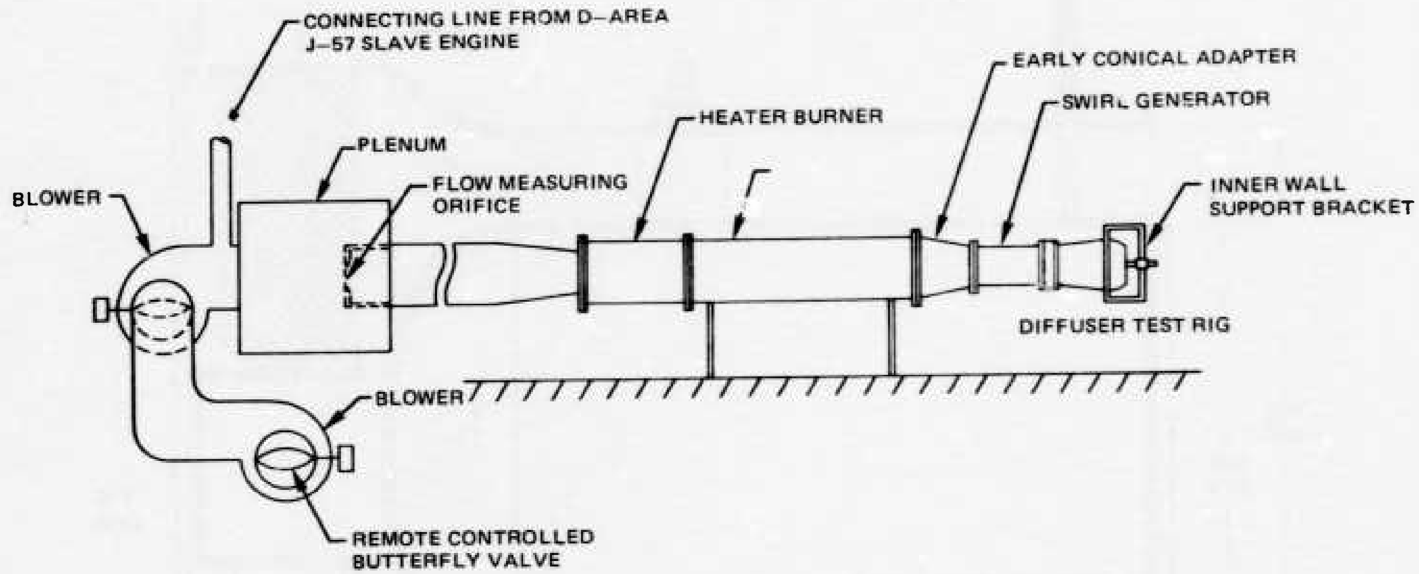

FIG. 4. SCHEMATIC OF D–32 STAND.

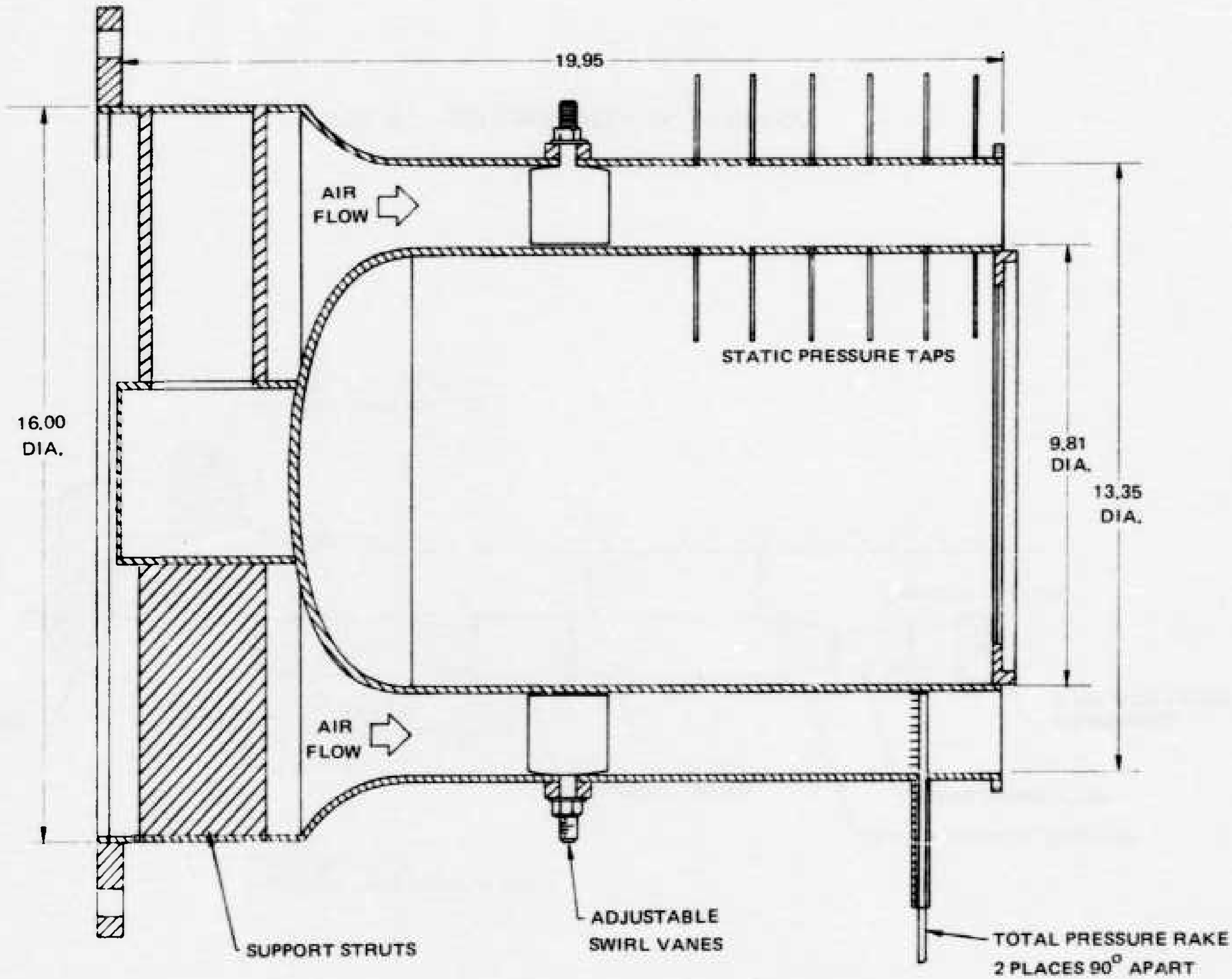

FIG. 5. SWIRL GENERATION SECTION.

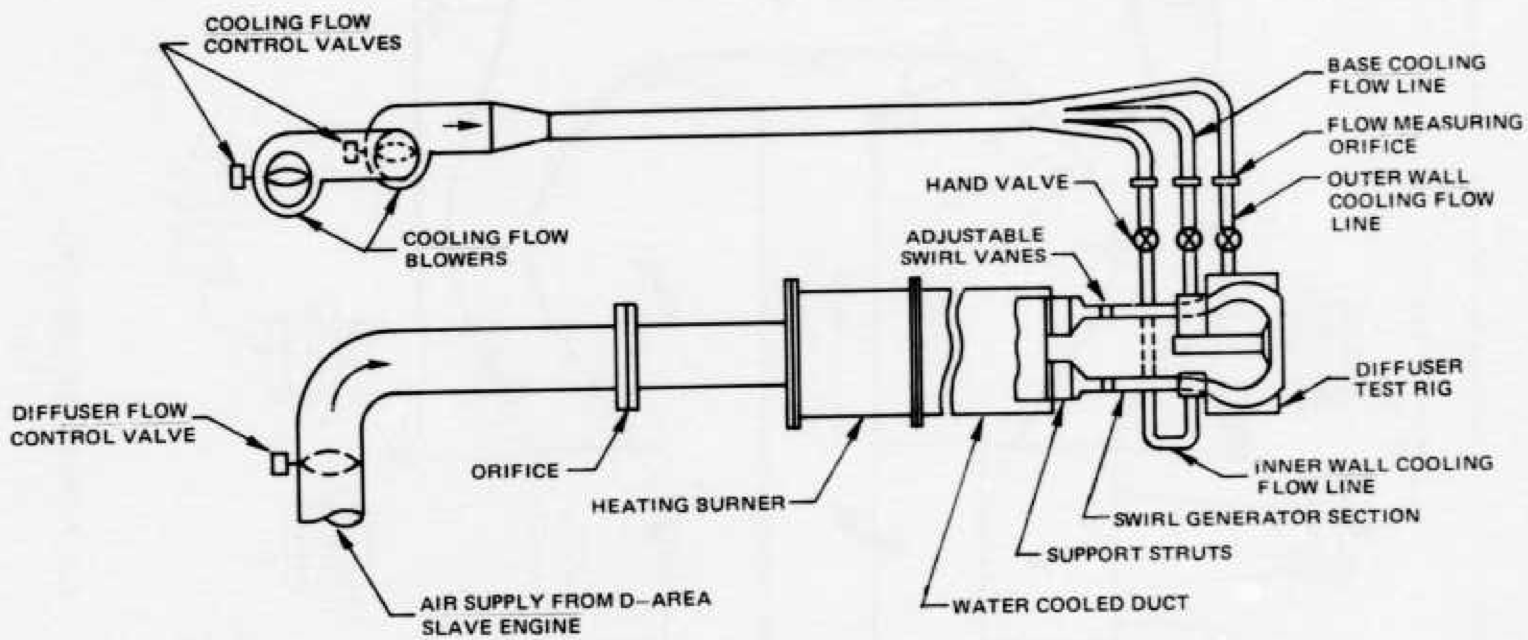

FIG. 6. INSTALLATION OF SLOT COOLING SYSTEM.

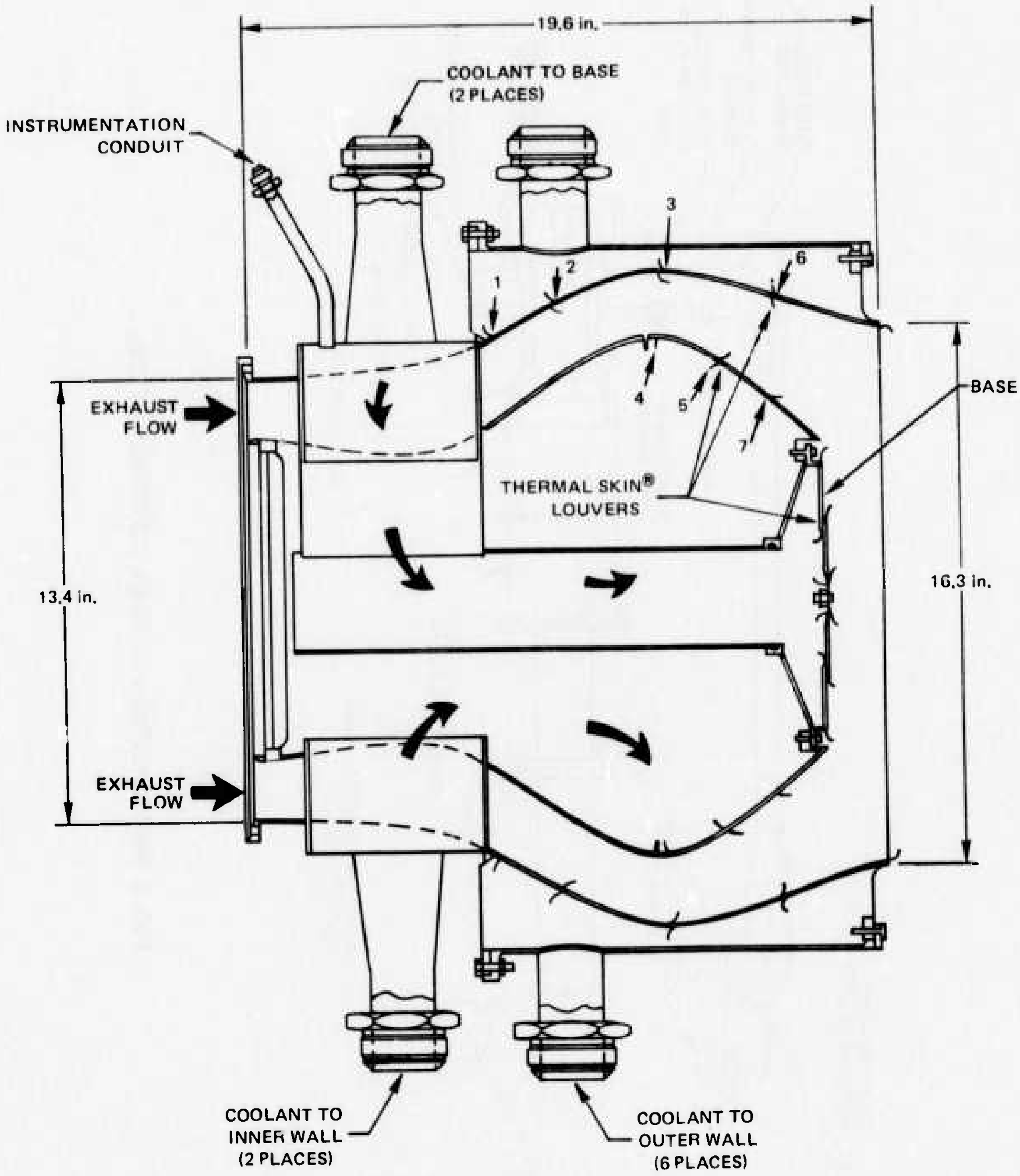

FIG. 7. DIFFUSER TEST RIG.

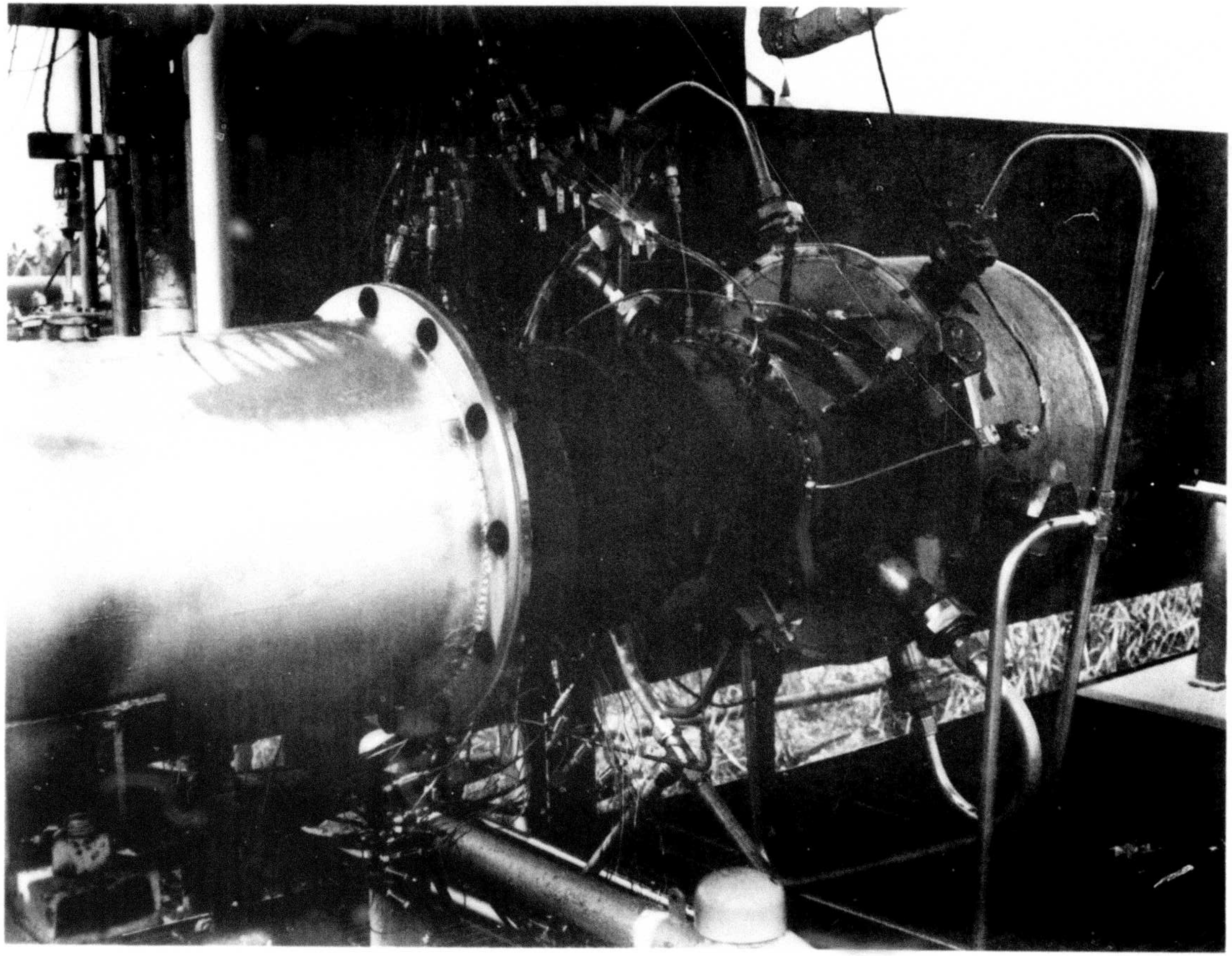

FIG. 8. SIDE VIEW OF TEST RIG.

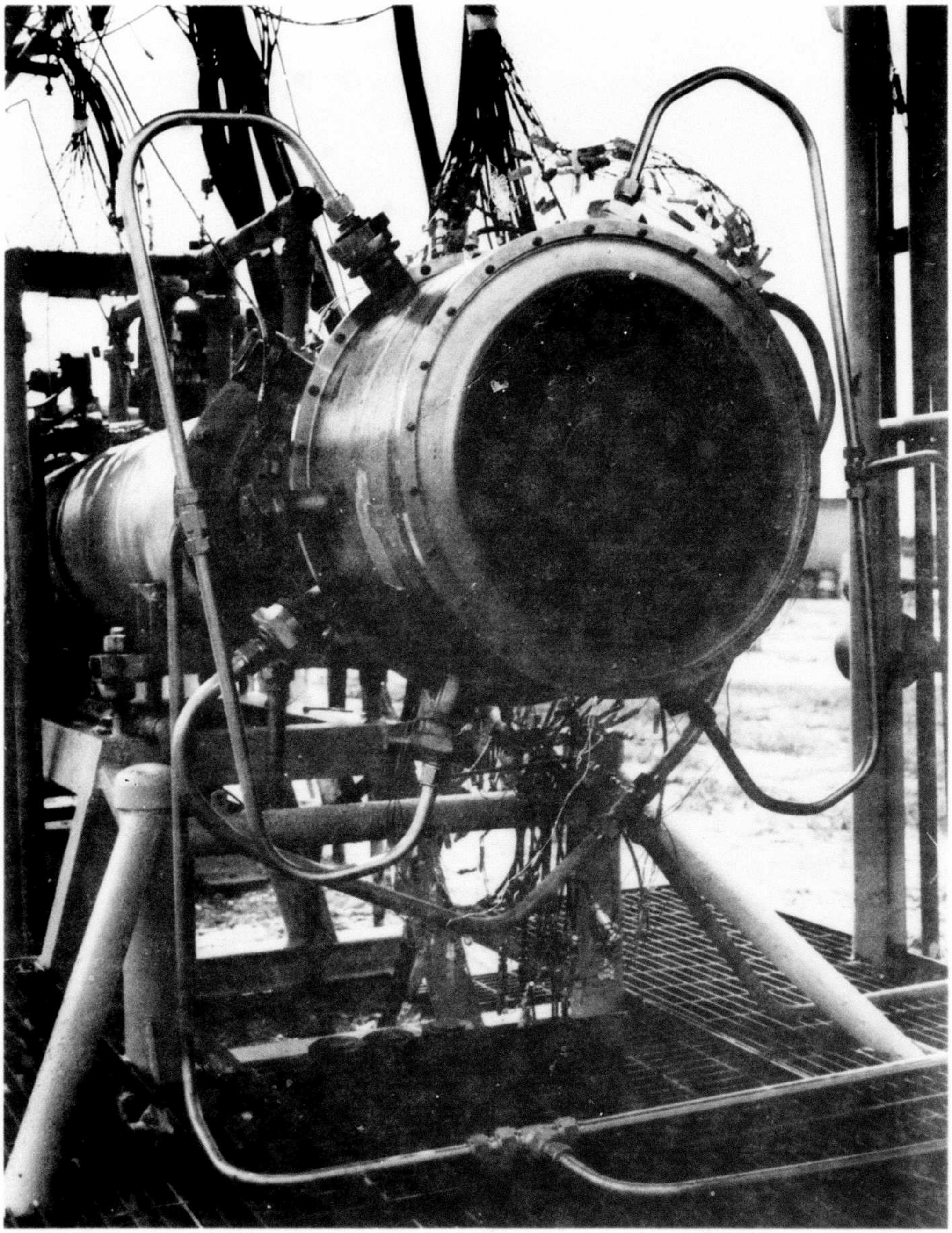

FIG. 9. AFT VIEW OF TEST RIG.

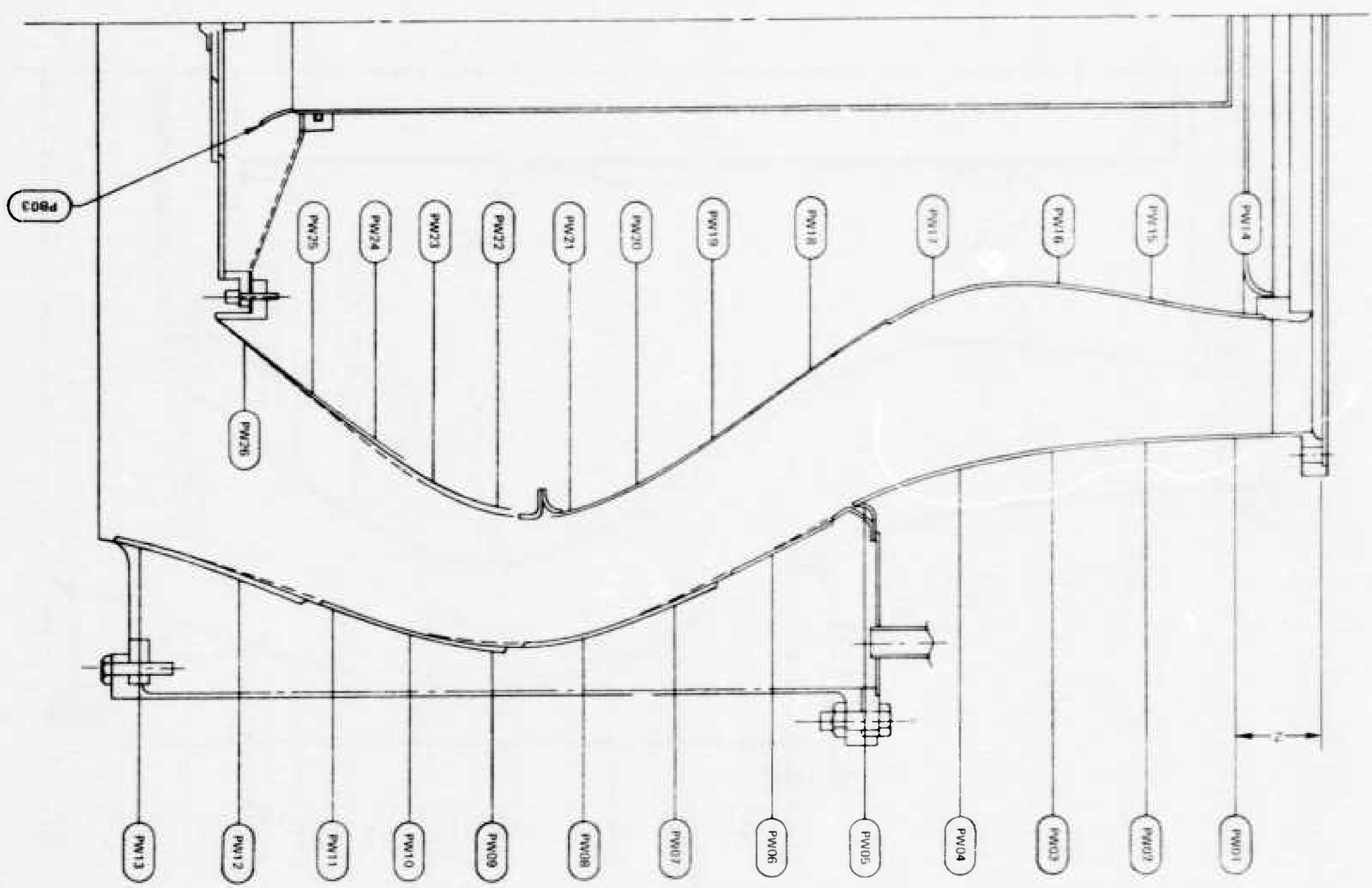

FIG. 10. LOCATION OF WALL STATIC PRESSURE TAPS.

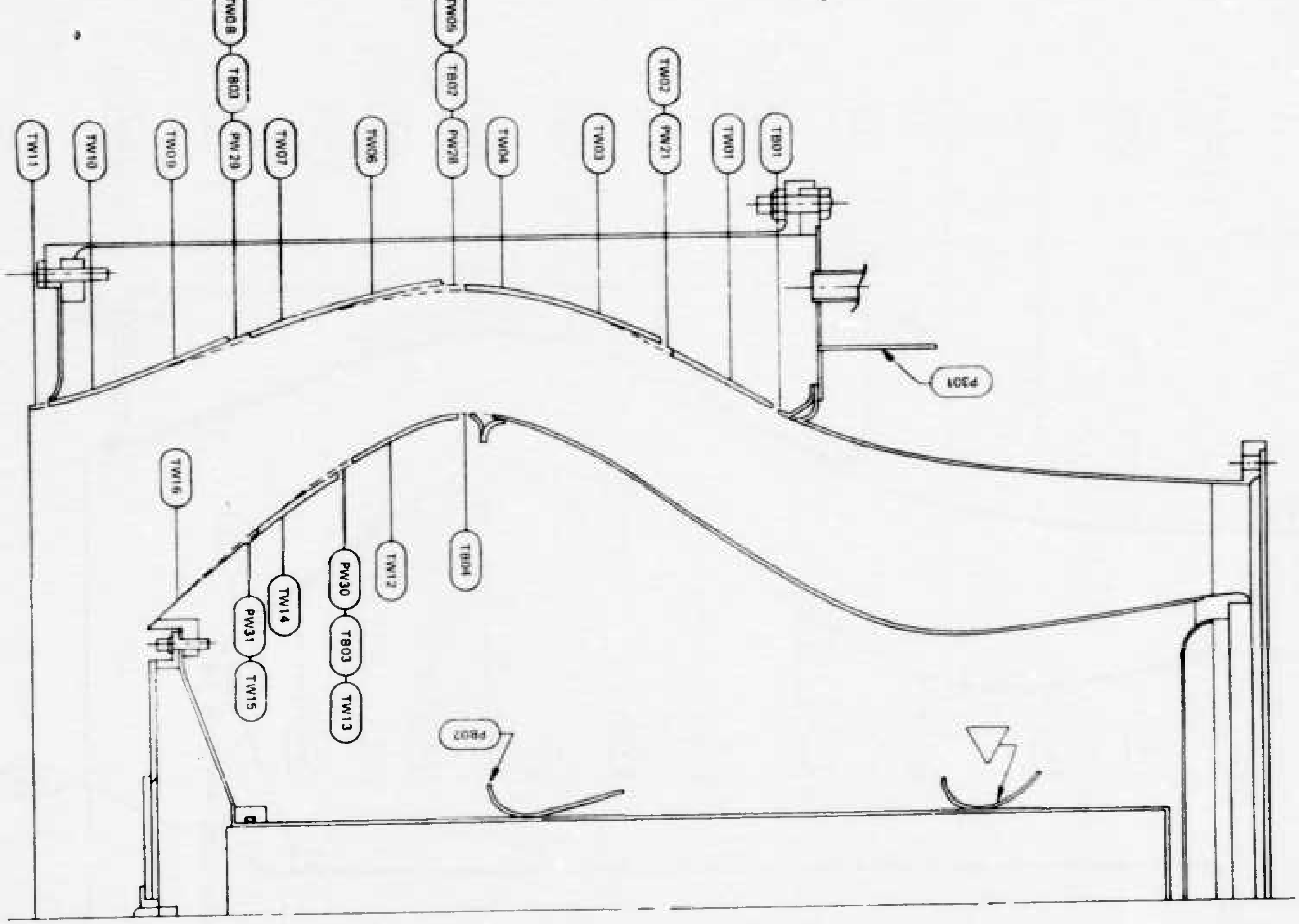

FIG. 11. LOCATION OF WALL THERMOCOUPLES.

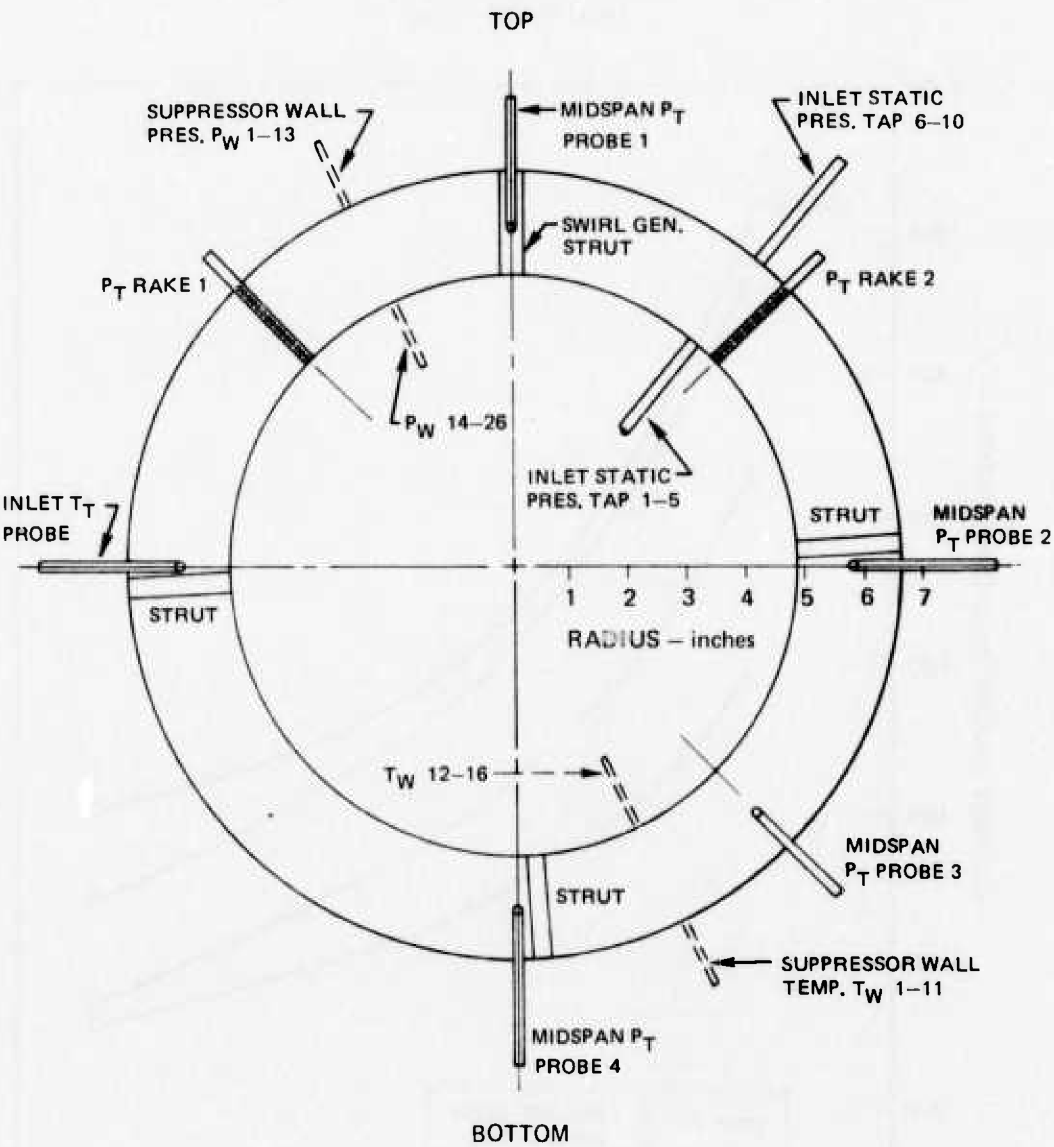

FIG. 12. INLET PLANE INSTRUMENTATION.

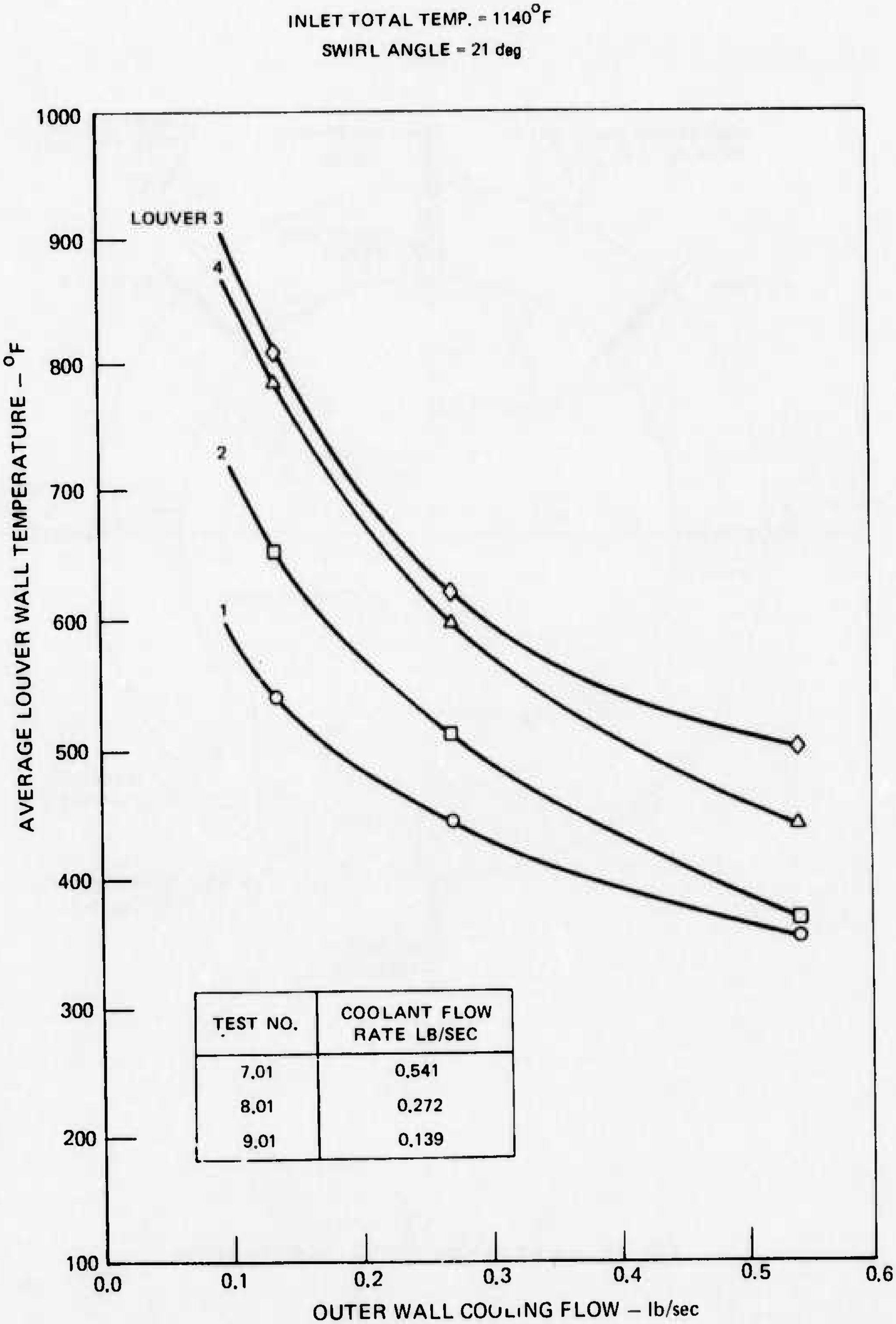

FIG. 13. OUTER WALL AVERAGE SURFACE TEMPERATURE FOR ST9 IR SUPPRESION DIFFUSER.

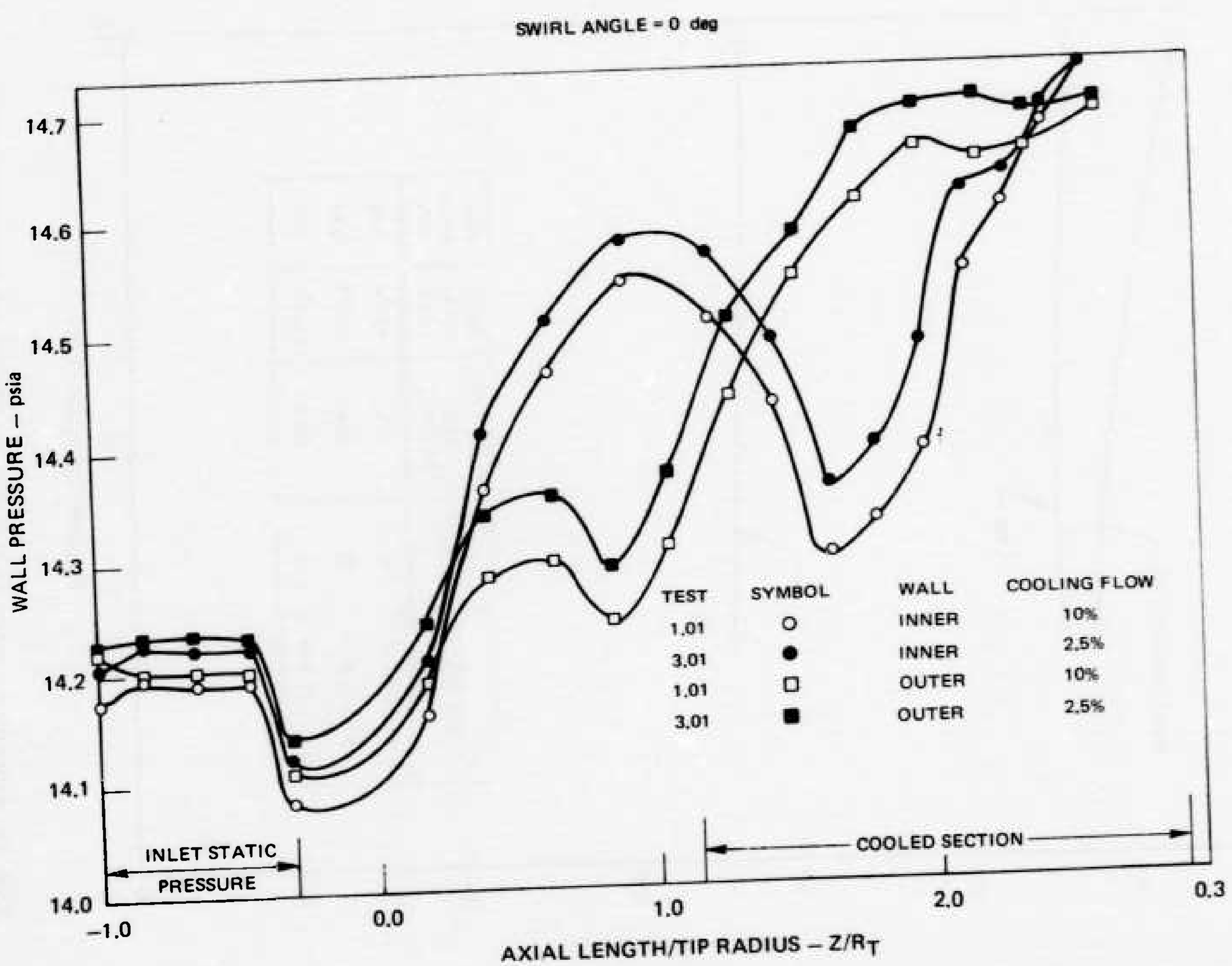

FIG. 14. EFFECT OF COOLANT FLOW ON WALL PRESSURES FOR ST9 IR SUPPRESSION DIFFUSER.

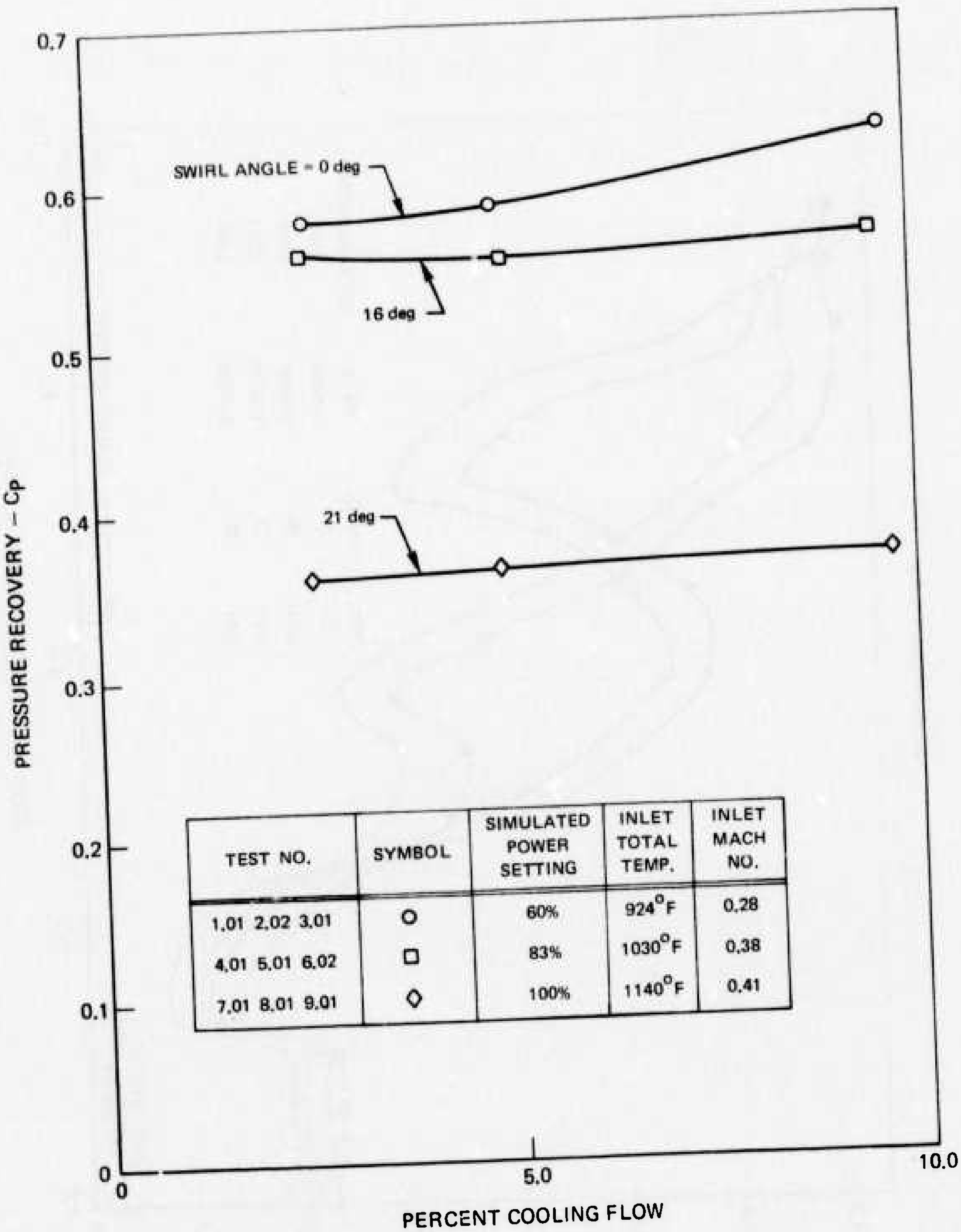

TEST NO.	SYMBOL	SIMULATED POWER SETTING	INLET TOTAL TEMP.	INLET MACH NO.
1.01 2.02 3.01	○	60%	924°F	0.28
4.01 5.01 6.02	□	83%	1030°F	0.38
7.01 8.01 9.01	◇	100%	1140°F	0.41

FIG. 15. EFFECT OF COOLANT FLOW ON PRESSURE RECOVERY FOR ST9 IR SUPPRESSION DIFFUSER.

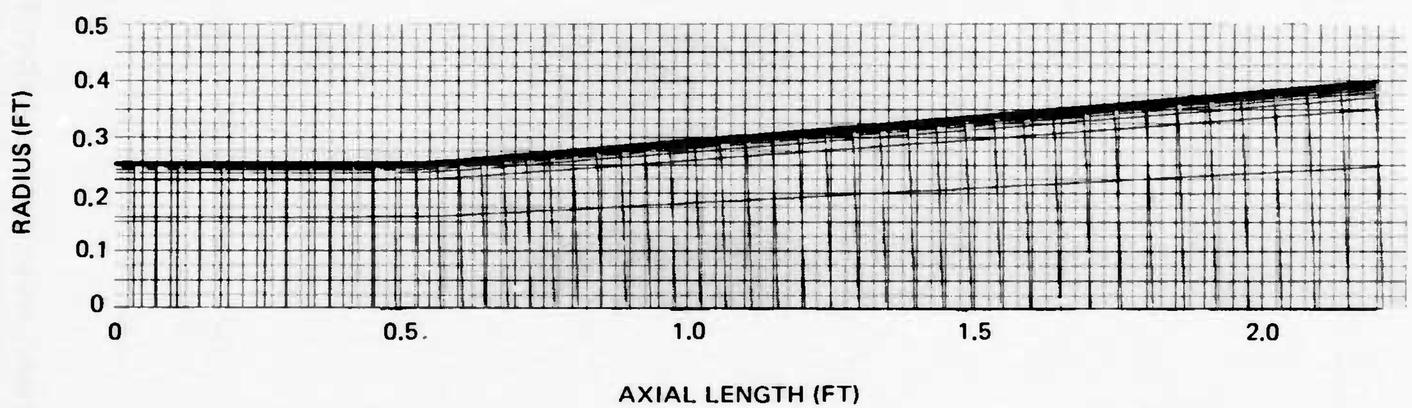

FIG. 16. STREAMLINE COORDINATES FOR FRASER FLOW "A" DIFFUSER.

FRASER FLOW "A" CONICAL DIFFUSER

AFOSR STANFORD CONFERENCE 1968

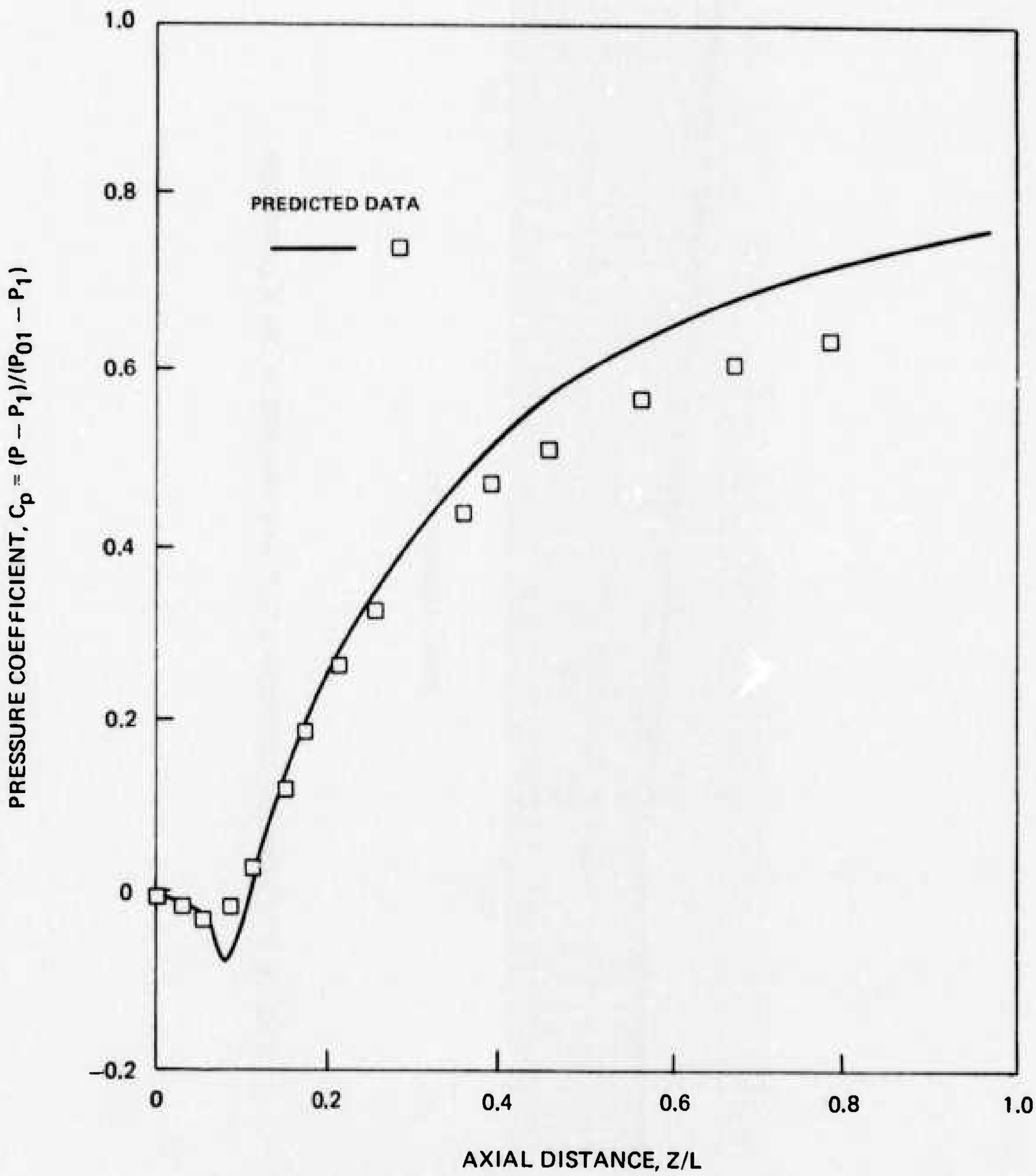

FIG. 17. COMPARISON OF EXPERIMENTAL AND PREDICTED WALL STATIC PRESSURE DISTRIBUTION FOR FRASER FLOW "A" DIFFUSER.

FRASER FLOW "A" CONICAL DIFFUSER

AFOSR STANFORD CONFERENCE 1968

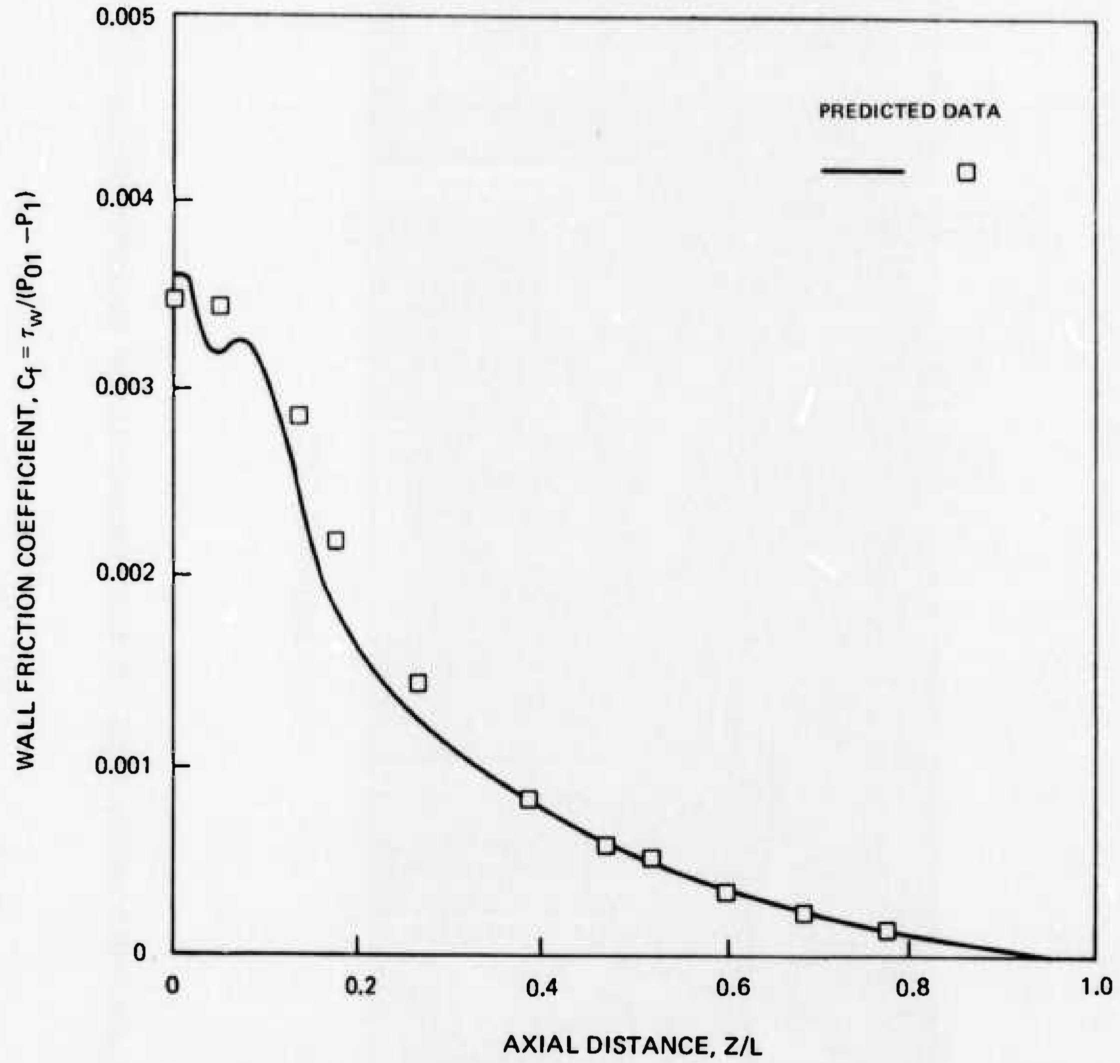

FIG. 18. COMPARISON OF EXPERIMENTAL AND PREDICTED WALL FRICTION COEFFICIENT DISTRIBUTION FOR FRASER FLOW "A" DIFFUSER.

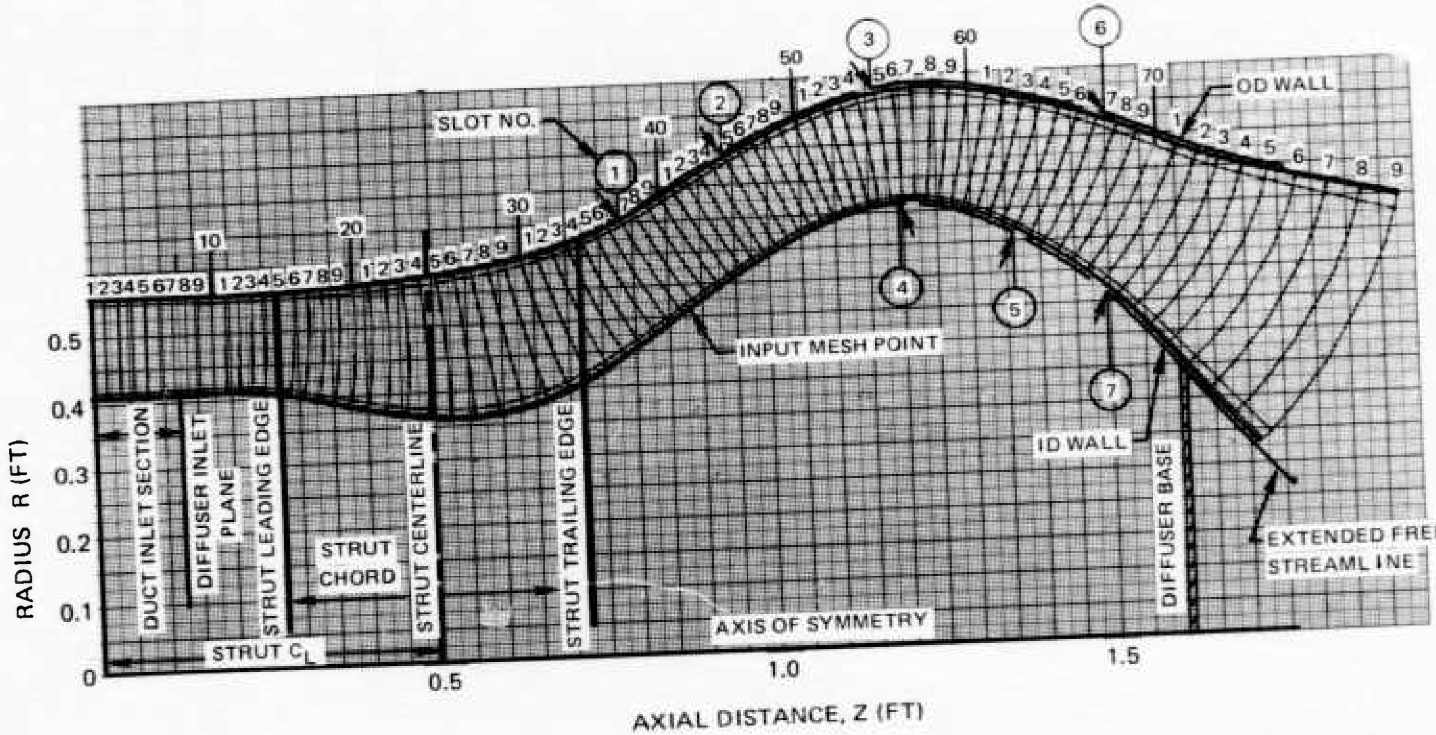

FIG. 19. STREAMLINE COORDINATES FOR ST9 DEMONSTRATOR IR SUPPRESSION DIFFUSER.

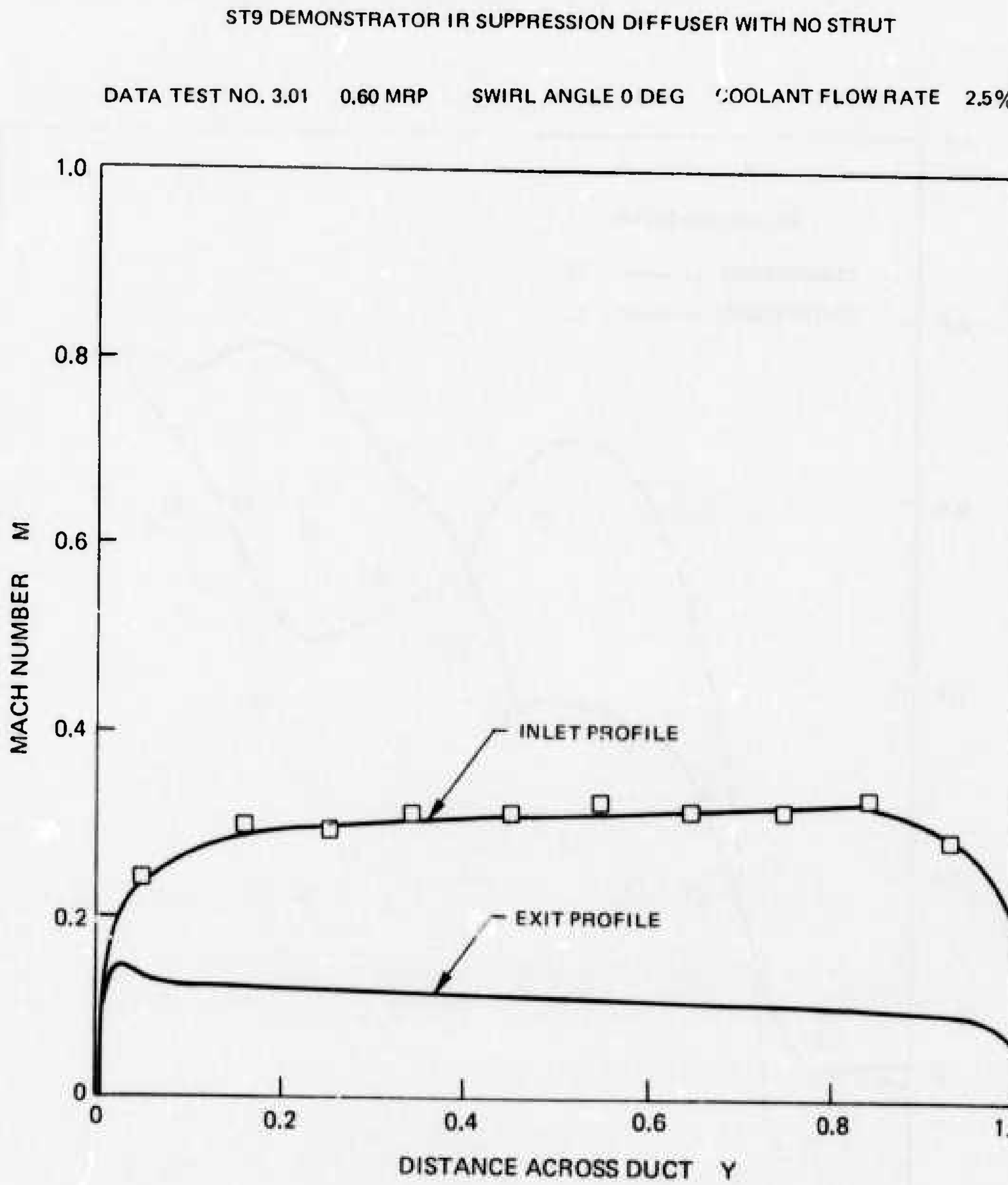

FIG. 20. INLET EXIT MACH NUMBER DISTRIBUTION.

ST9 DEMONSTRATOR IR DIFFUSER MODEL

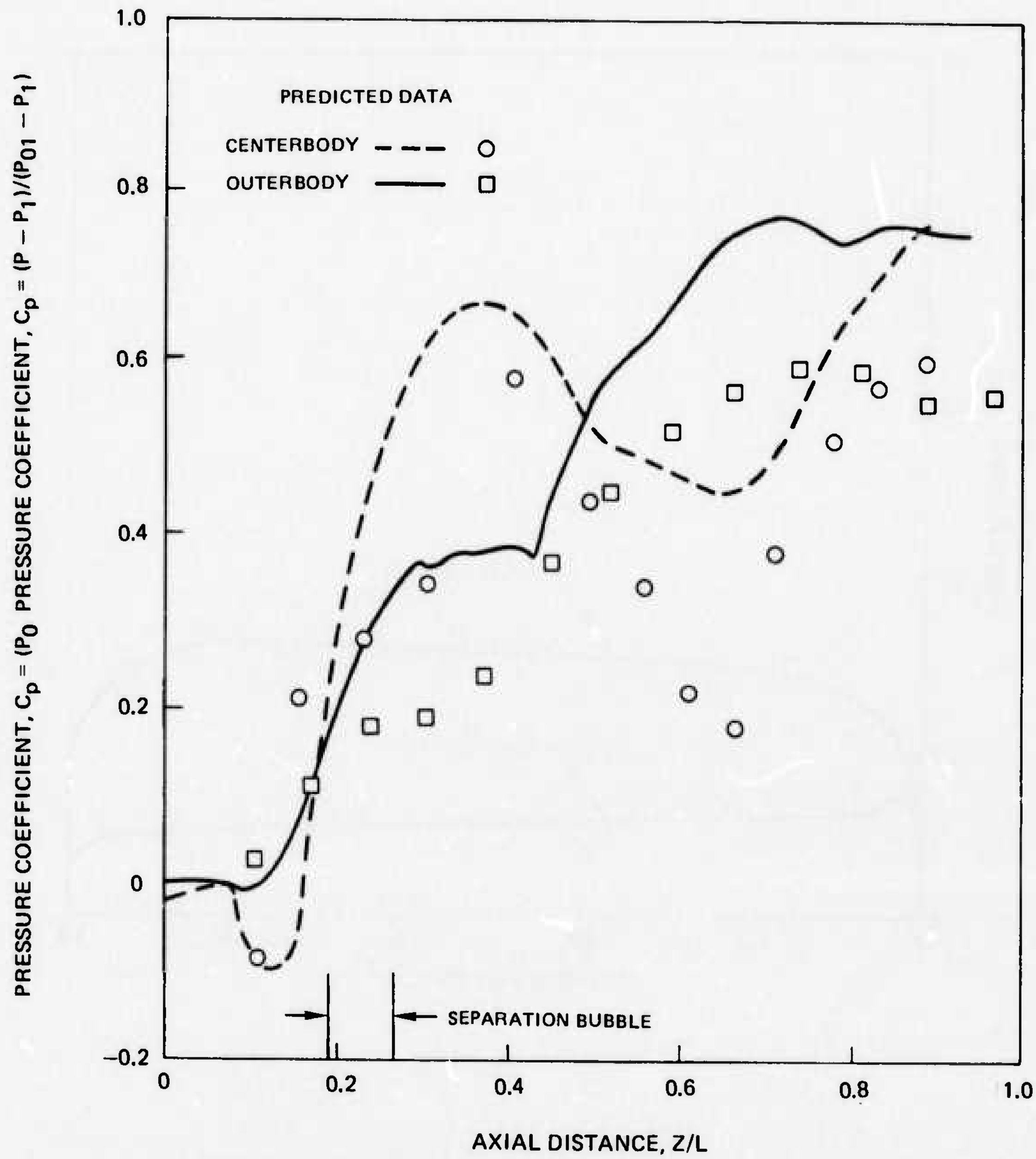

FIG. 21. COMPARISON OF EXPERIMENTAL AND PREDICTED WALL STATIC PRESSURE COEFFICIENTS FOR ST9 IR SUPPRESSOR DIFFUSER WITH NO FILM COOLING AND NO STRUTS.

ST9 DEMONSTRATOR IR SUPPRESSION DIFFUSER

TEST NO. 3.01   0.60 MRP   SWIRL ANGLE 0 DEG   COOLANT FLOW RATE 2.5 %

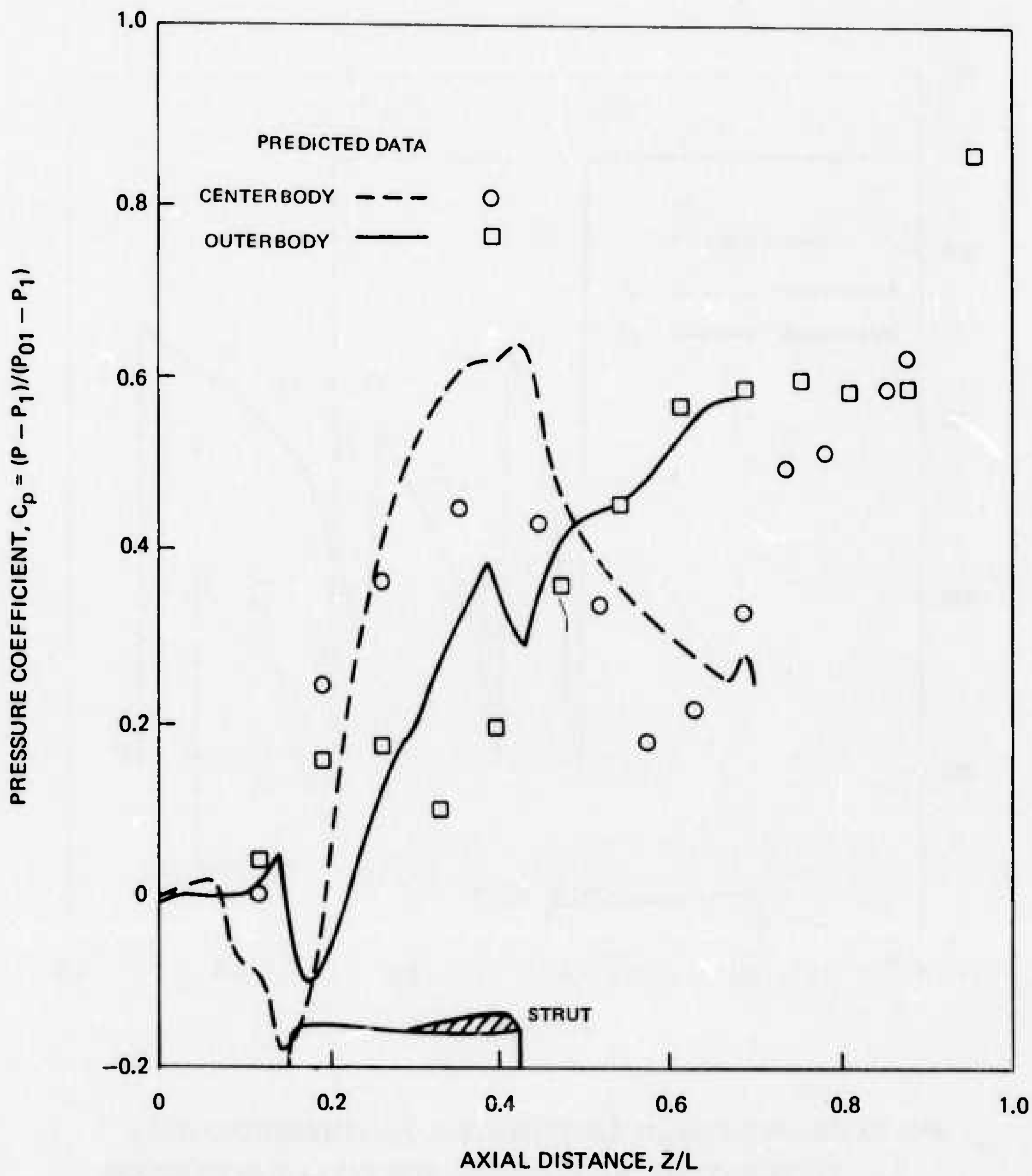

FIG. 22. COMPARISON OF EXPERIMENTAL AND PREDICTED WALL STATIC PRESSURE DISTRIBUTION FOR ST9 IR SUPPRESSION DIFFUSER WITH 2.5% INJECTED COOLING AIR.

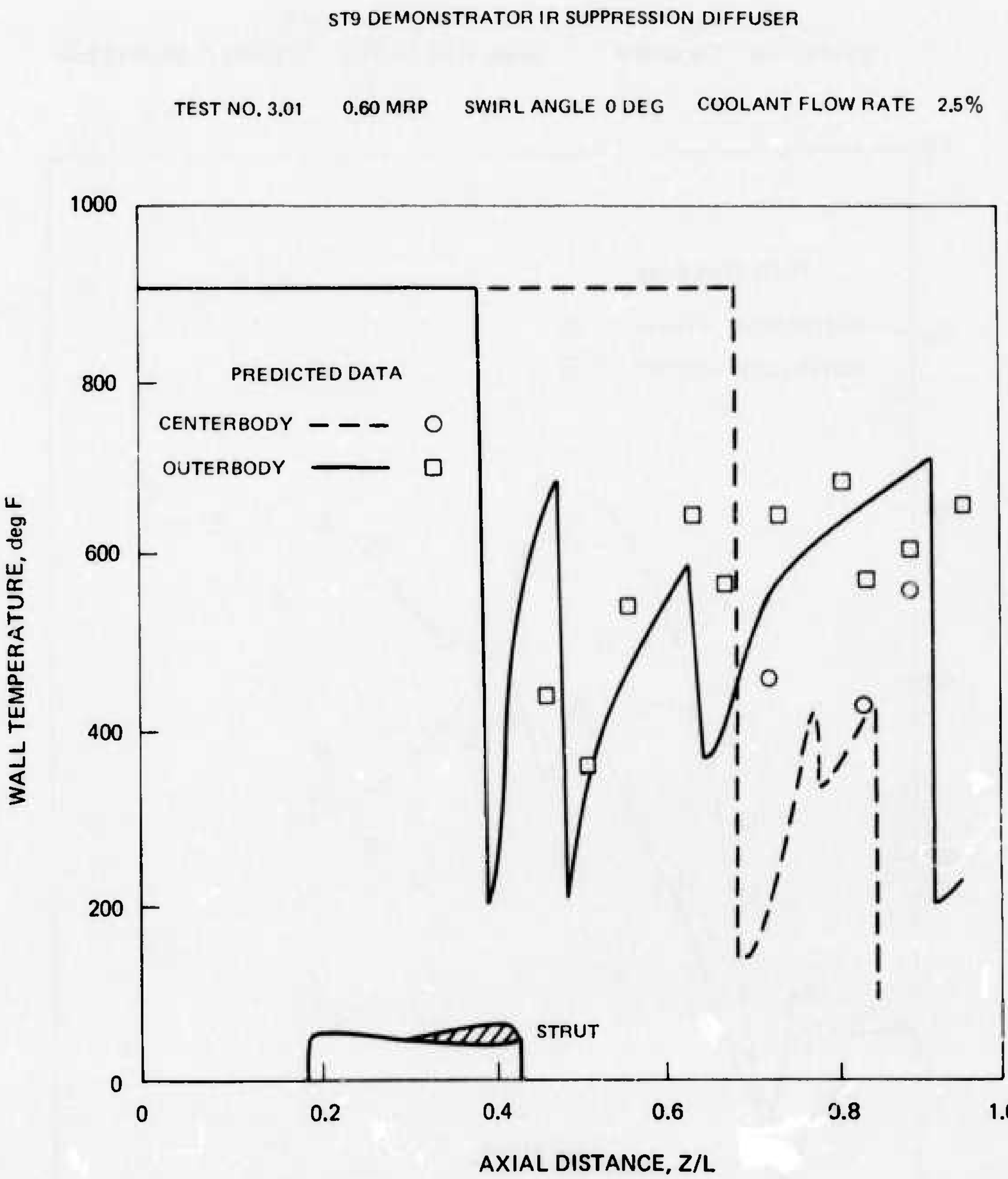

FIG. 23. COMPARISON OF EXPERIMENTAL AND PREDICTED WALL TEMPERATURE DISTRIBUTION FOR ST9 IR SUPPRESSSION DIFFUSER WITH 2.5% INJECTED COOLING AIR.

ST9 DEMONSTRATOR IR SUPPRESSION DIFFUSER

TEST NO. 2.02 0.60 MRP SWIRL ANGLE 0 DEG COOLANT FLOW RATE 5.0%

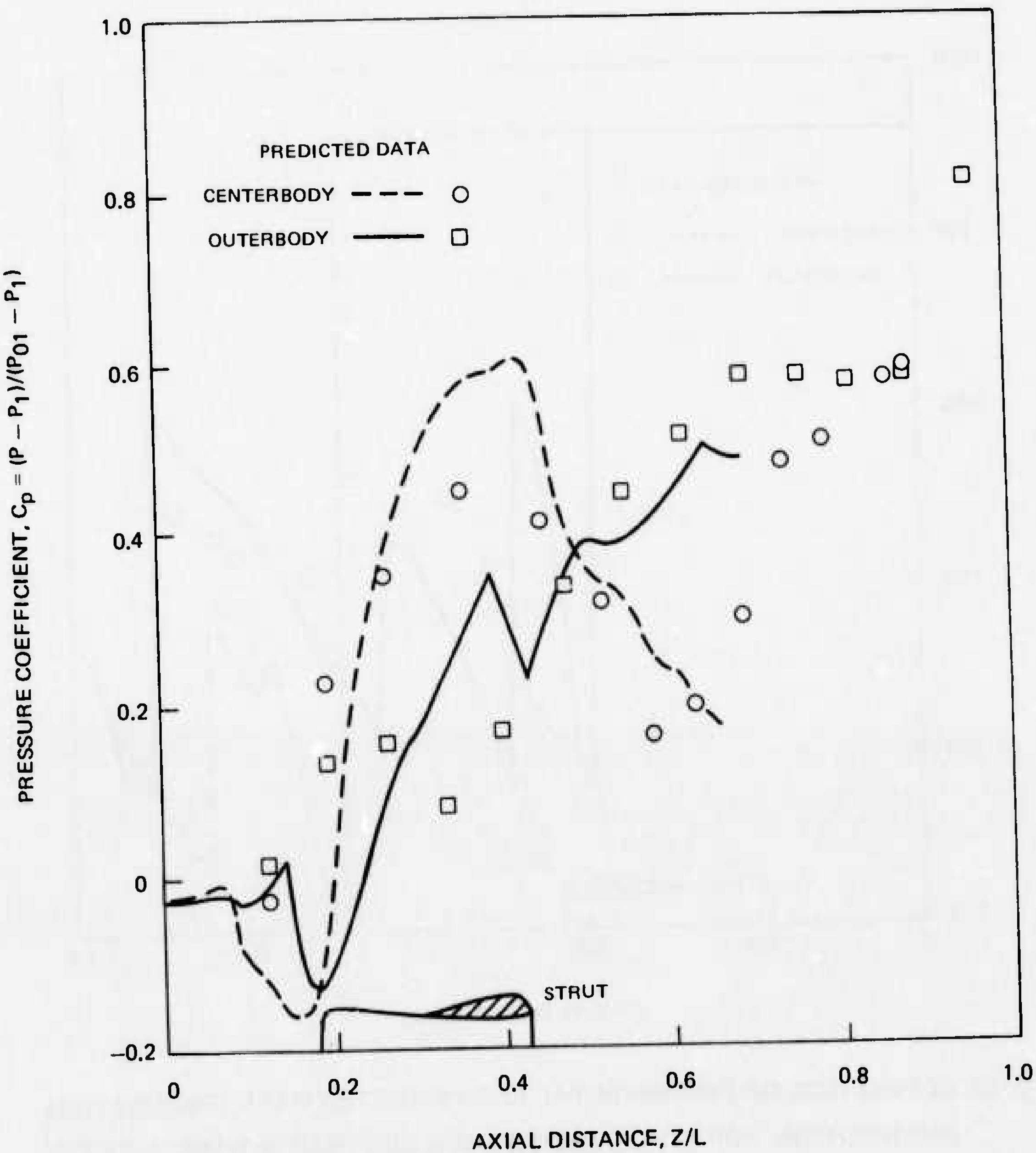

FIG. 24. COMPARISON OF EXPERIMENTAL AND PREDICTED WALL STATIC PRESSURE DISTRIBUTION FOR ST9 IR SUPPRESSION DIFFUSER WITH 5.0% INJECTED COOLING AIR.

ST9 DEMONSTRATOR IR SUPPRESSION DIFFUSER

TEST NO. 2 02 0.60 MRP SWIRL ANGLE 0 DEG COOLANT FLOW RATE 5%

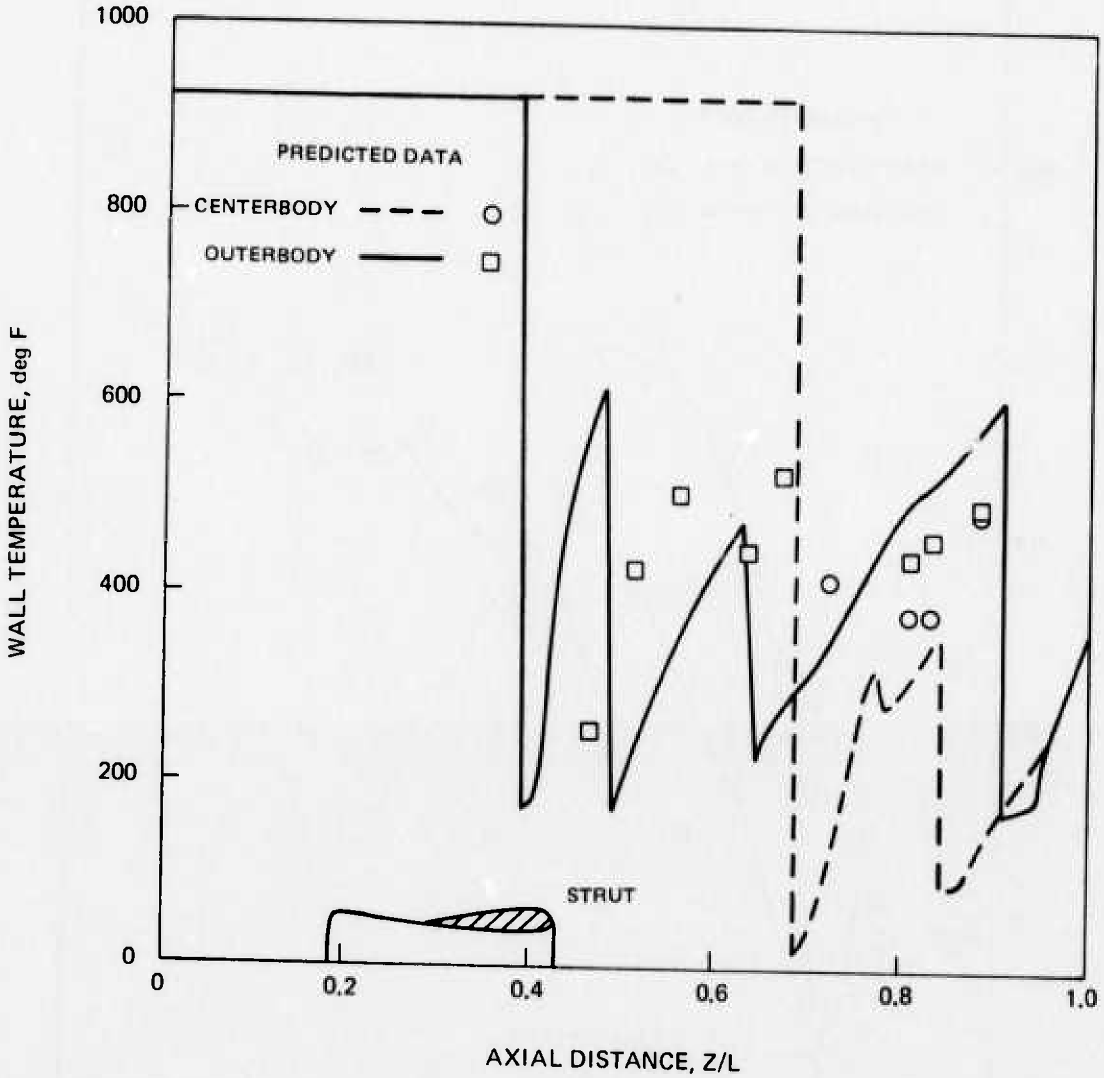

FIG. 25. COMPARISON OF EXPERIMENTAL AND PREDICTED WALL TEMPERATURE DISTRIBUTION FOR ST9 IR SUPPRESSION DIFFUSER WITH 5% INJECTED COOLING AIR.

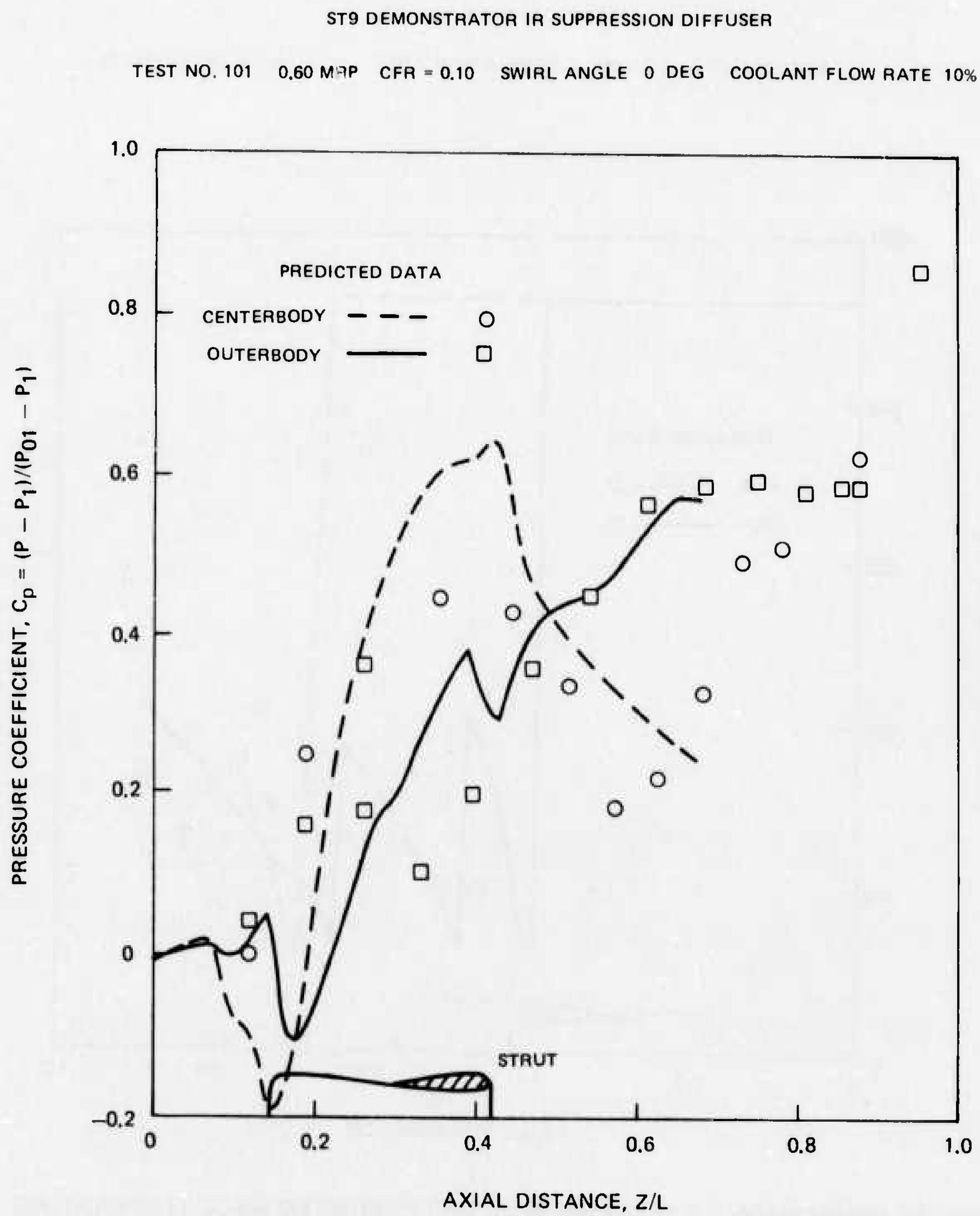

FIG. 26. COMPARISON OF EXPERIMENTAL AND PREDICTED WALL STATIC PRESSURE DISTRIBUTION IR SUPPRESSION DIFFUSER WITH 10% INJECTED COOLING AIR.

ST9 DEMONSTRATOR IR SUPPRESSION DIFFUSER

TEST NO. 1.01 0.60 MRP SWIRL ANGLE 0 DEG COOLANT FLOW RATE 10%

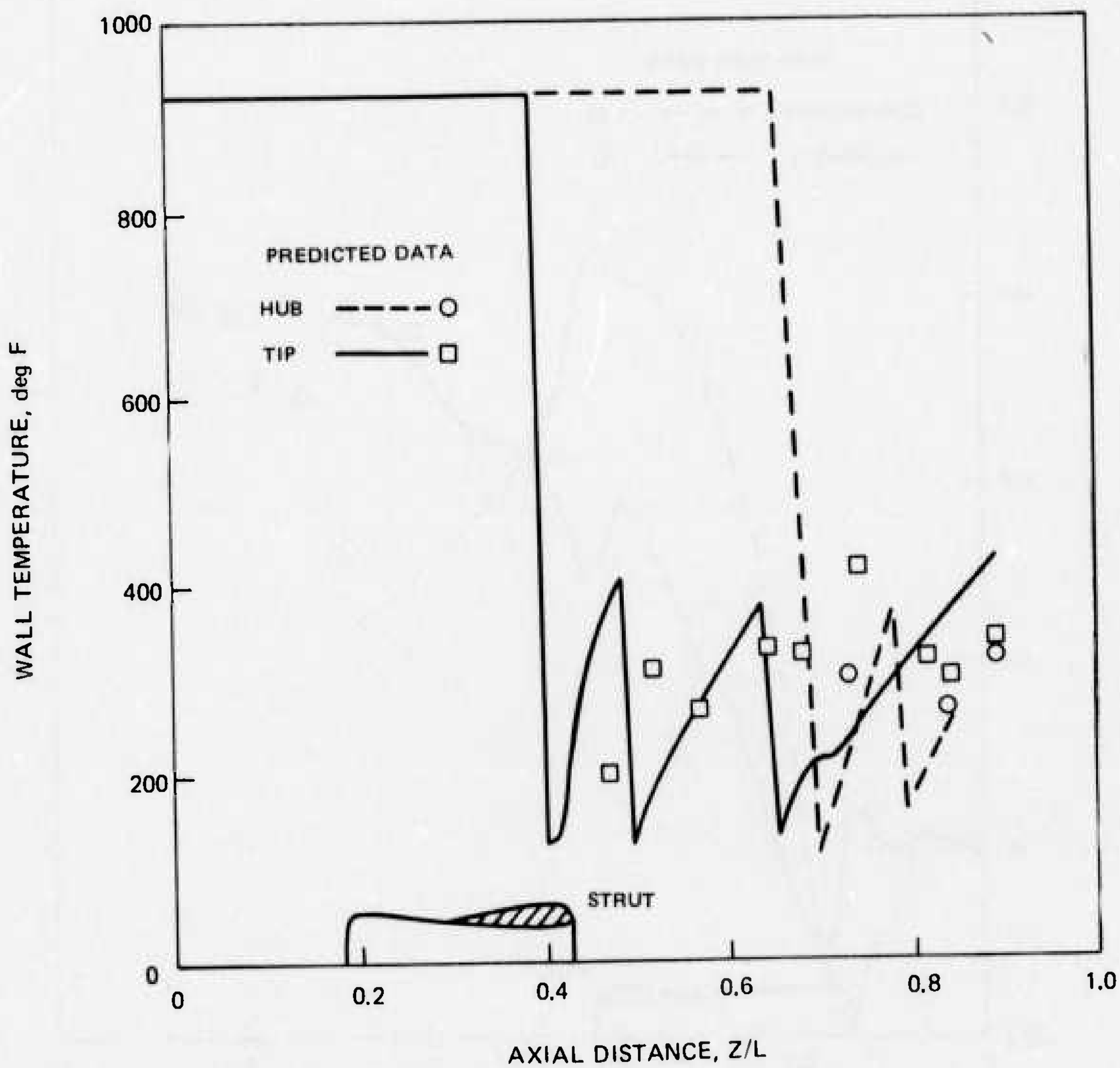

FIG. 27. COMPARISON OF EXPERIMENTAL AND PREDICTED WALL TEMPERATURE DISTRIBUTION FOR ST9 IR SUPPRESSION DIFFUSER WITH 10% INJECTED COOLING AIR.

TABLE 1. LOCATION OF PRESSURE AND TEMPERATURE INSTRUMENTATION

TABLE #1		
N CALBR	TYPE	I . INCHES
PW01	WALL PRESSURE	1.250
02		2.750
03		4.250
04		5.750
05		7.150
06		8.750
07		10.250
08		11.750
09		13.250
10		14.650
11		15.900
12		14.700
13		19 000
14		1.250
15		2.750
16		4.250
17		6.250
18		8.200
19		9.700
20		10.900
21		12.000
22		13.200
23		14.250
24		15.250
25		16.350
26		17.350
27		9.500
28		12.906
29		16.312
30		14.740
31		16.232
PB01	PLENUM PROCESS AS SHOWN	
02		
03		
TW01	WALL TEMPERATURE	2.852
02		9.500
03		10.548
04		12.120
05		12.906
06		14.216
07		15.7881
08		16.312
09		17.360
10		18.669
11		19.475
12		13.954
13		14.740
14		15.788
15		16.232
16		17.360
T801	BULK TEMPERATURE	7.712
02		12.706
03		16.312
04		12.574
05		14.740
06		AS SHOWN

TABLE 2. TEST LOG

DATE	TEST NO.	SUPPRESSOR INLET CONDITIONS: SIMULATED POWER SETTING % MRP	SWIRL ANGLE DEG	FLOW RATE LB/SEC	TOTAL TEMP °F	MACH NO	COOLANT FLOWS: PERCENT OF INLET FLOW	TOTAL FLOWRATE LB/SEC	OUTER WALL FLOWRATE LB/SEC	INNER WALL FLOWRATE LB/SEC	C_P	REMARKS
6/25/73	1.01	60	0	6.367	924	0.287	9.76	0.621	0.405	0.216	0.633	
6/25/73	2.01	60	0	6.095	925	0.274	5.21	0.317	0.217	0.100	0.611	INVALID DATA
6/25/73	2.02	60	0	6.377	924	0.287	4.93	0.314	0.217	0.097	0.588	REPEAT OF TEST 2.01
6/25/73	3.01	60	0	6.377	910	0.285	2.64	0.168	0.100	0.069	0.580	
6/25/73	4.01	83	16	7.887	1030	0.378	9.58	0.756	0.521	0.235	0.566	
6/25/73	5.01	83	16	7.850	1035	0.376	5.04	0.395	0.271	0.124	0.556	
6/25/73	6.01	83	16	7.852	1030	0.375	3.23	0.253	0.121	0.132	0.563	INVALID DATA[2]
6/25/73	6.02	83	16	7.882	1035	0.378	2.62	0.206	0.124	0.082	0.559	REPEAT OF TEST 6.01
6/26/73	7.01	100	21	8.470	1140	0.417	9.74	0.825	0.541	0.284	0.369	
6/26/73	8.01	100	21	8.377	1140	0.411	4.93	0.413	0.272	0.141	0.364	
6/26/73	9.01	100	21	8.379	1140	0.411	2.66	0.223	0.139	0.084	0.358	

1. INLET FLOW DECREASED DURING TEST
2. INNER WALL FLOW INCREASED DURING TEST

TABLE 3. TEST DATA

HOT FLOW TEST WITH 0.10 COOLING FLOW RATE
MRP = 60 SWIRL ANGLE = 0.0 NO IR DATA

RUN NO	DATA PT	P AMB. IN. HG	P AMB PSIA
1.0000	0.0100	29.9000	14.6868

WEIGHT FLOW RATE,PRIMARY

P1	DEL P	TEMP (R)	FLOW RATE
18.7147	4.8137	680.0001	6.2875

FUEL TO AIR RATIO = 0.0126 FUEL FLOW RATE = 0.0797 LBM/SEC

TOTAL PRIMARY FLOW RATE = 6.3672 LBM/SEC

WEIGHT FLOW RATE,COOLING AIR

OUTER WALL

P1	DEL P	TEMP (R)	FLOW RATE
67.1868	30.5000	543.0001	0.4049

INNER WALL

P1	DEL P	TEMP (R)	FLOW RATE
35.5868	16.5000	543.0001	0.2159

BASE

P1	DEL P	TEMP (R)	FLOW RATE
14.6868	0.0000	460.0000	0.0000

TOTAL TEMP. (AFT OF BURNER CAN) = 1445.000 DEG R INLET TOTAL TEMP. = 1384.000 DEG R

PLENUM (MANIFOLD) PRESSURES PSIA

OUTER WALL	INNER WALL	BASE
15.3950	18.4143	14.5697

INLET PROBE DATA (BASED ON INLET DATA)

PTB	PSI	PSBAR	A R	(PT1-PA)/Q1	DENSITY	CAL FLO RATE	UFLO	QA1	Q1
14.95391	14.16515	14.23713	2.49000	0.39775	0.00087	6.23049	0.81875	0.74677	0.80095

SPAN	VEL	PT	PS	Y
0.00000	0.00000	14.16515	14.16515	4.90600
0.04522	0.72707	14.71216	14.16515	4.98600
0.04522	0.84273	14.90004	14.16515	4.98600
0.15262	0.90660	15.01565	14.16515	5.17599
0.15262	0.88713	14.97953	14.16515	5.17599
0.24307	0.93504	15.06985	14.16515	5.33599
0.24307	0.86924	14.94701	14.16515	5.33599
0.33917	0.94617	15.09153	14.16515	5.50599
0.33917	0.87125	14.95062	14.16515	5.50599
0.44657	0.95352	15.10598	14.16515	5.69600
0.44657	0.88910	14.98314	14.16515	5.69600
0.54267	0.96806	15.13488	14.16515	5.86599
0.54267	0.87724	14.96146	14.16515	5.86599
0.63877	0.96082	15.12043	14.16515	6.03599
0.63877	0.90467	15.01204	14.16515	6.03599

0.74053	0.96082	15.12043	14.16515	6.21599
0.74053	0.91618	15.03372	14.16515	6.21599
0.83663	1.00000	15.19992	14.16515	6.38599
0.83663	0.90852	15.01927	14.16515	6.38599
0.92142	0.88713	14.97953	14.16515	6.53599
0.92142	0.80890	14.84223	14.16515	6.53599
1.00000	0.00000	14.16515	14.16515	6.67500

RUN NO	DATA PT	P AMB, IN. HG	P AMB PSIA
1.0000	0.0100	29.9000	14.6868

PRESSURE COEFFICIENTS (BASED ON INLET DATA)

INLET STATIC PRESSURES

IN TERMS OF ABSOLUTE PRESSURES

1	14.17383	2	14.19550	3	14.18828	4	14.18828	5	14.07989
6	14.21718	7	14.19912	8	14.19912	9	14.19550	10	14.10518
11	14.68687	12	14.68687	13	14.68687	14	14.68687	15	14.68687
16	14.68687	17	14.68687	18	14.68687	19	14.68687	20	14.68687

IN TERMS OF CP

1	-0.00044	2	0.02632	3	0.01740	4	0.01740	5	-0.11645
6	0.05309	7	0.03078	8	0.03078	9	0.02632	10	-0.08522
11	0.63316	12	0.63316	13	0.63316	14	0.63316	15	0.63316
16	0.63316	17	0.63316	18	0.63316	19	0.63316	20	0.63316

STATIC WALL PRESSURES

IN TERMS OF ABSOLUTE PRESSURES / IN TERMS OF CP

	TIP M		HUB M		TIP		HUB
1	14.18105	14	14.15215	1	0.00847	14	-0.02721
2	14.27499	15	14.35448	2	0.12449	15	0.22265
3	14.28944	16	14.45564	3	0.14233	16	0.34759
4	14.23163	17	14.53513	4	0.07094	17	0.44575
5	14.30028	18	14.49900	5	0.15572	18	0.40113
6	14.43035	19	14.42312	6	0.31635	19	0.30743
7	14.53513	20	14.28944	7	0.44575	20	0.14233
8	14.60377	21	14.31835	8	0.53053	21	0.17803
9	14.65074	22	14.37977	9	0.58854	22	0.25388
10	14.63990	23	14.53874	10	0.57515	23	0.45021
11	14.64713	24	14.59655	11	0.58408	24	0.52161
12	14.67965	25	14.66881	12	0.62423	25	0.61085
13	14.83139	26	14.72300	13	0.81164	26	0.67778

STATIC BASE PRESSURES

IN TERMS OF ABSOLUTE PRESSURES

1	14.64713	2	14.64713	3	14.65797

IN TERMS OF CP

1	0.58408	2	0.58408	3	0.59746

CP = 0.63316 ETA = 0.75492

RUN NO	DATA PT	P AMB. IN. HG	P AMB PSIA
1.0000	0.0100	29.9000	14.6868

CALCULATIONS BASED ON WEIGHT FLOW RATE

AIR FLO RATE	FUEL FLO RATE	FUEL AIR RATIO	TOT FLO RATE
6.28751	0.07972	0.01267	6.36723

MACH NO.	QFLOW	V AVG.	DENSITY
0.28673	0.78176	508.49285	0.02801

PRESSURE COEFFICIENTS

INLET STATIC PRESSURES, IN TERMS OF CP

1	-0.00046	2	0.02726	3	0.01802	4	0.01802	5	-0.12062
6	0.05499	7	0.03188	8	0.03188	9	0.02726	10	-0.08827
11	0.65580	12	0.65580	13	0.65580	14	0.65580	15	0.65580
16	0.65580	17	0.65580	18	0.65580	19	0.65580	20	0.65580

STATIC WALL PRESSURES, IN TERMS OF CP

	TIP		HUB
1	0.00878	14	-0.02819
2	0.12894	15	0.23061
3	0.14742	16	0.36002
4	0.07348	17	0.46169
5	0.16129	18	0.41548
6	0.32767	19	0.31842
7	0.46169	20	0.14742
8	0.54950	21	0.18440
9	0.60958	22	0.26296
10	0.59572	23	0.46631
11	0.60496	24	0.54026
12	0.64656	25	0.63269
13	0.84067	26	0.70202

STATIC BASE PRESSURES IN TERMS OF CP

1	0.60496	2	0.60496	3	0.61883

CP = 0.65580   ETA = 0.78192

RATIO OF RAKE AVE Q TO FLOW AVE Q = 1.03576

ST9 FULL SCALE DIFFUSER (IR SUPPRESSING)
SWIRL ANGLE = 0.00 DEGREES

RUN NO	DATA PT	P AMB IN. HG	P AMB PSIA
1.0000	0.0100	29.9000	14.6868

INLET STATIC PRESSURES, PSIA

1 14.17383	2 14.19550	3 14.18828	4 14.18828	5 14.07989
6 14.21718	7 14.19912	8 14.19912	9 14.19550	10 14.10518
11 14.68687	12 14.68687	13 14.68687	14 14.68687	15 14.68687
16 14.68687	17 14.68687	18 14.68687	19 14.68687	20 14.68687

STATIC WALL PRESSURES, PSIA

OUTER WALL

Pw 1 14.18105	Pw 2 14.27499	Pw 3 14.28944	Pw 4 14.23163	Pw 5 14.30028
Pw 6 14.43035	Pw 7 14.53513	Pw 8 14.60377	Pw 9 14.65074	Pw10 14.63990
Pw11 14.64713	Pw12 14.67965	Pw13 14.83139	Pw	

INNER WALL

Pw14 14.15215	Pw15 14.35448	Pw16 14.45564	Pw17 14.53513	Pw18 14.49900
Pw19 14.42312	Pw20 14.28944	Pw21 14.31835	Pw22 14.37977	Pw23 14.53874
Pw24 14.59655	Pw25 14.66881	Pw26 14.72300	Pw	

OUTER WALL DKJ-5600

COOLANT INLET TOTAL PRESSURE (PB01) = 15.3950 PSIA
COOLANT INLET TOTAL TEMPERATURE (TB01) = 120.000 F
COOLANT INLET TOTAL TEMPERATURE (TB02) = 125.000 F
COOLANT INLET TOTAL TEMPERATURE (TB03) = 0.000 F
OUTER WALL UNCOOLED TEMPERATURE (TWUCO) = 815.000 F
OUTER PANEL NO.1 WALL STATIC PRES. (PW27) = 14.47009 PSIA
OUTER PANEL NO.2 WALL STATIC PRES. (PW28) = 14.64713 PSIA
OUTER PANEL NO.3 WALL STATIC PRES. (PW29) = 14.62545 PSIA
TOTAL COOLANT FLOW RATE = 0.40496 LB/SEC

	Z (IN)	X (IN)	R (IN)	Tw (F)	
1	8.45200	8.71800	8.32200	265.00006	(Tw 1)
2	9.50000	9.92400	8.91600	200.00003	(Tw 2)
3	10.54800	11.10100	9.45400	310.00006	(Tw 3)
4	12.12000	12.74900	9.93500	265.00006	(Tw 4)
5	12.90600	13.53700	9.98500	330.00006	(Tw 5)
6	14.21600	14.86000	9.82400	325.00006	(Tw 6)
7	15.78800	16.49900	9.36600	415.00006	(Tw 7)
8	16.31200	17.05400	9.18000	320.00006	(Tw 8)
9	17.36000	18.16700	8.80300	300.00006	(Tw 9)
10	18.66900	19.54000	8.39700	340.00006	(Tw10)
11	19.47500	20.36900	8.19800	0.00000	(Tw11)

INNER WALL DKJ-5600

COOLANT INLET TOTAL PRESSURE (PB02) = 18.4143 PSIA
COOLANT INLET TOTAL TEMPERATURE (TB04) = 120.000 F
COOLANT INLET TOTAL TEMPERATURE (TB05) = 175.000 F
COOLANT INLET TOTAL TEMPERATURE (TB06) = 85.000 F
INNER WALL UNCOOLED TEMPERATURE (TWUCI) = 950.000 F
INNER PANEL NO.1 WALL STATIC PRES. (PW30) = 14.61823 PSIA
INNER PANEL NO.2 WALL STATIC PRES. (PW31) = 14.61461 PSIA
TOTAL COOLANT FLOW RATE = 0.21595 LB/SEC

	Z (IN)	X (IN)	R (IN)	TW (F)	
1	13.95400	15.02400	7.63600	300.00006	(TW12)
2	14.74000	15.93000	7.18700	0.00000	(TW13)
3	15.78800	17.24800	6.39000	0.00000	(TW14)
4	16.23200	17.83000	6.01200	265.00005	(TW15)
5	17.36000	19.33400	5.01800	320.00006	(TW16)

BASE REGION DKJ-5575

	RADIUS (IN)	STATIC PRESSURE (PSIA)	
1	0.00000	14.64713	P BASE 1
2	1.57000	14.64713	P BASE 2
3	3.10000	14.65797	P BASE 3

COOLANT INLET TOTAL PRESSURE (PB03) = 14.5697 PSIA
TOTAL COOLANT FLOW RATE = 0.00000 LB/SEC

	R (IN)	X (IN)	TW (F)	
1	1.20000	0.21990	0.00000	(TWB01)
2	1.92000	1.34310	510.00006	(TWB02)
3	2.62000	2.43100	560.00012	(TWB03)
4	3.58000	3.75300	0.00000	(TWB04)

BASE BULK TEMP (TBB1) = 515.00012 F

MIDSPAN INLET TOTAL PRESSURES

NO.	PT(PSIA)
1	15.015
2	15.040
3	15.131
4	14.957

HOT FLOW TEST WITH 0.05 COOLING FLOW RATE
MRP = 60 SWIRL ANGLE = 0.0 NO IR DATA PRIMARY FLOW CHANGED

RUN NO	DATA PT	P AMB. IN. HG	P AMB PSIA
2.0000	0.0100	29.9000	14.6868

WEIGHT FLOW RATE,PRIMARY

P1	DEL P	TEMP (R)	FLOW RATE
19.0094	4.2243	680.0001	6.0155

FUEL TO AIR RATIO = 0.0132 FUEL FLOW RATE = 0.0797 LBM/SEC

TOTAL PRIMARY FLOW RATE = 6.0952 LBM/SEC

WEIGHT FLOW RATE,COOLING AIR

OUTER WALL

P1	DEL P	TEMP (R)	FLOW RATE
37.6868	15.0000	545.0001	0.2169

INNER WALL

P1	DEL P	TEMP (R)	FLOW RATE
21.2868	5.0000	540.0001	0.1004

BASE

P1	DEL P	TEMP (R)	FLOW RATE
14.6868	0.0000	460.0000	0.0000

TOTAL TEMP. (AFT OF BURNER CAN) = 1460.000 DEG R INLET TOTAL TEMP. = 1385.000 DEG R

PLENUM (MANIFOLD) PRESSURES PSIA

OUTER WALL	INNER WALL	BASE
14.9867	15.7625	14.6229

INLET PROBE DATA (BASED ON INLET DATA)

PTB	PSI	PSBAR	A R	(PT1-PA)/Q1	DENSITY	CAL FLO RATE	WFLO	QW1	QI
14.99283	14.19695	14.26757	2.49000	0.42186	0.00087	6.14322	0.79588	0.72525	0.77801

SPAN	VEL	PT	PS	Y
0.00000	0.00000	14.19695	14.19695	4.90600
0.04522	0.7[illegible]938	14.74107	14.19695	4.98600
0.04522	0.81621	14.89643	14.19695	4.98600
0.15262	0.88304	15.01[illegible]65	14.19695	5.17599
0.15262	0.86929	14.99036	14.19695	5.17599
0.24307	0.90802	15.06262	14.19695	5.33599
0.24307	0.85533	14.96507	14.19695	5.33599
0.33917	0.91931	15.08430	14.19695	5.50599
0.33917	0.85129	14.95785	14.19695	5.50599
0.44657	0.92491	15.09514	14.19695	5.69600
0.44657	0.86929	14.99036	14.19695	5.69600
0.54267	0.96675	15.17824	14.19695	5.86599
0.54267	0.[illegible]6134	14.97591	14.19695	5.86599
0.63877	0.93232	15.10959	14.19695	6.03599
0.63877	0.88693	15.02288	14.19695	6.03599

0.74053	0.93232	15.10959	14.19695	6.21599
0.74053	0.89657	15.04095	14.19695	6.21599
0.83663	1.00000	15.24689	14.19695	6.38599
0.83663	0.88886	15.02549	14.19695	6.38599
0.92142	0.84724	14.95062	14.19695	6.53599
0.92142	0.80560	14.87836	14.19695	6.53599
1.00000	0.00000	14.19695	14.19695	6.67500

THIS REPORT HAS BEEN DELIMITED
AND CLEARED FOR PUBLIC RELEASE
UNDER DOD DIRECTIVE 5200.20 AND
NO RESTRICTIONS ARE IMPOSED UPON
ITS USE AND DISCLOSURE.

DISTRIBUTION STATEMENT A

APPROVED FOR PUBLIC RELEASE;
DISTRIBUTION UNLIMITED.

RUN NO	DATA PT	P AMB. IN. HG	P AMB PSIA
2.0000	0.0100	29.9000	14.6868

PRESSURE COEFFICIENTS (BASED ON INLET DATA)

INLET STATIC PRESSURES

IN TERMS OF ABSOLUTE PRESSURES

1 14.20634	2 14.22802	3 14.21718	4 14.21718	5 14.11602
6 14.24970	7 14.23163	8 14.23163	9 14.22802	10 14.13770
11 14.68687	12 14.68687	13 14.68687	14 14.68687	15 14.68687
16 14.68687	17 14.68687	18 14.68687	19 14.68687	20 14.68687

IN TERMS OF CP

1 0.00000	2 0.02756	3 0.01378	4 0.01378	5 -0.11484
6 0.05512	7 0.03215	8 0.03215	9 0.02756	10 -0.08728
11 0.61098	12 0.61098	13 0.61098	14 0.61098	15 0.61098
16 0.61098	17 0.61098	18 0.61098	19 0.61098	20 0.61098

STATIC WALL PRESSURES

IN TERMS OF ABSOLUTE PRESSURES		IN TERMS OF CP	
TIP	HUB	TIP	HUB
1 14.22802	14 14.19189	1 0.02756	14 -0.01837
2 14.32196	15 14.39422	2 0.14700	15 0.23887
3 14.34002	16 14.49538	3 0.16997	16 0.36750
4 14.27860	17 14.57848	4 0.09187	17 0.47316
5 14.35086	18 14.53513	5 0.18375	18 0.41803
6 14.48454	19 14.47009	6 0.35372	19 0.33534
7 14.57487	20 14.34364	7 0.46857	20 0.17456
8 14.62184	21 14.37615	8 0.52829	21 0.21591
9 14.67965	22 14.45925	9 0.60179	22 0.32156
10 14.67965	23 14.60016	10 0.60179	23 0.50072
11 14.67965	24 14.62184	11 0.60179	24 0.52829
12 14.68687	25 14.68326	12 0.61098	25 0.60638
13 14.87113	26 14.72661	13 0.84526	26 0.66151

STATIC BASE PRESSURES

IN TERMS OF ABSOLUTE PRESSURES

1	14.66519	2	14.66519	3	14.65797

IN TERMS OF CP

1	0.58341	2	0.58341	3	0.57422

CP = 0.61098 ETA = 0.72847

RUN NO	DATA PT	P AMB. IN. HG	P AMB PSIA
2.0000	0.0100	29.9000	14.6868

CALCULATIONS BASED ON WEIGHT FLOW RATE

AIR FLO RATE	FUEL FLO RATE	FUEL AIR RATIO	TOT FLO RATE
6.01556	0.07972	0.01325	6.09529

MACH NO.	QFLOW	V AVG.	DENSITY
0.27422	0.71617	486.61499	0.02802

PRESSURE COEFFICIENTS

INLET STATIC PRESSURES, IN TERMS OF CP

1	0.00000	2	0.03026	3	0.01513	4	0.01513	5	-0.12612
6	0.06053	7	0.03531	8	0.03531	9	0.03026	10	-0.09585
11	0.67096	12	0.67096	13	0.67096	14	0.67096	15	0.67096
16	0.67096	17	0.67096	18	0.67096	19	0.67096	20	0.67096

STATIC WALL PRESSURES, IN TERMS OF CP

	TIP		HUB
1	0.03026	14	-0.02017
2	0.16143	15	0.26233
3	0.18665	16	0.40358
4	0.10089	17	0.51961
5	0.20179	18	0.45908
6	0.38845	19	0.36827
7	0.51457	20	0.19170
8	0.58015	21	0.23710
9	0.66087	22	0.35314
10	0.66087	23	0.54988
11	0.66087	24	0.58015
12	0.67096	25	0.66591
13	0.92825	26	0.72645

STATIC BASE PRESSURES IN TERMS OF CP

1	0.64069	2	0.64069	3	0.63060

CP = 0.67096 ETA = 0.79999

RATIO OF RAKE AVE Q TO FLOW AVE Q = 1.09817

ST9 FULL SCALE DIFFUSER (IR SUPPRESSING)
SWIRL ANGLE = 0.00 DEGREES

RUN NO	DATA PT	P AMB IN. HG	P AMB PSIA
2.0000	0.0100	29.9000	14.6868

INLET STATIC PRESSURES, PSIA

1 14.20634	2 14.22802	3 14.21718	4 14.21718	5 14.11602
6 14.24970	7 14.23163	8 14.23163	9 14.22802	10 14.13770
11 14.68687	12 14.68687	13 14.68687	14 14.68687	15 14.68687
16 14.68687	17 14.68687	18 14.68687	19 14.68687	20 14.68687

STATIC WALL PRESSURES, PSIA

OUTER WALL

Pw 1 14.22802	Pw 2 14.32196	Pw 3 14.34002	Pw 4 14.27860	Pw 5 14.35086
Pw 6 14.48454	Pw 7 14.57487	Pw 8 14.62184	Pw 9 14.67965	Pw10 14.67965
Pw11 14.67965	Pw12 14.68687	Pw13 14.87113	Pw	

INNER WALL

Pw14 14.19189	Pw15 14.39422	Pw16 14.49538	Pw17 14.57848	Pw18 14.53513
Pw19 14.47009	Pw20 14.34364	Pw21 14.37615	Pw22 14.45925	Pw23 14.60016
Pw24 14.62184	Pw25 14.68326	Pw26 14.72661	Pw	

OUTER WALL DKJ-5600

COOLANT INLET TOTAL PRESSURE (PB01) = 14.9867 PSIA
COOLANT INLET TOTAL TEMPERATURE (TB01) = 155.000 F
COOLANT INLET TOTAL TEMPERATURE (TB02) = 210.000 F
COOLANT INLET TOTAL TEMPERATURE (TB03) = 0.000 F
OUTER WALL UNCOOLED TEMPERATURE (TWUCO) = 825.000 F
OUTER PANEL NO.1 WALL STATIC PRES. (PW27) = 14.53151 PSIA
OUTER PANEL NO.2 WALL STATIC PRES. (PW28) = 14.65797 PSIA
OUTER PANEL NO.3 WALL STATIC PRES. (PW29) = 14.64713 PSIA
TOTAL COOLANT FLOW RATE = 0.21694 LB/SEC

	Z (IN)	X (IN)	R (IN)	TW (F)	
1	8.45200	8.71800	8.32200	330.00006	(TW 1)
2	9.50000	9.92400	8.91600	240.00003	(TW 2)
3	10.54800	11.10100	9.45400	410.00006	(TW 3)
4	12.12000	12.74900	9.93500	475.00006	(TW 4)
5	12.90600	13.53700	9.98500	425.00006	(TW 5)
6	14.21600	14.86000	9.82400	500.00006	(TW 6)
7	15.78800	16.49900	9.36600	0.00000	(TW 7)
8	16.31200	17.05400	9.18000	420.00006	(TW 8)
9	17.36000	18.16700	8.80300	440.00006	(TW 9)
10	18.66900	19.54000	8.39700	470.00006	(TW10)
11	19.47500	20.36900	8.19800	0.00000	(TW11)

INNER WALL DKJ-5600

COOLANT INLET TOTAL PRESSURE (PB02) = 15.7625 PSIA
COOLANT INLET TOTAL TEMPERATURE (TB04) = 108.000 F
COOLANT INLET TOTAL TEMPERATURE (TB05) = 275.000 F
COOLANT INLET TOTAL TEMPERATURE (TB06) = 86.000 F
INNER WALL UNCOOLED TEMPERATURE (TWUCI) = 970.000 F
INNER PANEL NO.1 WALL STATIC PRES. (PW30) = 14.62545 PSIA
INNER PANEL NO.2 WALL STATIC PRES. (PW31) = 14.67965 PSIA
TOTAL COOLANT FLOW RATE = 0.10046 LB/SEC

	Z (IN)	X (IN)	R (IN)	TW (F)	
1	13.95400	15.02400	7.63600	395.00006	(TW12)
2	14.74000	15.93000	7.18700	0.00000	(TW13)
3	15.78800	17.24800	6.39000	0.00000	(TW14)
4	16.23200	17.83000	6.01200	365.00006	(TW15)
5	17.36000	19.33400	5.01800	465.00006	(TW16)

BASE REGION DKJ-5575

	RADIUS (IN)	STATIC PRESSURE (PSIA)	
1	0.00000	14.66519	P BASE 1
2	1.57000	14.66519	P BASE 2
3	3.10000	14.65797	P BASE 3

COOLANT INLET TOTAL PRESSURE (PB03) = 14.6229 PSIA
TOTAL COOLANT FLOW RATE = 0.00000 LB/SEC

	R (IN)	X (IN)	TW (F)	
1	1.20000	0.21990	0.00000	(TWB01)
2	1.92000	1.34310	640.00012	(TWB02)
3	2.62000	2.43100	705.00012	(TWB03)
4	3.58000	3.75300	0.00000	(TWB04)

BASE BULK TEMP (TBB1) = 690.00012 F

MIDSPAN INLET TOTAL PRESSURES

NO.	PT(PSIA)
1	15.004
2	15.040
3	15.127
4	14.954

HOT FLOW TEST WITH 0.05 COOLING FLOW RATE
MRP = 60 SWIRL ANGLE = 0.0 NO IR DATA

RUN NO	DATA PT	P AMB, IN. HG	P AMB PSIA
2.0000	0.0200	29.9000	14.6868

WEIGHT FLOW RATE,PRIMARY

P1	DEL P	TEMP (R)	FLOW RATE
18.7638	4.8137	680.0001	6.2973

FUEL TO AIR RATIO = 0.0126 FUEL FLOW RATE = 0.0797 LBM/SEC

TOTAL PRIMARY FLOW RATE = 6.3771 LBM/SEC

WEIGHT FLOW RATE,COOLING AIR

OUTER WALL

P1	DEL P	TEMP (R)	FLOW RATE
37.6868	15.0000	545.0001	0.2169

INNER WALL

P1	DEL P	TEMP (R)	FLOW RATE
20.1868	5.0000	545.0001	0.0969

BASE

P1	DEL P	TEMP (R)	FLOW RATE
14.6868	0.0000	460.0000	0.0000

TOTAL TEMP. (AFT OF BURNER CAN) = 1465.000 DEG R INLET TOTAL TEMP. = 1384.000 DEG R

PLENUM (MANIFOLD) PRESSURES PSIA

OUTER WALL	INNER WALL	BASE
14.9831	15.7944	14.6229

INLET PROBE DATA (BASED ON INLET DATA)

PTB	PSI	PSBAR	A R	(PT1-PA)/Q1	DENSITY	CAL FLO RATE	CFLO	QW1	QI
15.03236	14.18683	14.26133	2.49000	0.44808	0.00087	6.33730	0.84552	0.77103	0.82682

SPAN	VEL	PT	PS	Y
0.00000	0.00000	14.18683	14.18683	4.90600
0.04522	0.72901	14.74829	14.18683	4.98600
0.04522	0.84016	14.93256	14.18683	4.98600
0.15262	0.90861	15.05901	14.18683	5.17599
0.15262	0.89725	15.03733	14.18683	5.17599
0.24307	0.93641	15.11321	14.18683	5.33599
0.24307	0.87993	15.00482	14.18683	5.33599
0.33917	0.94911	15.13850	14.18683	5.50599
0.33917	0.87798	15.00120	14.18683	5.50599
0.44657	0.95450	15.14934	14.18683	5.69600
0.44657	0.89534	15.03372	14.18683	5.69600
0.54267	0.97225	15.18547	14.18683	5.86599
0.54267	0.88767	15.01927	14.18683	5.86599
0.63877	0.96342	15.16740	14.18683	6.03599
0.63877	0.91424	15.06985	14.18683	6.03599

0.74053	0.96696	15.17463	14.18683	6.21599
0.74053	0.92724	15.09514	14.18683	6.21599
0.83663	1.00000	15.24327	14.18683	6.38599
0.83663	0.91983	15.08069	14.18683	6.38599
0.92142	0.87798	15.00120	14.18683	6.53599
0.92142	0.82372	14.90365	14.18683	6.53599
1.00000	0.00000	14.18683	14.18683	6.67500

RUN NO	DATA PT	P AMB. IN. HG	P AMB PSIA
2.0000	0.0200	29.9000	14.6858

PRESSURE COEFFICIENTS (BASED ON INLET DATA)

INLET STATIC PRESSURES

IN TERMS OF ABSOLUTE PRESSURES

1	14.19550	2	14.21718	3	14.20996	4	14.20996	5	14.10157
6	14.23886	7	14.21718	8	14.21718	9	14.21357	10	14.12324
11	14.68687	12	14.68687	13	14.68687	14	14.68687	15	14.68687
16	14.68687	17	14.68687	18	14.68687	19	14.68687	20	14.68687

IN TERMS OF CP

1	0.00129	2	0.02716	3	0.01854	4	0.01854	5	-0.11080
6	0.05303	7	0.02716	8	0.02716	9	0.02285	10	-0.08493
11	0.58769	12	0.58769	13	0.58769	14	0.58769	15	0.58769
16	0.58769	17	0.58769	18	0.58769	19	0.58769	20	0.58769

STATIC WALL PRESSURES

IN TERMS OF ABSOLUTE PRESSURES				IN TERMS OF CP			
TIP		HUB		TIP		HUB	
1	14.21718	14	14.18105	1	0.02716	14	-0.01595
2	14.31473	15	14.39061	2	0.14358	15	0.23413
3	14.33280	16	14.49177	3	0.16514	16	0.35486
4	14.27138	17	14.57487	4	0.09184	17	0.45403
5	14.34364	18	14.54235	5	0.17807	18	0.41522
6	14.48093	19	14.46648	6	0.34192	19	0.32467
7	14.57126	20	14.33641	7	0.44971	20	0.16945
8	14.62906	21	14.36532	8	0.51870	21	0.20394
9	14.68687	22	14.44841	9	0.58769	22	0.30311
10	14.68687	23	14.60016	10	0.58769	23	0.48421
11	14.67965	24	14.62184	11	0.57907	24	0.51008
12	14.68687	25	14.68326	12	0.58769	25	0.58338
13	14.87836	26	14.69410	13	0.81621	26	0.59631

STATIC BASE PRESSURES

IN TERMS OF ABSOLUTE PRESSURES

1	14.66519	2	14.66158	3	14.65435

IN TERMS OF CP

1	0.56182	2	0.55751	3	0.54858

CP = 0.58769 ETA = 0.70071

RUN NO	DATA PT	P AMB. IN. HG	P AMB PSIA
2.0000	0.0200	29.9000	14.6868

CALCULATIONS BASED ON WEIGHT FLOW RATE

AIR FLO RATE	FUEL FLO RATE	FUEL AIR RATIO	TOT FLO RATE
6.29737	0.07972	0.01265	6.37710

MACH NO.	QFLOW	V AVG.	DENSITY
0.28689	0.78309	508.57031	0.02805

PRESSURE COEFFICIENTS

INLET STATIC PRESSURES, IN TERMS OF CP

1	0.00138	2	0.02906	3	0.01984	4	0.01984	5	-0.11857
6	0.05675	7	0.02906	8	0.02906	9	0.02445	10	-0.09088
11	0.62885	12	0.62885	13	0.62885	14	0.62885	15	0.62885
16	0.62885	17	0.62885	18	0.62885	19	0.62885	20	0.62885

STATIC WALL PRESSURES, IN TERMS OF CP

	TIP		HUB
1	0.02906	14	-0.01706
2	0.15364	15	0.25052
3	0.17670	16	0.37971
4	0.09827	17	0.48583
5	0.19055	18	0.44430
6	0.36587	19	0.34741
7	0.48121	20	0.18132
8	0.55503	21	0.21823
9	0.62885	22	0.32434
10	0.62885	23	0.51812
11	0.61962	24	0.54580
12	0.62885	25	0.62424
13	0.87338	26	0.63808

STATIC BASE PRESSURES IN TERMS OF CP

1	0.60117	2	0.59656	3	0.58733

CP = 0.62885 ETA = 0.74978

RATIO OF RAKE AVE Q TO FLOW AVE Q = 1.07003

ST9 FULL SCALE DIFFUSER (IR SUPPRESSING)
SWIRL ANGLE = 0.00 DEGREES

RUN NO	DATA PT	P AMB IN. HG	P AMB PSIA
2.0000	0.0200	29.9000	14.6868

INLET STATIC PRESSURES, PSIA

1 14.19550	2 14.21718	3 14.20996	4 14.20996	5 14.10157
6 14.23886	7 14.21718	8 14.21718	9 14.21357	10 14.12324
11 14.68687	12 14.68687	13 14.68687	14 14.68687	15 14.68687
16 14.68687	17 14.68687	18 14.68687	19 14.68687	20 14.68687

STATIC WALL PRESSURES, PSIA

OUTER WALL

PW 1 14.21718	PW 2 14.31473	PW 3 14.33280	PW 4 14.27138	PW 5 14.34364
PW 6 14.48093	PW 7 14.57126	PW 8 14.62906	PW 9 14.68687	PW10 14.68687
PW11 14.67965	PW12 14.68687	PW13 14.87836	PW	

INNER WALL

PW14 14.18105	PW15 14.39061	PW16 14.49177	PW17 14.57487	PW18 14.54235
PW19 14.46648	PW20 14.33641	PW21 14.36532	PW22 14.44841	PW23 14.60016
PW24 14.62184	PW25 14.68326	PW26 14.69410	PW	

OUTER WALL DKJ-5600

COOLANT INLET TOTAL PRESSURE (PB01) = 14.9831 PSIA
COOLANT INLET TOTAL TEMPERATURE (TB01) = 165.000 F
COOLANT INLET TOTAL TEMPERATURE (TB02) = 220.000 F
COOLANT INLET TOTAL TEMPERATURE (TB03) = 0.000 F
OUTER WALL UNCOOLED TEMPERATURE (TWUCO) = 842.000 F
OUTER PANEL NO.1 WALL STATIC PRES. (PW27) = 14.88197 PSIA
OUTER PANEL NO.2 WALL STATIC PRES. (PW28) = 14.71939 PSIA
OUTER PANEL NO.3 WALL STATIC PRES. (PW29) = 14.73023 PSIA
TOTAL COOLANT FLOW RATE = 0.21694 LB/SEC

	Z (IN)	X (IN)	R (IN)	TW (F)	
1	8.45200	8.71800	8.32200	345.00006	(TW 1)
2	9.50000	9.92400	8.91600	255.00003	(TW 2)
3	10.54800	11.10100	9.45400	425.00006	(TW 3)
4	12.12000	12.74900	9.93500	505.00006	(TW 4)
5	12.90600	13.53700	9.98500	445.00006	(TW 5)
6	14.21600	14.86000	9.82400	525.00012	(TW 6)
7	15.78800	16.49900	9.36600	0.00000	(TW 7)
8	16.31200	17.05400	9.18000	440.00006	(TW 8)
9	17.36000	18.16700	8.80300	460.00006	(TW 9)
10	18.66900	19.54000	8.39700	495.00006	(TW10)
11	19.47500	20.36900	8.19800	0.00000	(TW11)

DKJ-5600

INNER WALL

COOLANT INLET TOTAL PRESSURE (PB02) = 15.7944 PSIA
COOLANT INLET TOTAL TEMPERATURE (TB04) = 135.000 F
COOLANT INLET TOTAL TEMPERATURE (TB05) = 285.000 F
COOLANT INLET TOTAL TEMPERATURE (TB06) = 86.000 F
INNER WALL UNCOOLED TEMPERATURE (TWUCI) = 1000.000 F
INNER PANEL NO.1 WALL STATIC PRES. (PW30) = 14.75913 PSIA
INNER PANEL NO.2 WALL STATIC PRES. (PW31) = 14.70133 PSIA
TOTAL COOLANT FLOW RATE = 0.09693 LB/SEC

	Z (IN)	X (IN)	R (IN)	TW (F)	
1	13.95400	15.02400	7.63600	415.00006	(TW12)
2	14.74000	15.93000	7.18700	0.00000	(TW13)
3	15.78800	17.24800	6.39000	380.00006	(TW14)
4	16.23200	17.83000	6.01200	380.00006	(TW15)
5	17.36000	19.33400	5.01800	485.00006	(TW16)

DKJ-5575

BASE REGION

	RADIUS (IN)	STATIC PRESSURE (PSIA)	
1	0.00000	14.66519	P BASE 1
2	1.57000	14.66158	P BASE 2
3	3.10000	14.65435	P BASE 3

COOLANT INLET TOTAL PRESSURE (PB03) = 14.6229 PSIA
TOTAL COOLANT FLOW RATE = 0.00000 LB/SEC

	R (IN)	X (IN)	TW (F)	
1	1.20000	0.21990	0.00000	(TWB01)
2	1.92000	1.34310	650.00012	(TWB02)
3	2.62000	2.43100	725.00012	(TWB03)
4	3.58000	3.75300	0.00000	(TWB04)

BASE BULK TEMP (TBB1) = 702.00012 F

MIDSPAN INLET TOTAL PRESSURES

NO.	PT(PSIA)
1	14.318
2	14.274
3	14.177
4	14.372

HOT FLOW TEST WITH 0.05 COOLING FLOW RATE
MRP = 60 SWIRL ANGLE = 0.0 NO IR DATA

RUN NO	DATA PT	P AMB. IN. HG	P AMB PSIA
3.0000	0.0100	29.9000	14.6868

WEIGHT FLOW RATE,PRIMARY

P1	DEL P	TEMP (R)	FLOW RATE
18.7638	4.8137	680.0001	6.2973

FUEL TO AIR RATIO = 0.0126 FUEL FLOW RATE = 0.0797 LBM/SEC

TOTAL PRIMARY FLOW RATE = 6.3771 LBM/SEC

WEIGHT FLOW RATE,COOLING AIR

OUTER WALL

P1	DEL P	TEMP (R)	FLOW RATE
21.1868	5.0000	545.0001	0.0997

INNER WALL

P1	DEL P	TEMP (R)	FLOW RATE
18.6868	2.5000	545.0001	0.0686

BASE

P1	DEL P	TEMP (R)	FLOW RATE
14.6868	0.0000	460.0000	0.0000

TOTAL TEMP. (AFT OF BURNER CAN) = 1450.000 DEG R INLET TOTAL TEMP. = 1370.000 DEG R

PLENUM (MANIFOLD) PRESSURES PSIA

OUTER WALL	INNER WALL	BASE
14.7699	15.2193	14.6442

INLET PROBE DATA (BASED ON INLET DATA)

PTB	PSI	PSBAR	A R	(PT1-PA)/Q1	DENSITY	CAL FLO RATE	QFLO	QW1	QI
15.03476	14.19839	14.27232	2.49000	0.45628	0.00088	6.33597	0.83636	0.76243	0.81788

SPAN	VEL	PT	PS	Y
0.00000	0.00000	14.19839	14.19839	4.90600
0.04522	0.71796	14.75191	14.19839	4.98600
0.04522	0.82890	14.93617	14.19839	4.98600
0.15262	0.89525	15.05901	14.19839	5.17599
0.15262	0.88390	15.03733	14.19839	5.17599
0.24307	0.92301	15.11321	14.19839	5.33599
0.24307	0.86660	15.00482	14.19839	5.33599
0.33917	0.93388	15.13488	14.19839	5.50599
0.33917	0.86271	14.99759	14.19839	5.50599
0.44657	0.93927	15.14572	14.19839	5.69600
0.44657	0.88009	15.03011	14.19839	5.69600
0.54267	0.97788	15.22521	14.19839	5.86599
0.54267	0.87241	15.01565	14.19839	5.86599
0.63877	0.94818	15.16379	14.19839	6.03599
0.63877	0.90087	15.06985	14.19839	6.03599

0.74053	0.94995	15.16740	14.19839	6.21599
0.74053	0.91201	15.09153	14.19839	6.21599
0.83663	1.00000	15.27218	14.19839	6.38599
0.83663	0.90460	15.07708	14.19839	6.38599
0.92142	0.86271	14.99759	14.19839	6.53599
0.92142	0.81250	14.90727	14.19839	6.53599
1.00000	0.00000	14.19839	14.19839	6.67500

RUN NO	DATA PT	P AMB. IN. HG	P AMB PSIA
3.0000	0.0100	29.9000	14.6868

PRESSURE COEFFICIENTS (BASED ON INLET DATA)

INLET STATIC PRESSURES

IN TERMS OF ABSOLUTE PRESSURES

1	14.20634	2	14.22802	3	14.22080	4	14.22080	5	14.11602
6	14.25331	7	14.23163	8	14.23163	9	14.22802	10	14.13770
11	14.68687	12	14.68687	13	14.68687	14	14.68687	15	14.68687
16	14.68687	17	14.68687	18	14.68687	19	14.68687	20	14.68687

IN TERMS OF CP

1	-0.00130	2	0.02489	3	0.01615	4	0.01615	5	-0.11048
6	0.05546	7	0.02926	8	0.02926	9	0.02489	10	-0.08428
11	0.57950	12	0.57950	13	0.57950	14	0.57950	15	0.57950
16	0.57950	17	0.57950	18	0.57950	19	0.57950	20	0.57950

STATIC WALL PRESSURES

IN TERMS OF ABSOLUTE PRESSURES				IN TERMS OF CP			
	TIP		HUB		TIP		HUB
1	14.23525	14	14.20273	1	0.03362	14	-0.00567
2	14.33280	15	14.40506	2	0.15153	15	0.23887
3	14.34725	16	14.50261	3	0.16900	16	0.35678
4	14.28583	17	14.57126	4	0.09476	17	0.43976
5	14.36532	18	14.55680	5	0.19084	18	0.42229
6	14.49900	19	14.48093	6	0.35242	19	0.33058
7	14.57487	20	14.35086	7	0.44413	20	0.17337
8	14.66881	21	14.38338	8	0.55767	21	0.21267
9	14.68687	22	14.47371	9	0.57950	22	0.32185
10	14.69410	23	14.61100	10	0.58824	23	0.48779
11	14.68326	24	14.62545	11	0.57514	24	0.50526
12	14.68687	25	14.68687	12	0.57950	25	0.57950
13	14.91088	26	14.71939	13	0.85026	26	0.61881

STATIC BASE PRESSURES

IN TERMS OF ABSOLUTE PRESSURES

1	14.67603	2	14.67242	3	14.66158

IN TERMS OF CP

1	0.56640	2	0.56203	3	0.54893

CP = 0.57950 ETA = 0.69095

RUN NO	DATA PT	P AMB. IN. HG	P AMB PSIA
3.0000	0.0100	29.9000	14.6868

CALCULATIONS BASED ON WEIGHT FLOW RATE

AIR FLO RATE	FUEL FLO RATE	FUEL AIR RATIO	TOT FLO RATE
6.29737	0.07972	0.01265	6.37710

MACH NO.	QFLOW	V AVG.	DENSITY
0.28510	0.77456	503.03399	0.02836

PRESSURE COEFFICIENTS

INLET STATIC PRESSURES, IN TERMS OF CP

1	-0.00139	2	0.02658	3	0.01725	4	0.01725	5	-0.11801
6	0.05923	7	0.03125	8	0.03125	9	0.02658	10	-0.09002
11	0.61898	12	0.61898	13	0.61898	14	0.61898	15	0.61898
16	0.61898	17	0.61898	18	0.61898	19	0.61898	20	0.61898

STATIC WALL PRESSURES, IN TERMS OF CP

	TIP		HUB
1	0.03591	14	-0.00606
2	0.16186	15	0.25515
3	0.18051	16	0.38109
4	0.10122	17	0.46971
5	0.20384	18	0.45105
6	0.37642	19	0.35310
7	0.47438	20	0.18518
8	0.59565	21	0.22716
9	0.61898	22	0.34377
10	0.62831	23	0.52102
11	0.61431	24	0.53968
12	0.61898	25	0.61898
13	0.90818	26	0.66096

STATIC BASE PRESSURES IN TERMS OF CP

1	0.60499	2	0.60032	3	0.58633

CP = 0.61898 ETA = 0.73801

RATIO OF RAKE AVE Q TO FLOW AVE Q = 1.05811

ST9 FULL SCALE DIFFUSER (IR SUPPRESSING)
SWIRL ANGLE = 0.00 DEGREES

RUN NO	DATA PT	P AMB IN. HG	P AMB PSIA
3.0000	0.0100	29.9000	14.6868

INLET STATIC PRESSURES, PSIA

1 14.20634	2 14.22802	3 14.22080	4 14.22080	5 14.11602
6 14.25331	7 14.23163	8 14.23163	9 14.22802	10 14.13770
11 14.68687	12 14.68687	13 14.68687	14 14.68687	15 14.68687
16 14.68687	17 14.68687	18 14.68687	19 14.68687	20 14.68687

STATIC WALL PRESSURES, PSIA

OUTER WALL

PW 1 14.23525	PW 2 14.33280	PW 3 14.34725	PW 4 14.28583	PW 5 14.36532
PW 6 14.49900	PW 7 14.57487	PW 8 14.66881	PW 9 14.68687	PW10 14.69410
PW11 14.68326	PW12 14.68687	PW13 14.91088	PW	

INNER WALL

PW14 14.20273	PW15 14.40506	PW16 14.50261	PW17 14.57126	PW18 14.55680
PW19 14.48093	PW20 14.35086	PW21 14.38338	PW22 14.47371	PW23 14.61100
PW24 14.62545	PW25 14.68687	PW26 14.71939	PW	

OUTER WALL DKJ-5600

COOLANT INLET TOTAL PRESSURE (PB01) = 14.7699 PSIA
COOLANT INLET TOTAL TEMPERATURE (TB01) = 195.000 F
COOLANT INLET TOTAL TEMPERATURE (TB02) = 360.000 F
COOLANT INLET TOTAL TEMPERATURE (TB03) = 0.000 F
OUTER WALL UNCOOLED TEMPERATURE (TWUCO) = 825.000 F
OUTER PANEL NO.1 WALL STATIC PRES. (PW27) = 14.50261 PSIA
OUTER PANEL NO.2 WALL STATIC PRES. (PW28) = 14.64352 PSIA
OUTER PANEL NO.3 WALL STATIC PRES. (PW29) = 14.64352 PSIA
TOTAL COOLANT FLOW RATE = 0.09972 LB/SEC

	Z (IN)	X (IN)	R (IN)	TW (F)	
1	8.45200	8.71800	8.32200	435.00006	(TW 1)
2	9.50000	9.92400	8.91600	355.00006	(TW 2)
3	10.54800	11.10100	9.45400	535.00012	(TW 3)
4	12.12000	12.74900	9.93500	640.00012	(TW 4)
5	12.90600	13.53700	9.98500	560.00012	(TW 5)
6	14.21600	14.86000	9.82400	640.00012	(TW 6)
7	15.78800	16.49900	9.36600	680.00012	(TW 7)
8	16.31200	17.05400	9.18000	565.00012	(TW 8)
9	17.36000	18.16700	8.80300	600.00012	(TW 9)
10	18.66900	19.54000	8.39700	650.00012	(TW10)
11	19.47500	20.36900	8.19800	0.00000	(TW11)

INNER WALL DKJ-5600

COOLANT INLET TOTAL PRESSURE (PB02) = 15.2193 PSIA
COOLANT INLET TOTAL TEMPERATURE (TB04) = 135.000 F
COOLANT INLET TOTAL TEMPERATURE (TB05) = 335.000 F
COOLANT INLET TOTAL TEMPERATURE (TB06) = 90.000 F
INNER WALL UNCOOLED TEMPERATURE (TWUCI) = 1000.000 F
INNER PANEL NO.1 WALL STATIC PRES. (PW30) = 14.61823 PSIA
INNER PANEL NO.2 WALL STATIC PRES. (PW31) = 14.65797 PSIA
TOTAL COOLANT FLOW RATE = 0.06866 LB/SEC

	Z (IN)	X (IN)	R (IN)	TW (F)	
1	13.95400	15.02400	7.63600	455.00006	(TW12)
2	14.74000	15.93000	7.18700	0.00000	(TW13)
3	15.78800	17.24800	6.39000	0.00000	(TW14)
4	16.23200	17.83000	6.01200	425.00006	(TW15)
5	17.36000	19.33400	5.01800	555.00012	(TW16)

BASE REGION DKJ-5575

	RADIUS (IN)	STATIC PRESSURE (PSIA)	
1	0.00000	14.67603	P BASE 1
2	1.57000	14.67242	P BASE 2
3	3.10000	14.66158	P BASE 3

COOLANT INLET TOTAL PRESSURE (PB03) = 14.6442 PSIA
TOTAL COOLANT FLOW RATE = 0.00000 LB/SEC

	R (IN)	X (IN)	TW (F)	
1	1.20000	0.21990	0.00000	(TWB01)
2	1.92000	1.34310	690.00012	(TWB02)
3	2.62000	2.43100	750.00012	(TWB03)
4	3.58000	3.75300	0.00000	(TWB04)

BASE BULK TEMP (TBB1) = 735.00012 F

MIDSPAN INLET TOTAL PRESSURES

NO.	PT(PSIA)
1	15.051
2	15.091
3	15.185
4	15.001

HOT FLOW TEST WITH 0.10 COOLING FLOW RATE
MRP = 83 SWIRL ANGLE = 16 NO IR DATA

RUN NO	DATA PT	P AMB. IN. HG	P AMB PSIA
4.0000	0.0100	29.8760	14.6750

WEIGHT FLOW RATE.PRIMARY

P1	DEL P	TEMP (R)	FLOW RATE
20.9133	6.9259	675.0001	7.7758

FUEL TO AIR RATIO = 0.0143 FUEL FLOW RATE = 0.1113 LBM/SEC

TOTAL PRIMARY FLOW RATE = 7.8872 LBM/SEC

WEIGHT FLOW RATE.COOLING AIR

OUTER WALL

P1	DEL P	TEMP (R)	FLOW RATE
87.6750	40.0000	560.0001	0.5212

INNER WALL

P1	DEL P	TEMP (R)	FLOW RATE
38.6750	19.0000	560.0001	0.2353

BASE

P1	DEL P	TEMP (R)	FLOW RATE
14.6750	0.0000	460.0000	0.0000

TOTAL TEMP. (AFT OF BURNER CAN) = 1595.000 DEG R INLET TOTAL TEMP. = 1490.000 DEG R

PLENUM (MANIFOLD) PRESSURES PSIA

OUTER WALL	INNER WALL	BASE
15.9613	18.9989	14.5792

INLET PROBE DATA (BASED ON INLET DATA)

PTB	PSI	PSBAR	A R	(PT1-PA)/Q1	DENSITY	CAL FLO RATE	QFLO	QW1	QI
15.33864	13.72559	14.01472	2.49000	0.50120	0.00079	7.93781	1.61305	1.32391	1.53983

SPAN	VEL	PT	PS	Y
0.00000	0.00000	13.72559	13.72559	4.90600
0.04522	0.70976	14.68592	13.72676	4.98600
0.04522	0.77372	14.86657	13.72676	4.98600
0.15262	0.92541	15.36517	13.73461	5.17599
0.15262	0.97824	15.55666	13.73461	5.17599
0.24307	0.97307	15.54582	13.74299	5.33599
0.24307	1.00000	15.64698	13.74299	5.33599
0.33917	0.98904	15.61446	13.75197	5.50599
0.33917	0.98423	15.59640	13.75197	5.50599
0.44657	0.98458	15.60724	13.76148	5.69600
0.44657	0.96118	15.52053	13.76148	5.69600
0.54267	0.97567	15.58195	13.76946	5.86599
0.54267	0.93698	15.44104	13.76946	5.86599
0.63877	0.96485	15.54943	13.77693	6.03599
0.63877	0.92468	15.40491	13.77693	6.03599

0.74053	0.94991	15.50246	13.78440	6.21599
0.74053	0.92255	15.40491	13.78440	6.21599
0.83663	0.92169	15.40852	13.79104	6.38599
0.83663	0.89981	15.33265	13.79104	6.38599
0.92142	0.82341	15.08697	13.79604	6.53599
0.92142	0.81063	15.04722	13.79604	6.53599
1.00000	0.00000	13.79806	13.79806	6.67500

RUN NO	DATA PT	P AMB. IN. HG	P AMB PSIA
4.0000	0.0100	29.8760	14.6750

PRESSURE COEFFICIENTS (BASED ON INLET DATA)

INLET STATIC PRESSURES

IN TERMS OF ABSOLUTE PRESSURES

1	13.78629	2	13.79713	3	13.76461	4	13.73932	5	13.54060
6	13.96332	7	13.91636	8	13.90552	9	13.94526	10	13.72487
11	14.67509	12	14.67509	13	14.67509	14	14.67509	15	14.67509
16	14.67509	17	14.67509	18	14.67509	19	14.67509	20	14.67509

IN TERMS OF CP

1	-0.01440	2	-0.00731	3	-0.02856	4	-0.04509	5	-0.17494
6	0.10128	7	0.07059	8	0.06351	9	0.08945	10	-0.05453
11	0.56639	12	0.56639	13	0.56639	14	0.56639	15	0.56639
16	0.56639	17	0.56639	18	0.56639	19	0.56639	20	0.56639

STATIC WALL PRESSURES

IN TERMS OF ABSOLUTE PRESSURES				IN TERMS OF CP			
TIP		HUB		TIP		HUB	
1	13.78990	14	13.62731	1	-0.01203	14	-0.11828
2	13.97778	15	14.02474	2	0.11072	15	0.14142
3	14.01391	16	14.26682	3	0.13433	16	0.29960
4	13.89106	17	14.55947	4	0.05404	17	0.49084
5	14.02836	18	14.43301	5	0.14378	18	0.40820
6	14.25598	19	14.24875	6	0.29252	19	0.28780
7	14.40411	20	13.93442	7	0.38932	20	0.08239
8	14.50889	21	13.95610	8	0.45778	21	0.09656
9	14.54863	22	14.08617	9	0.48375	22	0.18155
10	14.55586	23	14.34992	10	0.48848	23	0.35390
11	14.57392	24	14.54140	11	0.50028	24	0.47903
12	14.66063	25	14.68592	12	0.55694	25	0.57347
13	14.88103	26	14.68592	13	0.70096	26	0.57347

STATIC BASE PRESSURES

IN TERMS OF ABSOLUTE PRESSURES

1	14.58476	2	14.61366	3	14.68954

IN TERMS OF CP

1	0.50736	2	0.52625	3	0.57583

CP = 0.56639 ETA = 0.67531

RUN NO	DATA PT	P AMB. IN. HG	P AMB PSIA
4.0000	0.0100	29.8760	14.6750

CALCULATIONS BASED ON WEIGHT FLOW RATE

AIR FLO RATE	FUEL FLO RATE	FUEL AIR RATIO	TOT FLO RATE
7.77587	0.11138	0.01432	7.88726

MACH NO.	QFLOW	V AVG.	DENSITY
0.37767	1.42103	717.26489	0.02559

PRESSURE COEFFICIENTS

INLET STATIC PRESSURES, IN TERMS OF CP

1	-0.01550	2	-0.00788	3	-0.03076	4	-0.04856	5	-0.18840
6	0.10907	7	0.07602	8	0.06839	9	0.09636	10	-0.05873
11	0.60995	12	0.60995	13	0.60995	14	0.60995	15	0.60995
16	0.60995	17	0.60995	18	0.60995	19	0.60995	20	0.60995

STATIC WALL PRESSURES, IN TERMS OF CP

	TIP		HUB
1	-0.01296	14	-0.12737
2	0.11924	15	0.15229
3	0.14466	16	0.32264
4	0.05822	17	0.52858
5	0.15483	18	0.43960
6	0.31501	19	0.30993
7	0.41926	20	0.08873
8	0.49299	21	0.10398
9	0.52096	22	0.19551
10	0.52604	23	0.38112
11	0.53875	24	0.51587
12	0.59977	25	0.61757
13	0.75487	26	0.61757

STATIC BASE PRESSURES IN TERMS OF CP

1	0.54638	2	0.56672	3	0.62012

CP = 0.60995 ETA = 0.72724

RATIO OF RAKE AVE Q TO FLOW AVE Q = 1.07690

ST9 FULL SCALE DIFFUSER (IR SUPPRESSING)
SWIRL ANGLE = 15.99 DEGREES

RUN NO	DATA PT	P AMB IN. HG	P AMB PSIA
4.0000	0.0100	29.8760	14.6750

INLET STATIC PRESSURES, PSIA

1 13.78629	2 13.79713	3 13.76461	4 13.73932	5 13.54060
6 13.96332	7 13.91636	8 13.90552	9 13.94526	10 13.72487
11 14.67509	12 14.67509	13 14.67509	14 14.67509	15 14.67509
16 14.67509	17 14.67509	18 14.67509	19 14.67509	20 14.67509

STATIC WALL PRESSURES, PSIA

OUTER WALL

PW 1 13.78990	PW 2 13.97778	PW 3 14.01391	PW 4 13.89106	PW 5 14.02836
PW 6 14.25598	PW 7 14.40411	PW 8 14.50889	PW 9 14.54863	PW10 14.55586
PW11 14.57392	PW12 14.66063	PW13 14.88103	PW	

INNER WALL

PW14 13.62731	PW15 14.02474	PW16 14.26682	PW17 14.55947	PW18 14.43301
PW19 14.24875	PW20 13.93442	PW21 13.95610	PW22 14.08617	PW23 14.34992
PW24 14.54140	PW25 14.68592	PW26 14.68592	PW	

OUTER WALL DKJ-5600

COOLANT INLET TOTAL PRESSURE (PB01) = 15.9613 PSIA
COOLANT INLET TOTAL TEMPERATURE (TB01) = 140.000 F
COOLANT INLET TOTAL TEMPERATURE (TB02) = 140.000 F
COOLANT INLET TOTAL TEMPERATURE (TB03) = 0.000 F
OUTER WALL UNCOOLED TEMPERATURE (TWUCO) = 945.000 F
OUTER PANEL NO.1 WALL STATIC PRES. (PW27) = 14.33546 PSIA
OUTER PANEL NO.2 WALL STATIC PRES. (PW28) = 14.55586 PSIA
OUTER PANEL NO.3 WALL STATIC PRES. (PW29) = 14.63534 PSIA
TOTAL COOLANT FLOW RATE = 0.52120 LB/SEC

	Z (IN)	X (IN)	R (IN)	TW (F)	
1	8.45200	8.71800	8.32200	310.00006	(TW 1)
2	9.50000	9.92400	8.91600	240.00003	(TW 2)
3	10.54800	11.10100	9.45400	330.00006	(TW 3)
4	12.12000	12.74900	9.93500	0.00000	(TW 4)
5	12.90600	13.53700	9.98500	360.00006	(TW 5)
6	14.21600	14.86000	9.82400	395.00006	(TW 6)
7	15.78800	16.49900	9.36600	0.00000	(TW 7)
8	16.31200	17.05400	9.18000	360.00006	(TW 8)
9	17.36000	18.16700	8.80300	35.00000	(TW 9)
10	18.66900	19.54000	8.39700	380.00006	(TW10)
11	19.47500	20.36900	8.19800	0.00000	(TW11)

INNER WALL DKJ-5600

COOLANT INLET TOTAL PRESSURE (PB02) = 18.9989 PSIA
COOLANT INLET TOTAL TEMPERATURE (TB04) = 0.000 F
COOLANT INLET TOTAL TEMPERATURE (TB05) = 205.000 F
COOLANT INLET TOTAL TEMPERATURE (TB06) = 100.000 F
INNER WALL UNCOOLED TEMPERATURE (TWUCI) = 1135.000 F
INNER PANEL NO.1 WALL STATIC PRES. (PW30) = 14.55947 PSIA
INNER PANEL NO.2 WALL STATIC PRES. (PW31) = 14.77264 PSIA
TOTAL COOLANT FLOW RATE = 0.23531 LB/SEC

	Z (IN)	X (IN)	R (IN)	TW (F)	
1	13.95400	15.02400	7.63600	400.00006	(TW12)
2	14.74000	15.93000	7.18700	0.00000	(TW13)
3	15.78800	17.24800	6.39000	0.00000	(TW14)
4	16.23200	17.83000	6.01200	340.00006	(TW15)
5	17.36000	19.33400	5.01800	435.00006	(TW16)

BASE REGION DKJ-5575

	RADIUS (IN)	STATIC PRESSURE (PSIA)	
1	0.00000	14.58476	P BASE 1
2	1.57000	14.61366	P BASE 2
3	3.10000	14.68954	P BASE 3

COOLANT INLET TOTAL PRESSURE (PB03) = 14.5792 PSIA
TOTAL COOLANT FLOW RATE = 0.00000 LB/SEC

	R (IN)	X (IN)	TW (F)	
1	1.20000	0.21990	0.00000	(TWB01)
2	1.92000	1.34310	640.00012	(TWB02)
3	2.62000	2.43100	740.00012	(TWB03)
4	3.58000	3.75300	0.00000	(TWB04)

BASE BULK TEMP (TBB1) = 690.00012 F

MIDSPAN INLET TOTAL PRESSURES

NO.	PT(PSIA)
1	15.097
2	15.451
3	15.368
4	15.365

HOT FLOW TEST WITH 0.05 COOLING FLOW RATE
MRP = 83 SWIRL ANGLE = 16 NO IR DATA

RUN NO	DATA PT	P AMB, IN. HG	P AMB PSIA
5.0000	0.0100	29.8760	14.6750

WEIGHT FLOW RATE, PRIMARY

P1	DEL P	TEMP (R)	FLOW RATE
20.9624	6.8768	680.0001	7.7382

FUEL TO AIR RATIO = 0.0143 FUEL FLOW RATE = 0.1113 LBM/SEC

TOTAL PRIMARY FLOW RATE = 7.8496 LBM/SEC

WEIGHT FLOW RATE, COOLING AIR

OUTER WALL

P1	DEL P	TEMP (R)	FLOW RATE
46.1750	20.0000	556.0001	0.2708

INNER WALL

P1	DEL P	TEMP (R)	FLOW RATE
23.6750	7.5000	556.0001	0.1241

BASE

P1	DEL P	TEMP (R)	FLOW RATE
14.6750	0.0000	460.0000	0.0000

TOTAL TEMP. (AFT OF BURNER CAN) = 1605.000 DEG R INLET TOTAL TEMP. = 1495.000 DEG R

PLENUM (MANIFOLD) PRESSURES PSIA

OUTER WALL	INNER WALL	BASE
15.1483	16.2193	14.6324

INLET PROBE DATA (BASED ON INLET DATA)

PTB	PSI	PSBAR	A R	(PT1-PA)/Q1	DENSITY	CAL FLO RATE	QFLO	GW1	QI
15.34888	13.74943	14.03609	2.49000	0.51325	0.00079	7.89666	1.59944	1.31278	1.52697

SPAN	VEL	PT	PS	Y
0.00000	0.00000	13.74943	13.74943	4.90600
0.04522	0.70799	14.69676	13.75059	4.98600
0.04522	0.77015	14.87019	13.75059	4.98600
0.15262	0.92367	15.36878	13.75832	5.17599
0.15262	0.97508	15.55304	13.75832	5.17599
0.24307	0.97381	15.55666	13.76661	5.33599
0.24307	1.00000	15.65421	13.76661	5.33599
0.33917	0.98993	15.62530	13.77552	5.50599
0.33917	0.97924	15.58556	13.77552	5.50599
0.44657	0.98644	15.62169	13.78492	5.69600
0.44657	0.96188	15.53137	13.78492	5.69600
0.54267	0.97748	15.59640	13.79285	5.86599
0.54267	0.93852	15.45549	13.79285	5.86599
0.63877	0.96659	15.56388	13.80029	6.03599
0.63877	0.92614	15.41936	13.80029	6.03599

0.74053	0.95157	15.51691	13.80772	6.21599
0.74053	0.92090	15.40852	13.80772	6.21599
0.83663	0.92420	15.42659	13.81430	6.38599
0.83663	0.89900	15.33988	13.81430	6.38599
0.92142	0.82648	15.10865	13.81927	6.53599
0.92142	0.81011	15.05806	13.81927	6.53599
1.00000	0.00000	13.82127	13.82127	6.67500

RUN NC	DATA PT	P AMB. IN. HG	P AMB PSIA
5.0000	0.0100	29.8760	14.6750

PRESSURE COEFFICIENTS (BASED ON INLET DATA)

INLET STATIC PRESSURES

IN TERMS OF ABSCLUTE PRESSURES

1	13.80797	2	13.81880	3	13.78629	4	13.76461	5	13.56951
6	13.98500	7	13.94165	8	13.93081	9	13.97055	10	13.75016
11	14.67509	12	14.67509	13	14.67509	14	14.67509	15	14.67509
16	14.67509	17	14.67509	18	14.67509	19	14.67509	20	14.67509

IN TERMS OF CP

1	-0.01620	2	-0.00905	3	-0.03049	4	-0.04479	5	-0.17345
6	0.10055	7	0.07195	8	0.06481	9	0.09101	10	-0.05432
11	0.55564	12	0.55564	13	0.55564	14	0.55564	15	0.55564
16	0.55564	17	0.55564	18	0.55564	19	0.55564	20	0.55564

STATIC WALL PRESSURES

IN TERMS OF ABSOLUTE PRESSURES				IN TERMS OF CP			
TIP		HUB		TIP		HUB	
1	13.80074	14	13.64538	1	-0.02096	14	-0.12342
2	13.98500	15	14.03558	2	0.10055	15	0.13390
3	14.02113	16	14.27404	3	0.12437	16	0.29116
4	13.89468	17	14.57031	4	0.04098	17	0.48654
5	14.04281	18	14.44747	5	0.13867	18	0.40553
6	14.27043	19	14.25959	6	0.28878	19	0.28163
7	14.40411	20	13.93803	7	0.37694	20	0.06957
8	14.47276	21	13.97416	8	0.42221	21	0.09340
9	14.54502	22	14.08978	9	0.46986	22	0.16964
10	14.56670	23	14.34992	10	0.48416	23	0.34120
11	14.58837	24	14.54140	11	0.49846	24	0.46748
12	14.66425	25	14.62812	12	0.54849	25	0.52467
13	14.85212	26	14.66425	13	0.67239	26	0.54849

STATIC BASE PRESSURES

IN TERMS OF ABSCLUTE PRESSURES

1	14.63534	2	14.64618	3	14.68592

IN TERMS OF CP

1	0.52943	2	0.53658	3	0.56279

CP = 0.55564 ETA = 0.66250

RUN NO	DATA PT	P AMB, IN. HG	P AMB PSIA
5.0000	0.0100	29.8760	14.6750

CALCULATIONS BASED ON WEIGHT FLOW RATE

AIR FLO RATE	FUEL FLO RATE	FUEL AIR RATIO	TOT FLO RATE
7.73825	0.11138	0.01439	7.84963

MACH NO.	QFLOW	V AVG.	DENSITY
0.37596	1.41011	715.16235	0.02554

PRESSURE COEFFICIENTS

INLET STATIC PRESSURES, IN TERMS OF CP

1	-0.01742	2	-0.00973	3	-0.03279	4	-0.04816	5	-0.18652
6	0.10812	7	0.07737	8	0.06969	9	0.09787	10	-0.05841
11	0.59750	12	0.59750	13	0.59750	14	0.59750	15	0.59750
16	0.59750	17	0.59750	18	0.59750	19	0.59750	20	0.59750

STATIC WALL PRESSURES, IN TERMS OF CP

	TIP		HUB
1	-0.02254	14	-0.13272
2	0.10812	15	0.14399
3	0.13374	16	0.31310
4	0.04407	17	0.52320
5	0.14912	18	0.43608
6	0.31054	19	0.30285
7	0.40534	20	0.07481
8	0.45402	21	0.10044
9	0.50526	22	0.18243
10	0.52064	23	0.36690
11	0.53601	24	0.50270
12	0.58982	25	0.56419
13	0.72305	26	0.58982

STATIC BASE PRESSURES IN TERMS OF CP

1	0.56932	2	0.57701	3	0.60519

CP = 0.59750 ETA = 0.71241

RATIO OF RAKE AVE Q TO FLOW AVE Q = 1.07533

ST9 FULL SCALE DIFFUSER (IR SUPPRESSING)
SWIRL ANGLE = 15.99 DEGREES

RUN NO	DATA PT	P AMB IN. HG	P AMB PSIA
5.0000	0.0100	29.8760	14.6750

INLET STATIC PRESSURES, PSIA

1 13.80797	2 13.81880	3 13.78629	4 13.76461	5 13.56951
6 13.98500	7 13.94165	8 13.93081	9 13.97055	10 13.75016
11 14.67509	12 14.67509	13 14.67509	14 14.67509	15 14.67509
16 14.67509	17 14.67509	18 14.67509	19 14.67509	20 14.67509

STATIC WALL PRESSURES, PSIA

OUTER WALL

Pw 1 13.80074	Pw 2 13.98500	Pw 3 14.02113	Pw 4 13.59468	Pw 5 14.04281
Pw 6 14.27043	Pw 7 14.40411	Pw 8 14.47276	Pw 9 14.54502	Pw10 14.56670
Pw11 14.58837	Pw12 14.66425	Pw13 14.85212	Pw	

INNER WALL

Pw14 13.64538	Pw15 14.03558	Pw16 14.27404	Pw17 14.57031	Pw18 14.44747
Pw19 14.25959	Pw20 13.93803	Pw21 13.97416	Pw22 14.08978	Pw23 14.34992
Pw24 14.54140	Pw25 14.62812	Pw26 14.66425	Pw	

OUTER WALL DKJ-5600

COOLANT INLET TOTAL PRESSURE (PB01) = 15.1483 PSIA
COOLANT INLET TOTAL TEMPERATURE (TB01) = 180.000 F
COOLANT INLET TOTAL TEMPERATURE (TB02) = 215.000 F
COOLANT INLET TOTAL TEMPERATURE (TB03) = 0.000 F
OUTER WALL UNCOOLED TEMPERATURE (TWUCO) = 930.000 F
OUTER PANEL NO.1 WALL STATIC PRES. (PW27) = 14.38604 PSIA
OUTER PANEL NO.2 WALL STATIC PRES. (PW28) = 14.57031 PSIA
OUTER PANEL NO.3 WALL STATIC PRES. (PW29) = 14.67147 PSIA
TOTAL COOLANT FLOW RATE = 0.27084 LB/SEC

	Z (IN)	X (IN)	R (IN)	TW (F)	
1	8.45200	8.71800	8.32200	380.00006	(TW 1)
2	9.50000	9.92400	8.91600	260.00006	(TW 2)
3	10.54800	11.10100	9.45400	460.00006	(TW 3)
4	12.12000	12.74900	9.93500	540.00012	(TW 4)
5	12.90600	13.53700	9.98500	460.00006	(TW 5)
6	14.21600	14.86000	9.82400	560.00012	(TW 6)
7	15.78800	16.49900	9.36600	630.00012	(TW 7)
8	16.31200	17.05400	9.18000	485.00006	(TW 8)
9	17.36000	18.16700	8.80300	505.00006	(TW 9)
10	18.66900	19.54000	8.39700	545.00012	(TW10)
11	19.47500	20.36900	8.19800	0.00000	(TW11)

INNER WALL DKJ-5600

COOLANT INLET TOTAL PRESSURE (PB02) = 16.2193 PSIA
COOLANT INLET TOTAL TEMPERATURE (TB04) = 0.000 F
COOLANT INLET TOTAL TEMPERATURE (TB05) = 310.000 F
COOLANT INLET TOTAL TEMPERATURE (TB06) = 100.000 F
INNER WALL UNCOOLED TEMPERATURE (TWUCI) = 1148.000 F
INNER PANEL NO.1 WALL STATIC PRES. (PW30) = 14.55586 PSIA
INNER PANEL NO.2 WALL STATIC PRES. (PW31) = 14.58954 PSIA
TOTAL COOLANT FLOW RATE = 0.12411 LB/SEC

	Z (IN)	X (IN)	R (IN)	TW (F)	
1	13.95400	15.02400	7.63600	510.00006	(TW12)
2	14.74000	15.93000	7.18700	0.00000	(TW13)
3	15.78800	17.24800	6.39000	0.00000	(TW14)
4	16.23200	17.83000	6.01200	440.00006	(TW15)
5	17.36000	19.33400	5.01800	585.00012	(TW16)

BASE REGION DKJ-5575

	RADIUS (IN)	STATIC PRESSURE (PSIA)	
1	0.00000	14.63534	P BASE 1
2	1.57000	14.64618	P BASE 2
3	3.10000	14.68592	P BASE 3

COOLANT INLET TOTAL PRESSURE (PB03) = 14.6324 PSIA
TOTAL COOLANT FLOW RATE = 0.00000 LB/SEC

	R (IN)	X (IN)	TW (F)	
1	1.20000	0.21990	0.00000	(TWB01)
2	1.92000	1.34310	760.00012	(TWB02)
3	2.62000	2.43100	860.00012	(TWB03)
4	3.58000	3.75300	0.00000	(TWB04)

BASE BULK TEMP (TBB1) = 815.00012 F

MIDSPAN INLET TOTAL PRESSURES

NO.	PT(PSIA)
1	15.115
2	15.462
3	15.383
4	15.376

HOT FLOW TEST WITH 0.033 COOLING FLOW RATE
MRP = 83 SWIRL ANGLE = 15 NO IR DATA INNER WALL FLOW CHANGED

RUN NO	DATA PT	P AMB, IN. HG	P AMB PSIA
6.0000	0.0100	29.8760	14.6750

WEIGHT FLOW RATE,PRIMARY

P1	DEL P	TEMP (R)	FLOW RATE
20.9624	7.0241	690.0001	7.7424

FUEL TO AIR RATIO = 0.0140 FUEL FLOW RATE = 0.1091 LBM/SEC

TOTAL PRIMARY FLOW RATE = 7.8515 LBM/SEC

WEIGHT FLOW RATE,COOLING AIR

	P1	DEL P	TEMP (R)	FLOW RATE
OUTER WALL	23.8750	7.0000	556.0001	0.1214
INNER WALL	24.6750	8.2000	556.0001	0.1317
BASE	14.6750	0.0000	460.0000	0.0000

TOTAL TEMP. (AFT OF BURNER CAN) = 1585.000 DEG R INLET TOTAL TEMP. = 1490.000 DEG R

PLENUM (MANIFOLD) PRESSURES PSIA

OUTER WALL	INNER WALL	BASE
14.7726	16.5175	14.6537

INLET PROBE DATA (BASED ON INLET DATA)

PTB	PSI	PSBAR	A R	(PT1-PA)/Q1	DENSITY	CAL FLO RATE	QFLO	QW1	QI
15.32675	13.75738	14.03874	2.49000	0.50594	0.00080	7.83468	1.56937	1.28800	1.49877

SPAN	VEL	PT	PS	Y
0.00000	0.00000	13.75738	13.75738	4.90600
0.04522	0.70986	14.69315	13.75852	4.98600
0.04522	0.76021	14.83044	13.75852	4.98600
0.15262	0.92851	15.36517	13.76609	5.17599
0.15262	0.96352	15.48801	13.76609	5.17599
0.24307	0.97534	15.53859	13.77415	5.33599
0.24307	1.00000	15.62892	13.77415	5.33599
0.33917	0.99077	15.60363	13.78291	5.50599
0.33917	0.98189	15.57111	13.78291	5.50599
0.44657	0.98726	15.60001	13.79218	5.69600
0.44657	0.96834	15.53137	13.79218	5.69600
0.54267	0.97916	15.57834	13.80004	5.86599
0.54267	0.94267	15.44827	13.80004	5.86599
0.63877	0.96913	15.54943	13.80739	6.03599
0.63877	0.92701	15.40130	13.80739	6.03599

0.74053	0.95391	15.50246	13.81472	6.21599
0.74053	0.91535	15.36878	13.81472	6.21599
0.83663	0.92720	15.41575	13.82117	6.38599
0.83663	0.88529	15.27484	13.82117	6.38599
0.92142	0.82807	15.09781	13.82598	6.53599
0.92142	0.79934	15.01109	13.82598	6.53599
1.00000	0.00000	13.82790	13.82790	6.67500

RUN NO	DATA PT	P AMB. IN. HG	P AMB PSIA
6.0000	0.0100	29.8760	14.6750

PRESSURE COEFFICIENTS (BASED ON INLET DATA)

INLET STATIC PRESSURES

IN TERMS OF ABSOLUTE PRESSURES

1	13.81519	2	13.82603	3	13.79713	4	13.76822	5	13.58035
6	13.98862	7	13.94165	8	13.92719	9	13.96694	10	13.75016
11	14.67509	12	14.67509	13	14.67509	14	14.67509	15	14.67509
16	14.67509	17	14.67509	18	14.67509	19	14.67509	20	14.67509

IN TERMS OF CP

1	-0.01405	2	-0.00678	3	-0.02617	4	-0.04556	5	-0.17160
6	0.10228	7	0.07077	8	0.06108	9	0.08774	10	-0.05768
11	0.56281	12	0.56281	13	0.56281	14	0.56281	15	0.56281
16	0.56281	17	0.56281	18	0.56281	19	0.56281	20	0.56281

STATIC WALL PRESSURES

IN TERMS OF ABSOLUTE PRESSURES				IN TERMS OF CP			
TIP		HUB		TIP		HUB	
1	13.79713	14	13.62370	1	-0.02617	14	-0.14252
2	13.97778	15	14.02113	2	0.09501	15	0.12410
3	14.01752	16	14.26320	3	0.12167	16	0.28649
4	13.89468	17	14.56670	4	0.03926	17	0.49010
5	14.04281	18	14.44385	5	0.13864	18	0.40769
6	14.27766	19	14.25959	6	0.29619	19	0.28407
7	14.39327	20	13.94165	7	0.37375	20	0.07077
8	14.49805	21	13.97055	8	0.44404	21	0.09016
9	14.55586	22	14.08978	9	0.48282	22	0.17015
10	14.57031	23	14.36075	10	0.49252	23	0.35194
11	14.59560	24	14.53779	11	0.50949	24	0.47071
12	14.66425	25	14.62812	12	0.55554	25	0.53130
13	14.87741	26	14.66063	13	0.69855	26	0.55312

STATIC BASE PRESSURES

IN TERMS OF ABSOLUTE PRESSURES

1	14.63895	2	14.64618	3	14.69315

IN TERMS OF CP

1	0.53857	2	0.54342	3	0.57493

CP = 0.56281 ETA = 0.67104

RUN NO	DATA PT	P AMB, IN. HG	P AMB PSIA
6.0000	0.0100	29.8760	14.6750

CALCULATIONS BASED ON WEIGHT FLOW RATE

AIR FLO RATE	FUEL FLO RATE	FUEL AIR RATIO	TOT FLO RATE
7.74240	0.10916	0.01409	7.85157

MACH NO.	QFLOW	V AVG.	DENSITY
0.37518	1.40574	712.77502	0.02563

PRESSURE COEFFICIENTS

INLET STATIC PRESSURES, IN TERMS OF CP

1	-0.01490	2	-0.00719	3	-0.02775	4	-0.04831	5	-0.18196
6	0.10846	7	0.07504	8	0.06476	9	0.09303	10	-0.06116
11	0.59679	12	0.59679	13	0.59679	14	0.59679	15	0.59679
16	0.59679	17	0.59679	18	0.59679	19	0.59679	20	0.59679

STATIC WALL PRESSURES, IN TERMS OF CP

	TIP		HUB
1	-0.02775	14	-0.15112
2	0.10075	15	0.13159
3	0.12902	16	0.30379
4	0.04163	17	0.51968
5	0.14701	18	0.43230
6	0.31407	19	0.30122
7	0.39631	20	0.07504
8	0.47085	21	0.09560
9	0.51197	22	0.18042
10	0.52225	23	0.37318
11	0.54024	24	0.49912
12	0.58908	25	0.56337
13	0.74072	26	0.58650

STATIC BASE PRESSURES IN TERMS OF CP

1	0.57108	2	0.57622	3	0.60964

CP = 0.59679　　ETA = 0.71155

RATIO OF RAKE AVE Q TO FLOW AVE Q = 1.06036

ST9 FULL SCALE DIFFUSER (IR SUPPRESSING)
SWIRL ANGLE = 15.99 DEGREES

RUN NO	DATA PT	P AMB IN. HG	P AMB PSIA
6.0000	0.0100	29.8760	14.6750

INLET STATIC PRESSURES. PSIA

1 13.81519	2 13.82603	3 13.79713	4 13.76822	5 13.58035
6 13.98862	7 13.94165	8 13.92719	9 13.96694	10 13.75016
11 14.67509	12 14.67509	13 14.67509	14 14.67509	15 14.67509
16 14.67509	17 14.67509	18 14.67509	19 14.67509	20 14.67509

STATIC WALL PRESSURES, PSIA

OUTER WALL

PW 1 13.79713	PW 2 13.97778	PW 3 14.01752	PW 4 13.89468	PW 5 14.04281
PW 6 14.27766	PW 7 14.39327	PW 8 14.49805	PW 9 14.55586	PW10 14.57031
PW11 14.59560	PW12 14.66425	PW13 14.87741	PW	

INNER WALL

PW14 13.62370	PW15 14.02113	PW16 14.26320	PW17 14.56670	PW18 14.44385
PW19 14.25959	PW20 13.94165	PW21 13.97055	PW22 14.08978	PW23 14.36075
PW24 14.53779	PW25 14.62812	PW26 14.66063	PW	

OUTER WALL DKJ-5600

COOLANT INLET TOTAL PRESSURE (PB01) = 14.7726 PSIA
COOLANT INLET TOTAL TEMPERATURE (TB01) = 210.000 F
COOLANT INLET TOTAL TEMPERATURE (TB02) = 375.000 F
COOLANT INLET TOTAL TEMPERATURE (TB03) = 0.000 F
OUTER WALL UNCOOLED TEMPERATURE (TWUCO) = 965.000 F
OUTER PANEL NO.1 WALL STATIC PRES. (PW27) = 14.39688 PSIA
OUTER PANEL NO.2 WALL STATIC PRES. (PW28) = 14.55224 PSIA
OUTER PANEL NO.3 WALL STATIC PRES. (PW29) = 14.67147 PSIA
TOTAL COOLANT FLOW RATE = 0.12146 LB/SEC

	Z (IN)	X (IN)	R (IN)	TW (F)	
1	8.45200	8.71800	8.32200	490.00006	(TW 1)
2	9.50000	9.92400	8.91600	390.00006	(TW 2)
3	10.54800	11.10100	9.45400	602.00012	(TW 3)
4	12.12000	12.74900	9.93500	705.00012	(TW 4)
5	12.90600	13.53700	9.98500	615.00012	(TW 5)
6	14.21600	14.86000	9.82400	720.00012	(TW 6)
7	15.78800	16.49900	9.36600	785.00012	(TW 7)
8	16.31200	17.05400	9.18000	650.00012	(TW 8)
9	17.36000	18.16700	8.80300	705.00012	(TW 9)
10	18.66900	19.54000	8.39700	750.00012	(TW10)
11	19.47500	20.36900	8.19800	0.00000	(TW11)

INNER WALL DKJ-5600

COOLANT INLET TOTAL PRESSURE (PB02) = 16.5175 PSIA
COOLANT INLET TOTAL TEMPERATURE (TB04) = 125.000 F
COOLANT INLET TOTAL TEMPERATURE (TB05) = 315.000 F
COOLANT INLET TOTAL TEMPERATURE (TB06) = 100.000 F
INNER WALL UNCOOLED TEMPERATURE (TWUCI) = 1150.000 F
INNER PANEL NO.1 WALL STATIC PRES. (PW30) = 14.54863 PSIA
INNER PANEL NO.2 WALL STATIC PRES. (PW31) = 14.68592 PSIA
TOTAL COOLANT FLOW RATE = 0.13172 LB/SEC

	Z (IN)	X (IN)	R (IN)	TW (F)	
1	13.95400	15.02400	7.63600	510.00006	(TW12)
2	14.74000	15.93000	7.18700	0.00000	(TW13)
3	15.78800	17.24800	6.39000	0.00000	(TW14)
4	16.23200	17.83000	6.01200	465.00006	(TW15)
5	17.36000	19.33400	5.01800	615.00012	(TW16)

BASE REGION DKJ-5575

	RADIUS (IN)	STATIC PRESSURE (PSIA)	
1	0.00000	14.63895	P BASE 1
2	1.57000	14.64618	P BASE 2
3	3.10000	14.69315	P BASE 3

COOLANT INLET TOTAL PRESSURE (PB03) = 14.6537 PSIA
TOTAL COOLANT FLOW RATE = 0.00000 LB/SEC

	R (IN)	X (IN)	TW (F)	
1	1.20000	0.21990	0.00000	(TWB01)
2	1.92000	1.34310	755.00012	(TWB02)
3	2.62000	2.43100	865.00012	(TWB03)
4	3.58000	3.75300	0.00000	(TWB04)

BASE BULK TEMP (TBB1) = 830.00012 F

MIDSPAN INLET TOTAL PRESSURES

NO.	PT(PSIA)
1	15.105
2	15.444
3	15.365
4	15.361

HOT FLOW TEST WITH 0.025 COOLING FLOW RATE
VRP = 83 SWIRL ANGLE = 16 NO IR DATA

RUN NO	DATA PT	P AMB. IN. HG	P AMB PSIA
6.0000	0.0200	29.8760	14.6750

WEIGHT FLOW RATE,PRIMARY

P1	DEL P	TEMP (R)	FLOW RATE
20.9624	7.0241	685.0001	7.7706

FUEL TO AIR RATIO = 0.0143 FUEL FLOW RATE = 0.1113 LBM/SEC

TOTAL PRIMARY FLOW RATE = 7.8820 LBM/SEC

WEIGHT FLOW RATE,COOLING AIR

OUTER WALL

P1	DEL P	TEMP (R)	FLOW RATE
24.6750	7.0000	552.0001	0.1243

INNER WALL

P1	DEL P	TEMP (R)	FLOW RATE
18.6750	3.8000	551.0001	0.0821

BASE

P1	DEL P	TEMP (R)	FLOW RATE
14.6750	0.0000	460.0000	0.0000

TOTAL TEMP. (AFT OF BURNER CAN) = 1595.000 DEG R INLET TOTAL TEMP. = 1495.000 DEG R

PLENUM (MANIFOLD) PRESSURES PSIA

OUTER WALL	INNER WALL	BASE
14.8051	15.3673	14.6857

INLET PROBE DATA (BASED ON INLET DATA)

PTB	PSI	PSBAR	A R	(PT1-PA)/Q1	DENSITY	CAL FLO RATE	GFLO	QW1	QI
15.34440	13.74293	14.03088	2.49000	0.50956	0.00079	7.89718	1.60147	1.31352	1.53002

SPAN	VEL	PT	PS	Y
0.00000	0.00000	13.74293	13.74293	4.90600
0.04522	0.71786	14.71483	13.74411	4.98600
0.04522	0.73109	14.75096	13.74411	4.98600
0.15262	0.93377	15.39407	13.75161	5.17599
0.15262	0.94399	15.43020	13.75161	5.17599
0.24307	0.98063	15.57111	13.75968	5.33599
0.24307	1.00000	15.64337	13.75968	5.33599
0.33917	0.99761	15.64337	13.76864	5.50599
0.33917	0.99183	15.62169	13.76864	5.50599
0.44657	0.99506	15.64337	13.77822	5.69600
0.44657	0.97854	15.58195	13.77822	5.69600
0.54267	0.98805	15.62530	13.78636	5.86599
0.54267	0.95045	15.48801	13.78636	5.86599
0.63877	0.97721	15.59279	13.79395	6.03599
0.63877	0.93303	15.43381	13.79395	6.03599

0.74053	0.96229	15.54582	13.80151	6.21599
0.74053	0.91320	15.37239	13.80151	6.21599
0.83663	0.93517	15.45549	13.80810	6.38599
0.83663	0.87257	15.24233	13.80810	6.38599
0.92142	0.83398	15.12310	13.81295	6.53599
0.92142	0.79028	14.98941	13.81295	6.53599
1.00000	0.00000	13.81484	13.81484	6.67500

RUN NO	DATA PT	P AMB, IN. HG	P AMB PSIA
6.0000	0.0200	29.8760	14.6750

PRESSURE COEFFICIENTS (BASED ON INLET DATA)

INLET STATIC PRESSURES

IN TERMS OF ABSOLUTE PRESSURES

1	13.80797	2	13.81519	3	13.77906	4	13.75377	5	13.55867
6	13.98862	7	13.93803	8	13.92719	9	13.95610	10	13.73571
11	14.67509	12	14.67509	13	14.67509	14	14.67509	15	14.67509
16	14.67509	17	14.67509	18	14.67509	19	14.67509	20	14.67509

IN TERMS OF CP

1	-0.01189	2	-0.00713	3	-0.03093	4	-0.04759	5	-0.17608
6	0.10707	7	0.07376	8	0.06662	9	0.08566	10	-0.05948
11	0.55918	12	0.55918	13	0.55918	14	0.55918	15	0.55918
16	0.55918	17	0.55918	18	0.55918	19	0.55918	20	0.55918

STATIC WALL PRESSURES

IN TERMS OF ABSOLUTE PRESSURES				IN TERMS OF CP			
TIP		HUB		TIP		HUB	
1	13.78629	14	13.61648	1	-0.02617	14	-0.13801
2	13.96694	15	14.01391	2	0.09280	15	0.12373
3	14.00668	16	14.25959	3	0.11897	16	0.28554
4	13.87661	17	14.57031	4	0.03331	17	0.49018
5	14.03197	18	14.44024	5	0.13563	18	0.40451
6	14.26682	19	14.24875	6	0.29030	19	0.27840
7	14.38604	20	13.91636	7	0.36882	20	0.05948
8	14.44385	21	13.95610	8	0.40689	21	0.08566
9	14.52695	22	14.08255	9	0.46162	22	0.16894
10	14.56670	23	14.33185	10	0.48780	23	0.33313
11	14.60282	24	14.53418	11	0.51159	24	0.46638
12	14.66786	25	14.59921	12	0.55442	25	0.50921
13	14.72205	26	14.64979	13	0.59012	26	0.54253

STATIC BASE PRESSURES

IN TERMS OF ABSOLUTE PRESSURES

1	14.66063	2	14.66063	3	14.70038

IN TERMS OF CP

1	0.54966	2	0.54966	3	0.57584

CP = 0.55918 ETA = 0.66672

RUN NO	DATA PT	P AMB, IN. HG	P AMB PSIA
6.0000	0.0200	29.8760	14.6750

CALCULATIONS BASED ON WEIGHT FLOW RATE

AIR FLO RATE	FUEL FLO RATE	FUEL AIR RATIO	TOT FLO RATE
7.77061	0.11138	0.01433	7.88200

MACH NO.	QFLOW	V AVG.	DENSITY
0.37757	1.42209	718.28015	0.02554

PRESSURE COEFFICIENTS

INLET STATIC PRESSURES, IN TERMS OF CP

1	-0.01270	2	-0.00762	3	-0.03302	4	-0.05081	5	-0.18800
6	0.11432	7	0.07875	8	0.07113	9	0.09146	10	-0.06351
11	0.59704	12	0.59704	13	0.59704	14	0.59704	15	0.59704
16	0.59704	17	0.59704	18	0.59704	19	0.59704	20	0.59704

STATIC WALL PRESSURES, IN TERMS OF CP

	TIP		HUB
1	-0.02794	14	-0.14735
2	0.09908	15	0.13211
3	0.12703	16	0.30487
4	0.03556	17	0.52336
5	0.14481	18	0.43190
6	0.30995	19	0.29725
7	0.39379	20	0.06351
8	0.43444	21	0.09146
9	0.49287	22	0.18038
10	0.52082	23	0.35568
11	0.54623	24	0.49796
12	0.59196	25	0.54369
13	0.63007	26	0.57926

STATIC BASE PRESSURES IN TERMS OF CP

1	0.58688	2	0.58688	3	0.61482

CP = 0.59704 ETA = 0.71185

RATIO OF RAKE AVE Q TO FLOW AVE Q = 1.06770

ST9 FULL SCALE DIFFUSER (IR SUPPRESSING)
SWIRL ANGLE = 15.99 DEGREES

RUN NO	DATA PT	P AMB IN. HG	P AMB PSIA
6.0000	0.0200	29.8760	14.6750

INLET STATIC PRESSURES. PSIA

1 13.80797	2 13.81519	3 13.77906	4 13.75377	5 13.55867
6 13.98862	7 13.93803	8 13.92719	9 13.95610	10 13.73571
11 14.67509	12 14.67509	13 14.67509	14 14.67509	15 14.67509
16 14.67509	17 14.67509	18 14.67509	19 14.67509	20 14.67509

STATIC WALL PRESSURES, PSIA

OUTER WALL

PW 1 13.78629	PW 2 13.96694	PW 3 14.00668	PW 4 13.87661	PW 5 14.03197
PW 6 14.26682	PW 7 14.38604	PW 8 14.44385	PW 9 14.52695	PW10 14.56670
PW11 14.60282	PW12 14.66786	PW13 14.72205	PW	

INNER WALL

PW14 13.61648	PW15 14.01391	PW16 14.25959	PW17 14.57031	PW18 14.44024
PW19 14.24875	PW20 13.91636	PW21 13.95610	PW22 14.08255	PW23 14.33185
PW24 14.53418	PW25 14.59921	PW26 14.64979	PW	

OUTER WALL DKJ-5600

COOLANT INLET TOTAL PRESSURE (PB01) = 14.8051 PSIA
COOLANT INLET TOTAL TEMPERATURE (TB01) = 240.000 F
COOLANT INLET TOTAL TEMPERATURE (TB02) = 390.000 F
COOLANT INLET TOTAL TEMPERATURE (TB03) = 0.000 F
OUTER WALL UNCOOLED TEMPERATURE (TWUCO) = 965.000 F
OUTER PANEL NO.1 WALL STATIC PRES. (PW27) = 14.40411 PSIA
OUTER PANEL NO.2 WALL STATIC PRES. (PW28) = 14.55947 PSIA
OUTER PANEL NO.3 WALL STATIC PRES. (PW29) = 14.67509 PSIA
TOTAL COOLANT FLOW RATE = 0.12435 LB/SEC

	Z (IN)	X (IN)	R (IN)	TW (F)	
1	8.45200	8.71800	8.32200	465.00006	(TW 1)
2	9.50000	9.92400	8.91600	365.00006	(TW 2)
3	10.54800	11.10100	9.45400	595.00012	(TW 3)
4	12.12000	12.74900	9.93500	700.00012	(TW 4)
5	12.90600	13.53700	9.98500	620.00012	(TW 5)
6	14.21600	14.86000	9.82400	720.00012	(TW 6)
7	15.78800	16.49900	9.36600	755.00012	(TW 7)
8	16.31200	17.05400	9.18000	640.00012	(TW 8)
9	17.36000	18.16700	8.80300	685.00012	(TW 9)
10	18.66900	19.54000	8.39700	735.00012	(TW10)
11	19.47500	20.36900	8.19800	0.00000	(TW11)

INNER WALL DKJ-5600

COOLANT INLET TOTAL PRESSURE (PB02) = 15.3673 PSIA
COOLANT INLET TOTAL TEMPERATURE (TB04) = 100.000 F
COOLANT INLET TOTAL TEMPERATURE (TB05) = 375.000 F
COOLANT INLET TOTAL TEMPERATURE (TB06) = 95.000 F
INNER WALL UNCOOLED TEMPERATURE (TWUCI) = 1145.000 F
INNER PANEL NO.1 WALL STATIC PRES. (PW30) = 14.56670 PSIA
INNER PANEL NO.2 WALL STATIC PRES. (PW31) = 14.64257 PSIA
TOTAL COOLANT FLOW RATE = 0.08212 LB/SEC

	Z (IN)	X (IN)	R (IN)	TW (F)	
1	13.95400	15.02400	7.63600	565.00012	(TW12)
2	14.74000	15.93000	7.18700	0.00000	(TW13)
3	15.78800	17.24800	6.39000	0.00000	(TW14)
4	16.23200	17.83000	6.01200	515.00012	(TW15)
5	17.36000	19.33400	5.01800	690.00012	(TW16)

BASE REGION DKJ-5575

	RADIUS (IN)	STATIC PRESSURE (PSIA)	
1	0.00000	14.66063	P BASE 1
2	1.57000	14.66063	P BASE 2
3	3.10000	14.70038	P BASE 3

COOLANT INLET TOTAL PRESSURE (PB03) = 14.6857 PSIA
TOTAL COOLANT FLOW RATE = 0.00000 LB/SEC

	R (IN)	X (IN)	TW (F)	
1	1.20000	0.21990	0.00000	(TWB01)
2	1.92000	1.34310	800.00012	(TWB02)
3	2.62000	2.43100	910.00012	(TWB03)
4	3.58000	3.75300	0.00000	(TWB04)

BASE BULK TEMP (TBB) 885.00012 F

MIDSPAN INLET TOTAL PRESSURES

NO.	PT(PSIA)
1	15.130
2	15.469
3	15.390
4	15.397

HOT FLOW TEST WITH 0.10 COOLING FLOW RATE
WRP = 100 SWIRL ANGLE = 16 NO IR DATA

RUN NO	DATA PT	P AMB. IN. HG	P AMB PSIA
7.0000	0.0100	29.8670	14.6706

WEIGHT FLOW RATE,PRIMARY

P1	DEL P	TEMP (R)	FLOW RATE
22.4316	7.8100	700.0001	8.3415

FUEL TO AIR RATIO = 0.0153 FUEL FLOW RATE = 0.1283 LBM/SEC

TOTAL PRIMARY FLOW RATE = 8.4698 LBM/SEC

WEIGHT FLOW RATE,COOLING AIR

OUTER WALL

P1	DEL P	TEMP (R)	FLOW RATE
89.6706	41.6000	550.0001	0.5407

INNER WALL

P1	DEL P	TEMP (R)	FLOW RATE
45.6706	23.3000	547.0001	0.2843

BASE

P1	DEL P	TEMP (R)	FLOW RATE
14.6706	0.0000	460.0000	0.0000

TOTAL TEMP. (AFT OF BURNER CAN) = 1605.000 DEG R INLET TOTAL TEMP. = 1600.000 DEG R

PLENUM (MANIFOLD) PRESSURES PSIA

OUTER WALL	INNER WALL	BASE
16.7589	20.0063	14.5641

INLET PROBE DATA (BASED ON INLET DATA)

PT2	PSI	PSBAR	A R	(PT1-PA)/Q1	DENSITY	CAL FLO RATE	QFLO	QW1	QI
15.98892	13.75224	14.28580	0.00000	0.77402	0.00075	8.75336	2.23668	1.70312	2.09535

SPAN	VEL	PT	PS	Y
0.00000	0.00000	13.75224	13.75224	4.90600
0.04522	0.81693	15.40410	13.75564	4.98600
0.04522	0.80339	15.34991	13.75564	4.98600
0.15262	0.94938	16.00025	13.77393	5.17599
0.15262	0.92043	15.86657	13.77393	5.17599
0.24307	0.97909	16.15922	13.79136	5.33599
0.24307	0.95336	16.03638	13.79136	5.33599
0.33917	0.99008	16.23148	13.81015	5.50599
0.33917	0.94859	16.03277	13.81015	5.50599
0.44657	0.99332	16.26761	13.83043	5.69600
0.44657	0.97699	16.18812	13.83043	5.69600
0.54267	0.99843	16.31097	13.84864	5.86599
0.54267	0.96718	16.15922	13.84864	5.86599
0.63877	0.99927	16.33264	13.86615	6.03599
0.63877	0.97182	16.19896	13.86615	6.03599

0.74053	1.00000	16.35432	13.88427	6.21599
0.74053	0.96652	16.19174	13.88427	6.21599
0.83663	0.98784	16.31097	13.90062	6.38599
0.83663	0.93536	16.06167	13.90062	6.38599
0.92142	0.88028	15.82682	13.91278	6.53599
0.92142	0.86435	15.75818	13.91278	6.53599
1.00000	0.00000	13.91782	13.91782	6.67500

RUN NO	DATA PT	P AMB. IN. HG	P AMB PSIA
7.0000	0.0100	29.8670	14.6706

PRESSURE COEFFICIENTS (BASED ON INLET DATA)

INLET STATIC PRESSURES

IN TERMS OF ABSOLUTE PRESSURES

1	13.83967	2	13.83245	3	13.81077	4	13.77464	5	13.50366
6	14.15400	7	14.07091	8	14.07091	9	14.08536	10	13.85774
11	14.67066	12	14.67066	13	14.67066	14	14.67066	15	14.67066
16	14.67066	17	14.67066	18	14.67066	19	14.67066	20	14.67066

IN TERMS OF CP

1	-0.02888	2	-0.03234	3	-0.04272	4	-0.06001	5	-0.18973
6	0.12159	7	0.08181	8	0.08181	9	0.08872	10	-0.02023
11	0.36892	12	0.36892	13	0.36892	14	0.36892	15	0.36892
16	0.36892	17	0.36892	18	0.36892	19	0.36892	20	0.36892

STATIC WALL PRESSURES

IN TERMS OF ABSOLUTE PRESSURES				IN TERMS OF CP			
TIP		HUB		TIP		HUB	
1	13.95890	14	13.60844	1	0.02819	14	-0.13957
2	13.95890	15	13.91916	2	0.02819	15	0.00916
3	13.88303	16	14.14678	3	-0.00812	16	0.11813
4	13.76019	17	14.63815	4	-0.06693	17	0.35335
5	13.89387	18	14.49001	5	-0.00294	18	0.28244
6	14.02755	19	14.13955	6	0.06105	19	0.11467
7	14.20820	20	13.77464	7	0.14753	20	-0.06001
8	14.35633	21	13.87942	8	0.21845	21	-0.00985
9	14.51531	22	14.14317	9	0.29455	22	0.11640
10	14.54782	23	14.36356	10	0.31011	23	0.22190
11	14.57673	24	14.49724	11	0.32395	24	0.28590
12	14.65983	25	14.67066	12	0.36373	25	0.36892
13	14.83325	26	14.67066	13	0.44675	26	0.36892

STATIC BASE PRESSURES

IN TERMS OF ABSOLUTE PRESSURES

1	14.62369	2	14.64537	3	14.65260

IN TERMS OF CP

1	0.34644	2	0.35681	3	0.36027

CP = 0.36892 ETA = -0.00000

RUN NO	DATA PT	P AMB, IN. HG	P AMB PSIA
7.0000	0.0100	29.8670	14.6706

CALCULATIONS BASED ON WEIGHT FLOW RATE

AIR FLO RATE	FUEL FLO RATE	FUEL AIR RATIO	TOT FLO RATE
8.34155	0.12833	0.01538	8.46988

MACH NO.	QFLOW	V AVG.	DENSITY
0.41655	1.84412	841.82678	0.02411

PRESSURE COEFFICIENTS

INLET STATIC PRESSURES, IN TERMS OF CP

1	-0.03271	2	-0.03663	3	-0.04839	4	-0.06798	5	-0.21492
6	0.13773	7	0.09267	8	0.09267	9	0.10050	10	-0.02292
11	0.41789	12	0.41789	13	0.41789	14	0.41789	15	0.41789
16	0.41789	17	0.41789	18	0.41789	19	0.41789	20	0.41789

STATIC WALL PRESSURES, IN TERMS OF CP

	TIP		HUB
1	0.03193	14	-0.15810
2	0.03193	15	0.01038
3	-0.00920	16	0.13381
4	-0.07582	17	0.40026
5	-0.00333	18	0.31993
6	0.06916	19	0.12989
7	0.16712	20	-0.06798
8	0.24744	21	-0.01116
9	0.33365	22	0.13185
10	0.35128	23	0.25136
11	0.36695	24	0.32385
12	0.41202	25	0.41789
13	0.50606	26	0.41789

STATIC BASE PRESSURES IN TERMS OF CP

1	0.39242	2	0.40418	3	0.40810

CP = 0.41789 ETA = -0.00000

RATIO OF RAKE AVE Q TO FLOW AVE Q = 1.13274

ST9 FULL SCALE DIFFUSER (IR SUPPRESSING)
SWIRL ANGLE = 21.00 DEGREES

RUN NO	DATA PT	P AMB IN. HG	P AMB PSIA
7.0000	0.0100	29.8670	14.6706

INLET STATIC PRESSURES, PSIA

1 13.83967	2 13.83245	3 13.81077	4 13.77464	5 13.50366
6 14.15400	7 14.07091	8 14.07091	9 14.08536	10 13.85774
11 14.67066	12 14.67066	13 14.67066	14 14.67066	15 14.67066
16 14.67066	17 14.67066	18 14.67066	19 14.67066	20 14.67066

STATIC WALL PRESSURES, PSIA

OUTER WALL

PW 1 13.95890	PW 2 13.95890	PW 3 13.88303	PW 4 13.76019	PW 5 13.89387
PW 6 14.02755	PW 7 14.20820	PW 8 14.35633	PW 9 14.51531	PW10 14.54782
PW11 14.57673	PW12 14.65983	PW13 14.83325	PW	

INNER WALL

PW14 13.60844	PW15 13.91916	PW16 14.14678	PW17 14.63815	PW18 14.49001
PW19 14.13955	PW20 13.77464	PW21 13.87942	PW22 14.14317	PW23 14.36356
PW24 14.49724	PW25 14.67066	PW26 14.67066	PW	

OUTER WALL DKJ-5600

COOLANT INLET TOTAL PRESSURE (PB01) = 16.7589 PSIA
COOLANT INLET TOTAL TEMPERATURE (TB01) = 135.000 F
COOLANT INLET TOTAL TEMPERATURE (TB02) = 145.000 F
COOLANT INLET TOTAL TEMPERATURE (TB03) = 0.000 F
OUTER WALL UNCOOLED TEMPERATURE (TWUCO) = 990.000 F
OUTER PANEL NO.1 WALL STATIC PRES. (PW27) = 14.07452 PSIA
OUTER PANEL NO.2 WALL STATIC PRES. (PW28) = 14.44666 PSIA
OUTER PANEL NO.3 WALL STATIC PRES. (PW29) = 14.66344 PSIA
TOTAL COOLANT FLOW RATE = 0.54077 LB/SEC

	Z (IN)	X (IN)	R (IN)	TW (F)	
1	8.45200	8.71800	8.32200	355.00006	(TW 1)
2	9.50000	9.92400	8.91600	252.00003	(TW 2)
3	10.54800	11.10100	9.45400	405.00006	(TW 3)
4	12.12000	12.74900	9.93500	450.00006	(TW 4)
5	12.90600	13.53700	9.98500	450.00006	(TW 5)
6	14.21600	14.86000	9.82400	475.00006	(TW 6)
7	15.78800	16.49900	9.36600	585.00012	(TW 7)
8	16.31200	17.05400	9.18000	415.00006	(TW 8)
9	17.36000	18.16700	8.80300	483.00006	(TW 9)
10	18.66900	19.54000	8.39700	425.00006	(TW10)
11	19.47500	20.36900	8.19800	0.00000	(TW11)

INNER WALL DKJ-5600

COOLANT INLET TOTAL PRESSURE (PB02) = 20.0063 PSIA
COOLANT INLET TOTAL TEMPERATURE (TB04) = 113.000 F
COOLANT INLET TOTAL TEMPERATURE (TB05) = 200.000 F
COOLANT INLET TOTAL TEMPERATURE (TB06) = 185.000 F
INNER WALL UNCOOLED TEMPERATURE (TWUCI) = 1135.000 F
INNER PANEL NO.1 WALL STATIC PRES. (PW30) = 14.54421 PSIA
INNER PANEL NO.2 WALL STATIC PRES. (PW31) = 14.79712 PSIA
TOTAL COOLANT FLOW RATE = 0.28437 LB/SEC

	Z (IN)	X (IN)	R (IN)	TW (F)	
1	13.95400	15.02400	7.63600	442.00006	(TW12)
2	14.74000	15.93000	7.18700	0.00000	(TW13)
3	15.78800	17.24800	6.39000	360.00006	(TW14)
4	16.23200	17.83000	6.01200	350.00006	(TW15)
5	17.36000	19.33400	5.01800	455.00006	(TW16)

BASE REGION DKJ-5575

	RADIUS (IN)	STATIC PRESSURE (PSIA)	
1	0.00000	14.62369	P BASE 1
2	1.57000	14.64537	P BASE 2
3	3.10000	14.65260	P BASE 3

COOLANT INLET TOTAL PRESSURE (PB03) = 14.5641 PSIA
TOTAL COOLANT FLOW RATE = 0.00000 LB/SEC

	R (IN)	X (IN)	TW (F)	
1	1.20000	0.21990	0.00000	(TWB01)
2	1.92000	1.34310	0.65000	(TWB02)
3	2.62000	2.43100	755.00012	(TWB03)
4	3.58000	3.75300	0.00000	(TWB04)

BASE BULK TEMP (TBB1) = 715.00012 F

MIDSPAN INLET TOTAL PRESSURES

NO.	PT(PSIA)
1	15.581
2	16.079
3	16.473
4	16.061

HOT FLOW TEST WITH 0.05 COOLING FLOW RATE
MRF = 100 SWIRL ANGLE = 21 NO IR DATA

RUN NO	DATA PT	P AMB, IN. HG	P AMB PSIA
8.0000	0.0100	29.8670	14.6706

WEIGHT FLOW RATE,PRIMARY

P1	DEL P	TEMP (R)	FLOW RATE
22.3333	7.7118	705.0001	8.2507

FUEL TO AIR RATIO = 0.0152 FUEL FLOW RATE = 0.1261 LBM/SEC

TOTAL PRIMARY FLOW RATE = 8.3768 LBM/SEC

WEIGHT FLOW RATE,COOLING AIR

	P1	DEL P	TEMP (R)	FLOW RATE
OUTER WALL	46.1706	20.0000	550.0001	0.2722
INNER WALL	25.6706	9.0000	550.0001	0.1405
BASE	14.6706	0.0000	460.0000	0.0000

TOTAL TEMP. (AFT OF BURNER CAN) = 1610.000 DEG R INLET TOTAL TEMP. = 1600.000 DEG R

PLENUM (MANIFOLD) PRESSURES PSIA

OUTER WALL	INNER WALL	BASE
15.4402	16.4918	14.6706

INLET PROBE DATA (BASED ON INLET DATA)

PTB	PSI	PSBAR	A R	(PT1-PA)/Q1	DENSITY	CAL FLO RATE	GFLO	QW1	QI
15.96672	13.78476	14.30528	2.49000	0.78007	0.00075	8.65054	2.18196	1.66144	2.04402

SPAN	VEL	PT	PS	Y
0.00000	0.00000	13.78476	13.78476	4.90600
0.04522	0.82219	15.41856	13.78812	4.98600
0.04522	0.80189	15.33907	13.78812	4.98600
0.15262	0.94988	15.98218	13.80596	5.17599
0.15262	0.91943	15.84489	13.80596	5.17599
0.24307	0.97732	16.12670	13.82293	5.33599
0.24307	0.95327	16.01470	13.82293	5.33599
0.33917	0.98794	16.19535	13.84123	5.50599
0.33917	0.94612	16.00025	13.84123	5.50599
0.44657	0.99213	16.23509	13.86097	5.69600
0.44657	0.97692	16.16283	13.86097	5.69600
0.54267	0.99747	16.27845	13.87873	5.86599
0.54267	0.96697	16.13393	13.87873	5.86599
0.63877	0.99917	16.30374	13.89583	6.03599
0.63877	0.97181	16.17367	13.89583	6.03599

0.74053	1.00000	16.32542	13.91352	6.21599
0.74053	0.96570	16.16283	13.91352	6.21599
0.83663	0.98914	16.28929	13.92949	6.38599
0.83663	0.93302	16.02915	13.92949	6.38599
0.92142	0.88330	15.82321	13.94137	6.53599
0.92142	0.86271	15.73650	13.94137	6.53599
1.00000	0.00000	13.94627	13.94627	6.67500

RUN NO	DATA PT	P AMB, IN. HG	P AMB PSIA
8.0000	0.0100	29.8670	14.6706

PRESSURE COEFFICIENTS (BASED ON INLET DATA)

INLET STATIC PRESSURES

IN TERMS OF ABSOLUTE PRESSURES

1	13.86858	2	13.86496	3	13.84329	4	13.80716	5	13.53980
6	14.17568	7	14.09258	8	14.09981	9	14.10704	10	13.88303
11	14.67066	12	14.67066	13	14.67066	14	14.67066	15	14.67066
16	14.67066	17	14.67066	18	14.67066	19	14.67066	20	14.67066

IN TERMS OF CP

1	-0.02924	2	-0.03101	3	-0.04164	4	-0.05937	5	-0.19052
6	0.12140	7	0.08064	8	0.08418	9	0.08773	10	-0.02215
11	0.36421	12	0.36421	13	0.36421	14	0.36421	15	0.36421
16	0.36421	17	0.36421	18	0.36421	19	0.36421	20	0.36421

STATIC WALL PRESSURES

IN TERMS OF ABSOLUTE PRESSURES				IN TERMS OF CP			
TIP		HUB		TIP		HUB	
1	13.86858	14	13.63735	1	-0.02924	14	-0.14267
2	13.98781	15	13.95168	2	0.02924	15	0.01152
3	13.91193	16	14.17207	3	-0.00797	16	0.11963
4	13.79270	17	14.65260	4	-0.06646	17	0.35535
5	13.91916	18	14.51531	5	-0.00443	18	0.28800
6	14.06007	19	14.17207	6	0.06469	19	0.11963
7	14.20459	20	13.80716	7	0.13558	20	-0.05937
8	14.34911	21	13.92639	8	0.20647	21	-0.00088
9	14.51892	22	14.17568	9	0.28978	22	0.12140
10	14.56950	23	14.37801	10	0.31459	23	0.22065
11	14.59840	24	14.52614	11	0.32877	24	0.29332
12	14.66344	25	14.62731	12	0.36067	25	0.34295
13	14.86938	26	14.66705	13	0.46169	26	0.36244

STATIC BASE PRESSURES

IN TERMS OF ABSOLUTE PRESSURES

1	14.67066	2	14.67066	3	14.66344

IN TERMS OF CP

1	0.36421	2	0.36421	3	0.36067

CP = 0.36421 ETA = 0.43426

RUN NO	DATA PT	P AMB, IN. HG	P AMB PSIA
8.0000	0.0100	29.8670	14.6706

CALCULATIONS BASED ON WEIGHT FLOW RATE

AIR FLO RATE	FUEL FLO RATE	FUEL AIR RATIO	TOT FLO RATE
8.25073	0.12611	0.01528	8.37684

MACH NO.	QFLOW	V AVG.	DENSITY
0.41133	1.80147	831.49365	0.02414

PRESSURE COEFFICIENTS

INLET STATIC PRESSURES, IN TERMS OF CP

1	-0.03309	2	-0.03509	3	-0.04713	4	-0.06718	5	-0.21559
6	0.13738	7	0.09125	8	0.09526	9	0.09927	10	-0.02506
11	0.41214	12	0.41214	13	0.41214	14	0.41214	15	0.41214
16	0.41214	17	0.41214	18	0.41214	19	0.41214	20	0.41214

STATIC WALL PRESSURES, IN TERMS OF CP

	TIP		HUB
1	-0.03309	14	-0.16144
2	0.03309	15	0.01303
3	-0.00902	16	0.13537
4	-0.07520	17	0.40211
5	-0.00501	18	0.32590
6	0.07320	19	0.13537
7	0.15342	20	-0.06718
8	0.23365	21	-0.00100
9	0.32791	22	0.13738
10	0.35599	23	0.24969
11	0.37203	24	0.33192
12	0.40813	25	0.38807
13	0.52245	26	0.41014

STATIC BASE PRESSURES IN TERMS OF CP

1	0.41214	2	0.41214	3	0.40813

CP = 0.41214 ETA = 0.49140

RATIO OF RAKE AVE Q TO FLOW AVE Q = 1.13159

ST9 FULL SCALE DIFFUSER (IR SUPPRESSING)
SWIRL ANGLE = 21.00 DEGREES

RUN NO	DATA PT	P AMB IN. HG	P AMB PSIA
8.0000	0.0100	29.8670	14.6706

INLET STATIC PRESSURES, PSIA

1 13.86858	2 13.86496	3 13.84329	4 13.80716	5 13.53980
6 14.17568	7 14.09258	8 14.09981	9 14.10704	10 13.88303
11 14.67066	12 14.67066	13 14.67066	14 14.67066	15 14.67066
16 14.67066	17 14.67066	18 14.67066	19 14.67066	20 14.67066

STATIC WALL PRESSURES, PSIA

OUTER WALL

PW 1 13.86858	PW 2 13.98781	PW 3 13.91193	PW 4 13.79270	PW 5 13.91916
PW 6 14.06007	PW 7 14.20459	PW 8 14.34911	PW 9 14.51892	PW10 14.56950
PW11 14.59840	PW12 14.66344	PW13 14.86938	PW	

INNER WALL

PW14 13.63735	PW15 13.95168	PW16 14.17207	PW17 14.65260	PW18 14.51531
PW19 14.17207	PW20 13.80716	PW21 13.92639	PW22 14.17568	PW23 14.37801
PW24 14.52614	PW25 14.62731	PW26 14.66705	PW	

DKJ-5600

OUTER WALL

COOLANT INLET TOTAL PRESSURE (PB01) = 15.4402 PSIA
COOLANT INLET TOTAL TEMPERATURE (TB01) = 190.000 F
COOLANT INLET TOTAL TEMPERATURE (TB02) = 260.000 F
COOLANT INLET TOTAL TEMPERATURE (TB03) = 0.000 F
COOLANT INLET TOTAL TEMPERATURE (TWUCO) = 1000.000 F
OUTER WALL UNCOOLED TEMPERATURE (TWUCO) = 1000.000 F
OUTER PANEL NO.1 WALL STATIC PRES. (PW27) = 14.18291 PSIA
OUTER PANEL NO.2 WALL STATIC PRES. (PW28) = 14.48279 PSIA
OUTER PANEL NO.3 WALL STATIC PRES. (PW29) = 14.67066 PSIA
TOTAL COOLANT FLOW RATE = 0.27229 LB/SEC

	Z (IN)	X (IN)	R (IN)	TW (F)	
1	8.45200	8.71800	8.32200	445.00006	(TW 1)
2	9.50000	9.92400	8.91600	325.00006	(TW 2)
3	10.54800	11.10100	9.45400	540.00012	(TW 3)
4	12.12000	12.74900	9.93500	675.00012	(TW 4)
5	12.90600	13.53700	9.98500	575.00012	(TW 5)
6	14.21600	14.86000	9.82400	665.00012	(TW 6)
7	15.78800	16.49900	9.36600	620.00012	(TW 7)
8	16.31200	17.05400	9.18000	570.00012	(TW 8)
9	17.36000	18.16700	8.80300	585.00012	(TW 9)
10	18.66900	19.54000	8.39700	635.00012	(TW10)
11	19.47500	20.36900	8.19800	0.00000	(TW11)

INNER WALL DKJ-5600

COOLANT INLET TOTAL PRESSURE (PB02) = 16.4918 PSIA
COOLANT INLET TOTAL TEMPERATURE (TB04) = 110.000 F
COOLANT INLET TOTAL TEMPERATURE (TB05) = 310.000 F
COOLANT INLET TOTAL TEMPERATURE (TB06) = 0.000 F
INNER WALL UNCOOLED TEMPERATURE (TWUCI) = 1140.000 F
INNER PANEL NO.1 WALL STATIC PRES. (PW30) = 14.51531 PSIA
INNER PANEL NO.2 WALL STATIC PRES. (PW31) = 14.69595 PSIA
TOTAL COOLANT FLOW RATE = 0.14055 LB/SEC

	Z (IN)	X (IN)	R (IN)	TW (F)	
1	13.95400	15.02400	7.63600	590.00012	(TW12)
2	14.74000	15.93000	7.18700	0.00000	(TW13)
3	15.78800	17.24800	6.39000	0.00000	(TW14)
4	16.23200	17.83000	6.01200	460.00006	(TW15)
5	17.36000	19.33400	5.01800	625.00012	(TW16)

BASE REGION DKJ-5575

	RADIUS (IN)	STATIC PRESSURE (PSIA)	
1	0.00000	14.67066	P BASE 1
2	1.57000	14.67066	P BASE 2
3	3.10000	14.66344	P BASE 3

COOLANT INLET TOTAL PRESSURE (PB03) = 14.6706 PSIA
TOTAL COOLANT FLOW RATE = 0.00000 LB/SEC

	R (IN)	X (IN)	TW (F)	
1	1.20000	0.21990	0.00000	(TWB01)
2	1.92000	1.34310	780.00012	(TWB02)
3	2.62000	2.43100	870.00012	(TWB03)
4	3.58000	3.75300	0.00000	(TWB04)

BASE BULK TEMP (TBB1) = 845.00012 F

MIDSPAN INLET TOTAL PRESSURES

NO.	PT(PSIA)
1	15.573
2	16.090
3	16.473
4	16.021

HOT FLOW TEST WITH 0.025 COOLING FLOW RATE
MRP = 100 SWIRL ANGLE = 21 NO IR DATA

RUN NO	DATA PT	P AMB, IN. HG	P AMB PSIA
9.0000	0.0100	29.8670	14.6706

WEIGHT FLOW RATE,PRIMARY

P1	DEL P	TEMP (R)	FLOW RATE
22.3825	7.7609	710.0001	8.2521

FUEL TO AIR RATIO = 0.0153 FUEL FLOW RATE = 0.1263 LBM/SEC

TOTAL PRIMARY FLOW RATE = 8.3785 LBM/SEC

WEIGHT FLOW RATE,COOLING AIR

OUTER WALL

P1	DEL P	TEMP (R)	FLOW RATE
26.6706	8.2000	550.0001	0.1389

INNER WALL

P1	DEL P	TEMP (R)	FLOW RATE
18.6706	4.0000	550.0001	0.0840

BASE

P1	DEL P	TEMP (R)	FLOW RATE
14.6706	0.0000	460.0000	0.0000

TOTAL TEMP. (AFT OF BURNER CAN) = 1605.000 DEG R INLET TOTAL TEMP. = 1600.000 DEG R

PLENUM (MANIFOLD) PRESSURES PSIA

OUTER WALL	INNER WALL	BASE
14.9452	15.3629	14.6706

INLET PROBE DATA (BASED ON INLET DATA)

PTB	PSI	PSBAR	A R	(PT1-PA)/Q1	DENSITY	CAL FLO RATE	QFLO	QW1	QI
15.99334	13.78620	14.31258	2.49000	0.78695	0.00075	8.70335	2.20714	1.68075	2.06746

SPAN	VEL	PT	PS	Y
0.00000	0.00000	13.78620	13.78620	4.90600
0.04522	0.82521	15.45468	13.78963	4.98600
0.04522	0.80710	15.38242	13.78963	4.98600
0.15262	0.94848	16.00748	13.80780	5.17599
0.15262	0.92082	15.88102	13.80780	5.17599
0.24307	0.97479	16.14838	13.82497	5.33599
0.24307	0.95178	16.03999	13.82497	5.33599
0.33917	0.98526	16.21703	13.84345	5.50599
0.33917	0.94312	16.01831	13.84345	5.50599
0.44657	0.98937	16.25677	13.86334	5.69600
0.44657	0.97584	16.19174	13.86334	5.69600
0.54267	0.99536	16.30374	13.88128	5.86599
0.54267	0.96521	16.15922	13.88128	5.86599
0.63877	0.99774	16.33264	13.89856	6.03599
0.63877	0.96919	16.19535	13.89856	6.03599

0.74053	1.00000	16.36155	13.91645	6.21599
0.74053	0.96388	16.18812	13.91645	6.21599
0.83663	0.98924	16.32542	13.93261	6.38599
0.83663	0.93155	16.05444	13.93261	6.38599
0.92142	0.88408	15.85573	13.94465	6.53599
0.92142	0.86122	15.75818	13.94465	6.53599
1.00000	0.00000	13.94960	13.94960	6.67500

RUN NO	DATA PT	P AMB, IN. HG	P AMB PSIA
9.0000	0.0100	29.8670	14.6706

PRESSURE COEFFICIENTS (BASED ON INLET DATA)

INLET STATIC PRESSURES

IN TERMS OF ABSOLUTE PRESSURES

1	13.86858	2	13.86496	3	13.84329	4	13.81077	5	13.54341
6	14.18291	7	14.09981	8	14.10342	9	14.11787	10	13.89026
11	14.67066	12	14.67066	13	14.67066	14	14.67066	15	14.67066
16	14.67066	17	14.67066	18	14.67066	19	14.67066	20	14.67066

IN TERMS OF CP

1	-0.03103	2	-0.03278	3	-0.04330	4	-0.05908	5	-0.18881
6	0.12149	7	0.08117	8	0.08292	9	0.08993	10	-0.02051
11	0.35817	12	0.35817	13	0.35817	14	0.35817	15	0.35817
16	0.35817	17	0.35817	18	0.35817	19	0.35817	20	0.35817

STATIC WALL PRESSURES

IN TERMS OF ABSOLUTE PRESSURES				IN TERMS OF CP			
TIP		HUB		TIP		HUB	
1	13.87942	14	13.64818	1	-0.02577	14	-0.13797
2	13.99142	15	13.88664	2	0.02857	15	-0.02226
3	13.91555	16	14.17568	3	-0.00823	16	0.11799
4	13.80354	17	14.67066	4	-0.06258	17	0.35817
5	13.93361	18	14.52614	5	0.00052	18	0.28804
6	14.07452	19	14.18652	6	0.06890	19	0.12325
7	14.20459	20	13.82522	7	0.13201	20	-0.05206
8	14.38162	21	13.95529	8	0.21792	21	0.01104
9	14.52976	22	14.19013	9	0.28980	22	0.12500
10	14.59118	23	14.39969	10	0.31960	23	0.22668
11	14.61647	24	14.52976	11	0.33187	24	0.28980
12	14.67066	25	14.61285	12	0.35817	25	0.33012
13	14.89828	26	14.65983	13	0.46862	26	0.35291

STATIC BASE PRESSURES

IN TERMS OF ABSOLUTE PRESSURES

1	14.68873	2	14.68873	3	14.68150

IN TERMS OF CP

1	0.36694	2	0.36694	3	0.36343

CP = 0.35817 ETA = 0.42705

RUN NO	DATA PT	P AMB. IN. HG	P AMB PSIA
9.0000	0.0100	29.8670	14.6706

CALCULATIONS BASED ON WEIGHT FLOW RATE

AIR FLO RATE	FUEL FLO RATE	FUEL AIR RATIO	TOT FLO RATE
8.25214	0.12638	0.01531	8.37853

MACH NO.	QFLOW	V AVG.	DENSITY
0.41124	1.80162	831.39392	0.02415

PRESSURE COEFFICIENTS

INLET STATIC PRESSURES, IN TERMS OF CP

1	-0.03549	2	-0.03750	3	-0.04953	4	-0.06758	5	-0.21598
6	0.13897	7	0.09285	8	0.09485	9	0.10287	10	-0.02346
11	0.40970	12	0.40970	13	0.40970	14	0.40970	15	0.40970
16	0.40970	17	0.40970	18	0.40970	19	0.40970	20	0.40970

STATIC WALL PRESSURES, IN TERMS OF CP

	TIP		HUB
1	-0.02947	14	-0.15782
2	0.03268	15	-0.02546
3	-0.00942	16	0.13496
4	-0.07159	17	0.40970
5	0.00060	18	0.32949
6	0.07881	19	0.14098
7	0.15100	20	-0.05956
8	0.24927	21	0.01263
9	0.33149	22	0.14298
10	0.36558	23	0.25930
11	0.37962	24	0.33149
12	0.40970	25	0.37762
13	0.53604	26	0.40369

STATIC BASE PRESSURES IN TERMS OF CP

1	0.41973	2	0.41973	3	0.41572

CP = 0.40970 ETA = 0.48849

RATIO OF RAKE AVE Q TO FLOW AVE Q = 1.14386

ST9 FULL SCALE DIFFUSER (IR SUPPRESSING)
SWIRL ANGLE = 21.00 DEGREES

RUN NO	DATA PT	P AMB IN. HG	P AMB PSIA
9.0000	0.0100	29.8670	14.6706

INLET STATIC PRESSURES, PSIA

1 13.86858	2 13.86496	3 13.84329	4 13.81077	5 13.54341
6 14.18291	7 14.09981	8 14.10342	9 14.11787	10 13.89026
11 14.67066	12 14.67066	13 14.67066	14 14.67066	15 14.67066
16 14.67066	17 14.67066	18 14.67066	19 14.67066	20 14.67066

STATIC WALL PRESSURES, PSIA

OUTER WALL

PW 1 13.87942	PW 2 13.99142	PW 3 13.91555	PW 4 13.80354	PW 5 13.93361
PW 6 14.07452	PW 7 14.20459	PW 8 14.38162	PW 9 14.52976	PW10 14.59118
PW11 14.61647	PW12 14.67066	PW13 14.89828	PW	

INNER WALL

PW14 13.64818	PW15 13.88664	PW16 14.17568	PW17 14.67066	PW18 14.52614
PW19 14.18652	PW20 13.82522	PW21 13.95529	PW22 14.19013	PW23 14.39969
PW24 14.52976	PW25 14.61285	PW26 14.65983	PW	

OUTER WALL DKJ-5600

COOLANT INLET TOT L PRESSURE (PB01) = 14.9452 PSIA
COOLANT INLET TOTAL TEMPERATURE (TB01) = 260.000 F
COOLANT INLET TOTAL TEMPERATURE (TB02) = 430.000 F
COOLANT INLET TOTAL TEMPERATURE (TB03) = 0.000 F
OUTER WALL UNCOOLED TEMPERATURE (TWUCO) = 990.000 F
OUTER PANEL NO.1 WALL STATIC PRES. (PW27) = 14.21904 PSIA
OUTER PANEL NO.2 WALL STATIC PRES. (PW28) = 14.48640 PSIA
OUTER PANEL NO.3 WALL STATIC PRES. (PW29) = 14.67066 PSIA
TOTAL COOLANT FLOW RATE = 0.13896 LB/SEC

	Z (IN)	X (IN)	R (IN)	TW (F)	
1	8.45200	8.71800	8.32200	540.00012	(TW 1)
2	9.50000	9.92400	8.91600	430.00006	(TW 2)
3	10.54800	11.10100	9.45400	695.00012	(TW 3)
4	12.12000	12.74900	9.93500	830.00012	(TW 4)
5	12.90600	13.53700	9.98500	730.00012	(TW 5)
6	14.21600	14.86000	9.82400	840.00012	(TW 6)
7	15.78800	16.49900	9.36600	850.00012	(TW 7)
8	16.31200	17.05400	9.18000	745.00012	(TW 8)
9	17.36000	18.16700	8.80300	780.00012	(TW 9)
10	18.66900	19.54000	8.39700	830.00012	(TW10)
11	19.47500	20.36900	8.19800	0.00000	(TW11)

DKJ-5600

INNER WALL

COOLANT INLET TOTAL PRESSURE (PB02) = 15.3629 PSIA
COOLANT INLET TOTAL TEMPERATURE (TB04) = 118.000 F
COOLANT INLET TOTAL TEMPERATURE (TB05) = 400.000 F
COOLANT INLET TOTAL TEMPERATURE (TB06) = 90.000 F
INNER WALL UNCOOLED TEMPERATURE (TWUCI) = 1150.000 F
INNER PANEL NO.1 WALL STATIC PRES. (PW30) = 14.52614 PSIA
INNER PANEL NO.2 WALL STATIC PRES. (PW31) = 14.65983 PSIA
TOTAL COOLANT FLOW RATE = 0.08400 LB/SEC

	Z (IN)	X (IN)	R (IN)	TW (F)	
1	13.95400	15.02400	7.63600	720.00012	(TW12)
2	14.74000	15.93000	7.18700	0.00000	(TW13)
3	15.78800	17.24800	6.39000	0.00000	(TW14)
4	16.23200	17.83000	6.01200	805.00012	(TW15)
5	17.36000	19.33400	5.01800	800.00012	(TW16)

DKJ-5575

BASE REGION

	RADIUS (IN)	STATIC PRESSURE (PSIA)	
1	0.00000	14.68873	P BASE 1
2	1.57000	14.68873	P BASE 2
3	3.10000	14.68150	P BASE 3

COOLANT INLET TOTAL PRESSURE (PB03) = 14.6706 PSIA
TOTAL COOLANT FLOW RATE = 0.00000 LB/SEC

	R (IN)	X (IN)	TW (F)	
1	1.20000	0.21990	0.00000	(TWB01)
2	1.92000	1.34310	845.00012	(TWB02)
3	2.62000	2.43100	925.00012	(TWB03)
4	3.58000	3.75300	0.00000	(TWB04)

BASE BULK TEMP (TBB1) = 925.00012 F

MIDSPAN INLET TOTAL PRESSURES

NO.	PT(PSIA)
1	15.588
2	16.123
3	16.509
4	14.663

LIST OF SYMBOLS

a	Area (ft^2)
A	Area, a/r_r^2 (dimensionless)
A^+	Van Driest constant (26.0)
A^*	Critical area ratio (dimensionless)
$\bar{\bar{A}}$	Block tridiagonal matrix (dimensionless)
$\bar{\bar{A}}^k$	Diagonal block matrix (dimensionless)
b	Chord (ft)
B	Chord, b/r_r (dimensionless)
b_I	Location of pole in z plane (dimensionless)
$\bar{\bar{B}}^k$	Left diagonal block matrix (dimensionless)
c	Speed of sound (ft/sec)
C_D	Drag coefficient, $2D/(\rho_2 U_2^2 b)$ (dimensionless)
C_f	Friction coefficient, $T_w/(P_{01} - P_1)$ (dimensionless)
C_L	Lift coefficient, $2L/(\rho_2 U_2^2 b)$ (dimensionless)
C_p	Specific heat pressure $ft^2/(sec^2$ deg R)
C_p	Pressure coefficient, $(P - P_1)/(P_{01} - P_1)$ (dimensionless)
C_v	Specific heat volume $ft^2/(sec^2$ deg R)
$\bar{\bar{C}}^k$	Right diagonal block matrix (dimensionless)
D	Drag/span (lb/ft)
$\bar{\bar{D}}^k$	Block operator matrix (dimensionless)
e_{ns}	Streamwise strain (1/sec)
$e_{n\phi}$	Tangential strain (1/sec)
$\bar{\bar{E}}^k$	Block operator matrix (dimensionless)

$\bar{\bar{f}}^k$	Solution matrix (dimensionless)
f	Force/area (lb/ft^2)
f	Force/span (lb/ft)
F	Complex variable source solution (dimensionless)
g	Gap between walls (ft)
g_B	Gap between chord lines (ft)
G	Gap between walls, g/r_r (dimensionless)
G_B	Gap between chord lines (dimensionless)
h^+	Enthalpy (ft^2/sec^2)
h	Height of inlet duct (dimensionless)
H^+	Universal stagnation enthalpy, $(h_{QW}-h_Q)\rho_w U^*/q_w$ (dimensionless)
H_A^*	Universal adiabatic stagnation enthalpy, $(h_{OAW}-h_{OA})/(U^*)^2$ (dimensionless)
I	Entropy ft^2/(sec^2 deg R)
l_{IJ}^k	Element of $\bar{\bar{L}}^k$ matrix
L	Lift/span (lb/ft)
$\bar{\bar{L}}^k$	Matrix for k+1 point (dimensionless)
m	Mass flow (slugs/sec)
M	Mass flow, $m/(N_B r_r^2 \rho_r U_r)$ (dimensionless)
$\mathring{m}$	Mass flow/area slugs/(ft^2 sec)
m^+	Universal mass flow parameter, $\mathring{m}_W/(\rho_W U^*)$ (dimensionless)
$\mathring{M}$	Mass flow/area, $\mathring{m}/(\rho_r U_r)$ slugs/(ft^2 sec)
M	Mach number, U/C (dimensionless)

M_S	Streamwise Mach number (dimensionless)
m_{IK}^{k}	Element of $\bar{\bar{M}}$ matrix
$\bar{\bar{M}}$	Boundary condition matrix (dimensionless)
n	Normal coordinate (dimensionless)
η	Normal coordinate, $n/(r_r v_r)$ (dimensionless)
N_B	Number of struts (dimensionless)
N_R	Reynolds number, $r_r \rho_r U_r/\mu_r$ (dimensionless)
p	Pressure (lb/ft^2)
p^+	Universal pressure gradient parameter, $\frac{\mu_w}{\rho_w U^*} \frac{1}{\rho_w U^{*2}} \frac{dp}{dx}$ (dimensionless)
P_R	Prandtl number, $\left(\frac{\mu C_p}{\lambda}\right)$ (dimensionless)
P_{RT}	Prandtl number turbulent, $\left(\frac{\mu C_p}{\lambda}\right)_T$ (dimensionless)
q	Heat flux, $-\lambda \frac{\partial T}{\partial Y}$ lb/(ft sec)
$\bar{q}_1$	Average inlet dynamic pressure (lb/ft^2)
Q	Heat flux, $q/(\rho_r U_r C_p T_r)$ (dimensionless)
Q^+	Universal heat flux, q/q_W (dimensionless)
Q_A^+	Universal heat flux (adiabatic), $q/(\rho_W U^{*3})$ (dimensionless)
$\underset{\sim}{\bar{\bar{Q}}}{}^k$	Column matrix (dimensionless)
$\bar{\bar{q}}^k$	Split column matrix (dimensionless)
r	Radius (ft)
R_C	Recovery factor, Eq. (3.2.35) (dimensionless)
R	Radius, r/r_r (dimensionless)
$\mathcal{R}$	Gas constant $ft^2/(sec^2$ deg R)

r_J	Radius in z plane Eq. (3.7.2) (dimensionless)
$\bar{r}$	Radial coordinate $(\bar{r},\bar{z})$ plane (dimensionless)
r^k_{IJ}	Element of $\bar{\bar{R}}^k$ matrix
$\bar{\bar{R}}^k$	Matrix for k^{th} point (dimensionless)
s	Streamwise coordinate (dimensionless)
S	Streamwise coordinate, $s/(r_r V_r)$ (dimensionless)
S_t	Stanton number (dimensionless)
t	Blade thickness (ft)
T	Temperature (deg R)
T^+	Universal temperature, $C_p T/U^{*2}$ (dimensionless)
$\bar{\bar{T}}^k$	Column matrix for k point (dimensionless)
u_s	Streamwise velocity (ft/sec)
u_n	Normal velocity (ft/sec)
u_ϕ	Tangential velocity (ft/sec)
u	Magnitude of velocity (ft/sec)
u_B	Blade velocity (ft/sec)
u^*	Friction velocity, $\sqrt{\tau_w/\rho_w}$ (ft/sec)
U_S	Streamwise velocity, U_S/U_r (dimensionless)
U_n	Normal velocity, U_n/U_r (dimensionless)
U_ϕ	Tangential velocity, U_ϕ/U_r (dimensionless)
U	Magnitude of velocity, U/U_r (dimensionless)
U_B	Blade velocity, U_B/U_r (dimensionless)

U^+	Universal velocity, U/U^* (dimensionless)
U^*	Friction velocity, U^*/U_r (dimensionless)
v	Metric scale coefficient (dimensionless)
V	Metric scale coefficient, v/v_r (dimensionless)
$\forall$	Volume (ft^3)
w	Complex variable w plane (dimensionless)
W^+	Stream function inner layer (dimensionless)
x	Distance along streamline (ft)
X	Distance along streamline, x/r_r (dimensionless)
x	Real part of Z (dimensionless
y	Imaginary part of z (dimensionless)
y	Distance normal to wall (ft)
Y	Distance normal to wall, y/r_r (dimensionless)
$\tilde{X}$	Real part of dw/dz (dimensionless)
$\tilde{Y}$	Imaginary part of dw/dz (dimensionless)
Y^+	Universal distance from wall, $Y\rho_w U^*/\mu_w$ (dimensionless)
z	Complex variable - z plane (dimensionless)
Z	Axial distance (ft)
Z	Axial distance, z/r_r (dimensionless)
Z_B	Loss coefficient (dimensionless)
$\bar{Z}$	Axial coordinate $(\bar{r},\bar{z})$ plane (dimensionless)
$\bar{\bar{Z}}^k$	Column operator matrix (dimensionless)

α	Swirl angle to axis (deg)
α_s	Chord angle to axis (deg)
α_I	Angle Schwartz-Christoffel transformation (dimensionless)
γ	Ratio of specific heats, C_p/C_v (dimensionless)
δ	Boundary layer thickness (ft)
δ^*	Displacement thickness (ft)
Δ	Boundary layer thickness, δ/r_r (dimensionless)
Δ^*	Displacement thickness, δ^*/r_r (dimensionless)
E_{ns}	Streamwise strain, $r_r e_{ns}/U_r$ (dimensionless)
$E_{n\phi}$	Tangential strain, $r_r e_{n\phi}/U_r$ (dimensionless)
ϵ	Small angle in z plane
η	Transformed normal coordinate (dimensionless)
η	Imaginary part of w (dimensionless)
H	Blade/force area, $r_r f/(\rho_r u_r^2)$ (dimensionless)
θ	Angle of streamline to axis (deg)
θ^*	Momentum thickness (ft)
Θ	Temperature ratio, T/T_r (dimensionless)
Θ^*	Momentum thickness, θ^*/T_r (dimensionless)
i	$\sqrt{-1}$
I	Entropy, $(I-I_r)/R$ (dimensionless)
κ	Von Karman constant (0.41)
λ	Thermal conductivity lb/(sec deg R)

μ	Viscosity slugs/(ft sec)
Ξ	Plade force/span, $f/(r_r \rho_r U_r^2)$ (dimensionless)
ξ	Real part of w (dimensionless)
π	3.14159
Π	Pressure ratio, p/p_r (dimensionless)
ρ	Density (slugs/ft^3)
ρ_s, ρ_n	Radius of curvature (ft)
P	Density ratio, ρ/ρ_r (dimensionless)
P_s, P_n	Radius of curvature (dimensionless)
σ	Solidity, b/g_B (dimensionless)
Σ_{ns}	Streamwise stress, $\tau_{ns}/(\rho_r U_r^2)$ (dimensionless)
$\Sigma_{n\phi}$	Tangential stress, $\tau_{n\phi}/(\rho_r U_r^2)$ (dimensionless)
τ_{ns}	Streamwise stress (lb/ft^2)
$\tau_{n\phi}$	Tangential stress (lb/ft^2)
τ^+	Stress, τ/τ_w (dimensionless)
$\bar{\bar{\tau}}^k$	Column matrix for boundary conditions (dimensionless)
ϕ	Tangential coordinate (radians)
ϕ_c	Chamber angle (deg)
ϕ_J	Angle in z plane Eq. (3.7.3) (dimensionless)
ϕ_B	Blade dissipation function lb/(sec ft^2)
Φ_B	Blade dissipation function (dimensionless)

χ Clauser constant (0.016) (dimensionless)

χ Normal coordinate transform, $d\eta/dn$ (dimensionless)

ψ Stream function (slugs/ft)

Ψ Stream function (dimensionless)

Matrix Operators

T Transpose

-1 Inverse

Superscripts

ν Iteration number

$-$ Mean or average quantity

$\wedge$ Variables for blade force calculation

$'$ Deviation from mean quantity

Subscripts

O Stagnation conditions

1 Inlet conditions

2 Upstream of strut

3 Downstream of strut

A Adiabatic

E Effective turbulent

H Hub conditions

I Incompressible conditions

M Midspan conditions

r	Reference conditions*
T	Tip conditions
W	Wall conditions
∞	Free stream or edge of boundary layer

*Reference conditions are based on standard sea level atmosphere conditions for all thermodynamic quantities. The reference radius, r_r, is the inlet outer radius, and the velocity is the mean inlet velocity.